TiAM
kwartalnik naukowo-techniczny
e-ISSN-2450-8217

TECHNOLOGIA I AUTOMATYZACJA MONTAŻU

ZESPOŁÓW • MASZYN • URZĄDZEŃ

1/2020

Wydawca: Łukasiewicz - IMBiGS • Wydawnictwo SIGMA-NOT • Patronat: SIMP • Istnieje od 1993 r. • Open Access on www.sigma-not.pl • Zeszyt nr 1-2020 (107)

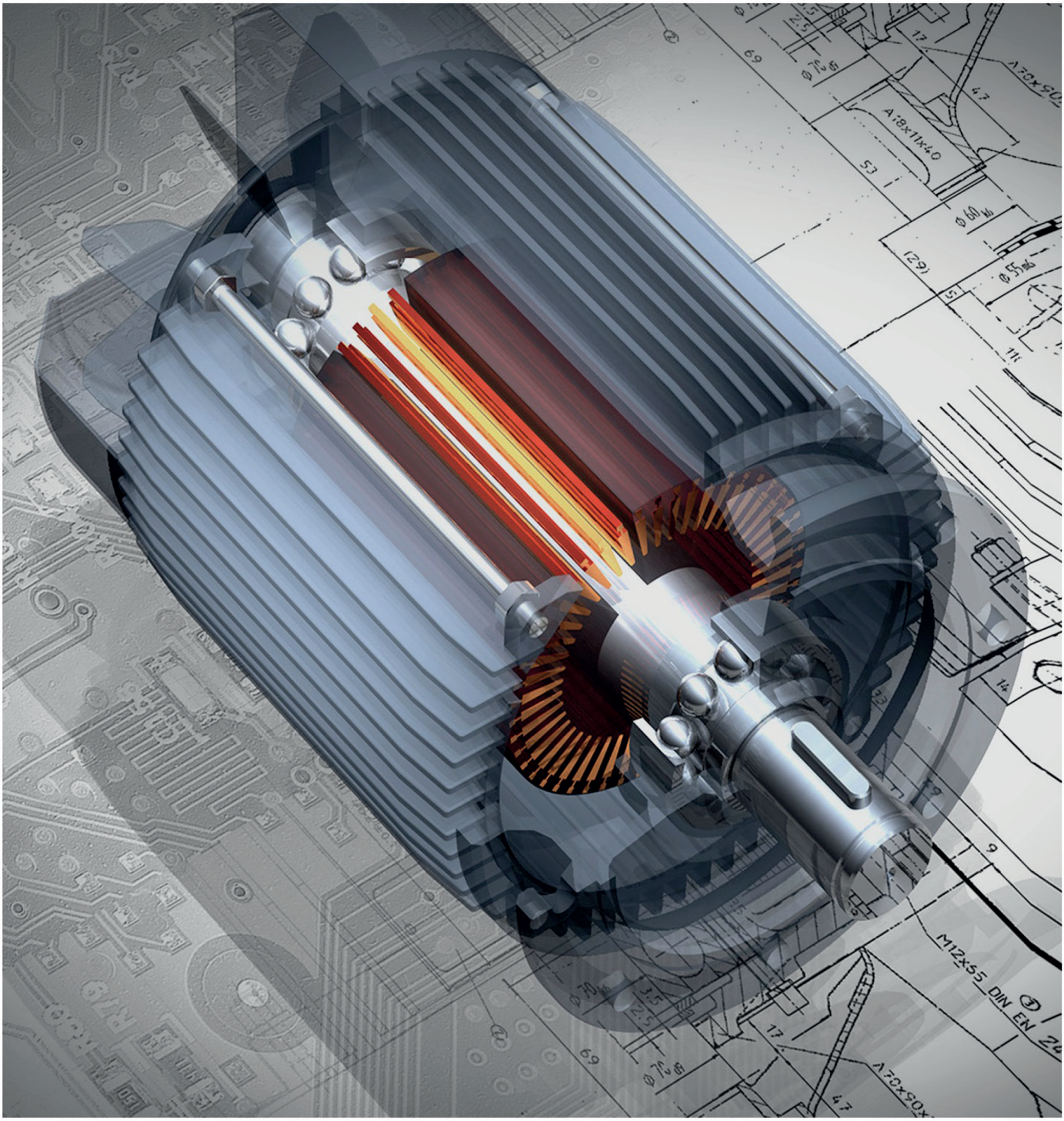

PRASA FACHOWA
SIGMA-NOT
www.sigma-not.pl

Łukasiewicz
IMBiGS

TiAM
kwartalnik naukowo-techniczny
TECHNOLOGIA I AUTOMATYZACJA MONTAŻU
ZESPOŁÓW • MASZYN • URZĄDZEŃ
ASSEMBLY TECHNIQUES AND TECHNOLOGIES

e-ISSN-2450-8217

ZESPÓŁ REDAKCYJNY:
Redaktor Naczelny – prof. dr hab. inż. Jerzy Łunarski
Z-ca Redaktora Naczelnego – dr inż. Martyna Jachimowicz
tel. 663 311 966
Redaktorzy tematyczni:
Dr inż. Rafał Kluz (technologia, automatyzacja)
Dr inż. Katarzyna Antosz (niezawodność, eksploatacja)
Dr inż. Mirosław Chłosta (inżynieria, produkcja)
Dr inż. Andrzej Kubit (struktury i systemy montażu)

RADA PROGRAMOWO-NAUKOWA:
Prof. Dario Antonelli (Politecnico di Torino, Włochy), prof. Bronius Baksys (Kaunas University of Technology, Litwa), prof. Marek Balaziński (Ecole Politechnique Montreal, Kanada), prof. Adam BARYLSKI (Politechnika Gdańska), mgr inż. Magdalena Borek-Daruk (SIGMA-NOT), prof. Józef Gawlik (Politechnika Krakowska) – z-ca przewodniczącego, prof. Jan Godzimirski (WAT), prof. Stefan Góralczyk (IMBiGS), prof. Mikulas Hajduk (Technicka Univerzita v Kosiciach, Słowacja), prof. Michael Kheifetz (Połocki Gosudarstwiennyj Uniwersytet, Białoruś), doc. dr inż. Radek Knoflicek (FME Brno, Czechy), prof. Mark Kristal (Volgograd State Technical University, Rosja), prof. Józef Kuczmaszewski (Politechnika Lubelska), prof. Piotr Łebkowski (AGH), prof. Antonio Maffei (KTH Royal Institute of Technology, Szwecja), prof. Ignace Martens (Katholieke Universiteit Leuven, Belgia), prof. Jacek Mucha (Politechnika Rzeszowska), prof. Vitaliy Pasichnyk (Nacjonalnyj Techniczeskij Uniwersitet Ukrainy „Kijewskij Politechniczeskij Instytut", Ukraina), prof. R. M. Chandima Ratnayake (University of Stavanger, Norwegia), prof. Emil Spisak (Technika Univerzita v Kosiciach, Słowacja), dr inż. Dorota Stadnicka (Politechnika Rzeszowska), prof. Jerzy Stamirowski (Politechnika Świętokrzyska), prof. Michaił W. Wartanow (Moskowskij Gosudarstwiennyj Maszinostroitielnyj Uniwersytet, Rosja), prof. Władimir P. Woronienko (Moskowskij Gosudarstwiennyj Technologiczeskij Uniwersytet, Rosja), prof. Jan Żurek (Politechnika Poznańska) – przewodniczący

ADRES REDAKCJI:
Kwartalnik „Technologia i Automatyzacja Montażu"
ul. Ratuszowa 11, pok. 740
00-950 Warszawa, skr. poczt. 1004
Tel. 22 853 81 13
e-mail: tiam@sigma-not.pl
www.tiam.pl

PRENUMERATA:
Zakład Kolportażu Wydawnictwa SIGMA-NOT Sp. z o.o.
ul. Ku Wiśle 7
tel. 22 840 30 86
tel./fax: 22 827 43 65, 619 22 41 w. 215
e-mail: prenumerata@sigma-not.pl
portal: www.sigma-not.pl

REKLAMA:
Redakcja: tel. 22 853 81 13
e-mail: tiam@sigma-not.pl
Dział Reklamy i Marketingu
tel./fax: 22 827 43 65
e-mail: reklama@sigma-not.pl

SKŁAD I ŁAMANIE:
Wydawnictwo SIGMA-NOT
ul. Ratuszowa 11, 00-950 Warszawa
e-mail: sekretariat@sigma-not.pl

WYDAWCA:
Łukasiewicz
IMBiGS
Sieć Badawcza Łukasiewicz
Instytut Mechanizacji Budownictwa i Górnictwa Skalnego
ul. Racjonalizacji 6/8, 02-673 Warszawa

PRASA FACHOWA SIGMA-NOT www.sigma-not.pl
Wydawnictwo SIGMA-NOT
ul. Ratuszowa 11 skr. poczt. 1004, 00-950 Warszawa

PATRONAT:
Stowarzyszenie Inżynierów Mechaników i Techników Polskich

Za treść ogłoszeń i artykułów promocyjnych redakcja nie odpowiada

Wersja pierwotna: elektroniczna

WSKAZÓWKI DOTYCZĄCE PRZYGOTOWANIA ARTYKUŁÓW

- Artykuły przeznaczone do opublikowania w kwartalniku „Technologia i Automatyzacja Montażu" powinny mieć oryginalny i naukowo-techniczny charakter i być zgodne z problematyką czasopisma. Redakcja przyjmuje artykuły w jęz. polskim, jęz. angielskim i jęz. rosyjskim.
- Artykuł o maksymalnej objętości 5 stron A4 wraz z ilustracjami powinien być napisany czcionką Times Roman lub Arial 12 pkt, z interlinią 12 pkt. Formatowany tekst nie powinien mieć podziału na kolumny.
- Tytuł artykułu należy podać w jęz. polskim i jęz. angielskim. Tytuł nieprzekraczający 10 słów powinien odzwierciedlać istotne elementy treści artykułu.
- Struktura artykułów naukowo-technicznych prezentujących prace autora(ów) powinna być następująca: wstęp (wprowadzenie); metodyka (badań, analiz, pracy z podaniem ewentualnie materiałów, założeń itp.); wyniki (badań, analiz); omówienie wyników; wnioski; spis literatury.
- Podpisy pod ilustracjami oraz tytuły tablic należy podać w jęz. artykułu i jęz. angielskim.
- Ilustracje należy dołączyć również jako osobne pliki w formacie: .jpg, .tiff, z rozdzielczością co najmniej 300 dpi. Wszystkie zamieszczane ilustracje powinny być własnością autora(ów) lub należy podać źródło pochodzenia rysunków.
- Wzory matematyczne pisane w edytorze równań Microsoft Equation i powinny być oznaczane kolejnym numerem w nawiasie okrągłym. Wszystkie symbole powinny być objaśnione. Należy stosować jednostki układu SI.
- Spis literatury należy podać w kolejności cytowania w tekście, a odnośniki w tekściepo winny być ponumerowane cyframi arabskimi i umieszczone w nawiasach kwadratowych. W przypadku korzystania z Internetu należy podać adres strony i datę odczytu. Liczbę autocytowań należy ograniczyć do niezbędnych.
- Do artykułu należy dołączyć streszczenie w jęz. artykułu i jęz. angielskim, zawierające minimum 200–250 słów.
- Pod streszczeniem należy podać 3–6 słów kluczowych w jęz. artykułu i jęz. angielskim, zwracając uwagę, by nie były one powtórzeniem tytułu pracy.
- Po spisie literatury zaleca się podanie źródła finansowania pracy.
- Na końcu artykułu należy podać: imiona i nazwiska autorów, tytuły naukowe lub zawodowe, telefon, faks, e-mail, miejsce zatrudnienia wraz z adresem do korespondencji.

PROCEDURA RECENZOWANIA

Procedura recenzowania artykułów w czasopiśmie jest zgodna z zaleceniami Ministerstwa Naukii Szkolnictwa Wyższego zawartymi w opracowaniu „Dobre praktyki w procedurach recenzyjnych w nauce", Warszawa 2011.

Wszystkie artykuły naukowo-techniczne publikowane w kwartalniku „Technologia i Automatyzacja Montażu" są recenzowane.

Nadesłane artykuły są poddawane redakcyjnej ocenie formalnej i otrzymują numer redakcyjny, identyfikujący je na dalszych etapach procesu wydawniczego, a redakcja wysyła do autorów informację o przyjęciu artykułu i wysłaniu go do recenzentów. Do oceny każdej publikacji powołuje się co najmniej dwóch niezależnych recenzentów. Redakcja dobiera recenzentów rzetelnych i kompetentnych w danej dziedzinie. Nadesłane artykuły nie są nigdy wysyłane do recenzentów z tej samej placówki, z której pochodzi autor. Prace recenzentów są poufne i anonimowe. Recenzja musi mieć formę pisemną i kończyć się jednoznacznym wnioskiem o dopuszczeniu artykułu do publikacji w czasopiśmie lub jego odrzuceniu. W przypadku pracy w języku obcym, co najmniej jeden z recenzentów jest afiliowany w instytucji zagranicznej innej niż narodowość autora pracy. Autorzy są informowani o wynikach recenzji oraz otrzymują je do wglądu. W sytuacjach spornych redakcja powołuje dodatkowych recenzentów.

Lista recenzentów publikowana jest w ostatnim zeszycie każdego rocznika.

Kwartalnik „Technologia i Automatyzacja Montażu" ukazuje się formie elektronicznej w otwartym dostępnie (Open Access) i jest dostępny na Portalu Informacji Technicznej Wydawnictwa SIGMA-NOT www.sigma-not.pl

CONTENTS / W NUMERZE / B HOMEPE

4

LOSKA A.:

The way of exploitation assessment in the conditions of object-oriented servicing of selected production machines and equipment

Sposób oceny eksploatacyjnej w warunkach obiektowego serwisowania wybranych maszyn i urządzeń produkcyjnych

10

BUCIOR M., KLUZ R., KUBIT A.:

Robotization of the process of removal of the gating system in an enterprise from the automotive industry

Robotyzacja procesu usuwania układów wlewowych w przedsiębiorstwie z branży motoryzacyjnej

16

BARSZCZ A., CHŁOSTA M.:

Electric car crash energy absorbing structure

Struktura pochłaniająca energię zderzenia dla samochodów elektrycznych

23

ANTOSZ K., KLUZ R.:

Application of selected balancing methods for analysis and evaluation of the working efficiency of the assembly line on the example of a selected product

Zastosowanie wybranych metod balansowania do analizy i oceny wydajności pracy linii montażowej na przykładzie wybranego produktu

30

KUBIT A., BUCIOR M., KLUZ R.:

Effect of temperature on the shear strength of GFRP-aluminium alloy 2024-T3 single lap joint

Wpływ temperatury na wytrzymałość na ścinanie połączenia adhezyjnego pomiędzy kompozytem GFRP a blachą ze stopu aluminium 2024-T3

36

BUKOWSKA B., STADNICKA D.:

Value stream mapping of a unique complex product manufacturing process

Mapowanie strumienia wartości procesu produkcji niepowtarzalnego wyrobu

45

ŻÓŁKOŚ M.:

Analysis of the grinding force components and surface roughness in grinding with the use of a glass-crystalline bonded grinding wheel

Analiza składowych siły szlifowania oraz chropowatości powierzchni podczas szlifowania z użyciem ściernicy ze spoiwem szklanokrystalicznym

52

FRĄCZYK A.:

Possibilities to reduce surface roughness in pre-assembly face milling using WIPER inserts

Możliwości obniżenia chropowatości powierzchni w przedmontażowym frezowaniu czołowym z wykorzystaniem płytek typu WIPER

Kwartalnik notowany na liście czasopism punktowanych Ministerstwa Nauki i Szkolnictwa Wyższego – 20 pkt.

TECHNOLOGIA I AUTOMATYZACJA MONTAŻU

e-kwartalnik naukowo-techniczny

w otwartym dostępie na:

www.tiam.com.pl

www.sigma-not.pl

Autorów zapraszamy do publikacji
na łamach kwartalnika – 20 pkt. MNiSW
kontakt: tiam@sigma-not.pl
tel. 22 853 81 13

WYDAWNICTWO *SIGMA-NOT*

THE PROBLEMS OF ASSESSING ASSEMBLY TECHNOLOGIES

Jerzy ŁUNARSKI

Significant progress may be observed in the improvement of particular technologies in the assembly production. It consists mainly in their automation and computerisation based on current achievements of artificial intelligence. General aspects of the assessment of automated assembly machines were discussed in TiAM No. 4/2017 ("Problems of quality assessment of automated assembly machines"), whereas the assessment of the modernity level of the technology used requires a slightly different approach. This assessment is often necessary because technology is one of important factors which determine an organisation's competitiveness.

When considering the whole of assembly technologies used in an organisation that are quite different depending on the organisation's operating profile, a general division into the following groups should be first made:

1. Technologies that create a competitive advantage and bring different benefits for an organisation because of their use (they may be called - modern).
2. Technologies typical of the considered manufacturing sector, commonly used and necessary for the implementation of basic production – as they are frequently used they do not contribute to building a competitive advantage.
3. Obsolete technologies that constitute the remains of the process used earlier of the productivity clearly lower than in the typical technologies and which should be exchanged (renovated) in the first place.

The criteria of the division into these three groups may be as follows: productivity sometimes characterised by the calculated time of a product manufacturing; a percentage share of service works in the general production work time of assembly machines; or a percentage share of manual work in the general production work time of assembly machines. In regard to a manufacturing sector these factors may differ. However, based on the mentioned indicators, decomposition of assembly stands into three groups may be done (i.e. modern, typical, obsolete). In an organisation's strategy and its management system there should be guidelines considering the percentage shares of the particular groups as well as the procedures of liquidating the third-group machines and obtaining the machines of the first and the second group.

A lot of modern assembly machines are designed for particular tasks as well as for the estimated production scale with a small or no possibility of the changeover to other similar tasks. Their solutions are unique and the analogous counterparts, which enable comparison and relative assessment, are mostly absent on the market. The assessment of technological advancement of machines that should guarantee 100% of service and property safety may be performed on the basis of the following criteria:

1. Operation reliability of a machine characterised by e.g. the ratio of the total time of downtimes from technical reasons to the available working time of a machine in the established period of time (e.g. one month).
2. Energy consumption of a machine characterised by the average energy consumption on manufacturing one unit of a product or on realizing a particular value of assembly production.
3. Simplicity of maintenance and service work characterised by the ratio of the total time of the mentioned work realisation to the total time of production work of the machine in the established period of time.
4. Productivity of a machine characterised by the ratio of the amount of the products (expressed in their number or monetary value) per one square metre of a production space occupied by the machine in the established period of time.
5. An exploitation wear and tear degree characterised by the ratio of the previous operation time to the expected period of a machine amortisation.
6. Possibility of the autonomous operation of a machine with operator-free service characterised by the ratio of the autonomous operation time to the available shift time (or two work shifts).

One or a few from the indicated criteria are often sufficient for the approximate assessment of technologies. In case of the specialised processes other criteria characteristic of the given technology (e.g. in food production - the shelf-life) may be applied.

Periodic conduct of such assessment will show preferable directions of the particular technologies' improvement. As a result, it will facilitate the improvement of an organisation's competitiveness. In many specific situations there is a need to develop assumptions and, possibly, a concept of a new technology effectively supporting assembly processes of a company. Physical implementation of such technologies may be realised by dedicated companies or in the organisation itself, if it possesses the appropriate research and development potential.

THE WAY OF EXPLOITATION ASSESSMENT IN THE CONDITIONS OF OBJECT-ORIENTED SERVICING OF THE SELECTED PRODUCTION MACHINES AND EQUIPMENT

Sposób oceny eksploatacyjnej w warunkach obiektowego serwisowania wybranych maszyn i urządzeń produkcyjnych

Andrzej LOSKA **ORCID: 0000-0003-0041-795X**

DOI: 10.15199/160.2020.1.1

Abstract: The article discusses issues related to the ways of maintenance management of selected groups of production machines and devices. The first part identifies and characterizes two organizational models of machine servicing, i.e. the process model and the object model. It was justified that the object-oriented approach to machine servicing is an unusual concept, and it can be the basis for developing the models for the exploitation assessment of machines being the products of manufacturing processes, that require servicing tasks. As a result, it was proposed to use taxonomic methods for the purposes of developing a model, the analysis of which will allow the interpretation of the exploitation policy realized in the conditions of object-oriented servicing of machines and devices. The case study presented in the article confirms the possibility of building such models, and also justifies such analyzes for the purposes of shaping the exploitation decision-making process.
Keyword: maintenance, exploitation process, service of machines, taxonomy methods

Streszczenie: Artykuł omawia problemy zarządzania eksploatacją i utrzymaniem ruchu wybranych grup maszyn i urządzeń produkcyjnych. W pierwszej części zidentyfikowano i scharakteryzowano dwa organizacyjne modele serwisowania maszyn, to znaczy model procesowy i model obiektowy. Uzasadniono, że obiektowe podejście do serwisowania maszyn jest koncepcją nietypową i może być podstawą budowy modeli oceny eksploatacyjnej maszyn będących produktami procesów produkcyjnych i wymagającymi serwisowania. W efekcie zaproponowano wykorzystanie metod taksonomicznych dla potrzeb budowy modeli, których analiza pozwoli na interpretację polityki eksploatacyjnej prowadzonej w warunkach obiektowego serwisowania maszyn i urządzeń. Zaprezentowane w artykule studium przypadku potwierdza możliwość budowy takich modeli, a także uzasadnia prowadzenie tego typu analiz na potrzeby kształtowania eksploatacyjnego procesu decyzyjnego.
Słowa kluczowe: utrzymanie ruchu, procesy eksploatacyjne, serwisowanie maszyn, metody taksonomiczne

Introduction

In industrial practice, the need to achieve and maintain high operational efficiency applies not only to individual machines and devices, but primarily to complex technical systems (e.g. industrial installations, technological lines, network technical systems). Different durability and diagnostic and repair susceptibility of components of complex technical systems often impede rational exploitation. However, the total value (e.g. replacement cost) often exceeds the amounts that are currently available to maintain their efficiency. These factors cause, that in the aspect of the exploitation decision-making process of complex technical systems, it is necessary to jointly consider their constituents and together operating machines and devices. In the aspect of rapid development of operational methods as well as IT tools, it becomes justified to conduct the research related to the development of rational decision-making process concerning, among others, long-term operational processes as a part of the appropriate models of technical management.

Two separate processes are considered in the exploitation of machines and devices [8]:

a. exploitation process, which is an ordered collection of intentional and unintentional events occurring in the operation phase, as well as during the realization of maintenance tasks and procedures,
b. decision-making process, which is a sequence of decisions, whose effects relate to the way and scope of operate and/or maintenance proceedings, in relation to the exploited machines and devices, and also significantly affect the participants and the resources of the realized exploitation processes.

There is a clear and significant relationship between the operational process and the decision-making process. The specific steps in the decision-making process result not only from decision theory, but also from the specifics of the human-technical object relationship. This is reflected in the methods and conditions of operate, as well as conducting maintenance work.

Review of organizational models of machine servicing

The set of factors/criteria, necessary to be taken into account in the exploitation decision-making process, is multi-faceted in nature, related itself to the exploited technical object, as well as related to its broadly understood environment.

Long-term research of various authors [1, 4, 10] showed that the way of maintenance management, in particular, the realization of tasks defined by the pair: exploitation process - decision-making process, depends primarily on the selected method of organization of operating activities and maintenance works, as well as the technical and organizational context. Therefore, two main ways of servicing machines can be specified:

- process-oriented machine servicing,
- object-oriented machine servicing.

♦ Service and assessment of machines in the process-oriented system

The process-oriented way of machine service is strictly determined by the characteristics of the production process. The implementation of operational and decision-making processes results from the systemic ordering of machinery and devices. Such a system is located in the specific stationary organizational and technical conditions and is operated by the maintenance staff of the given (production) enterprise [2, 6]. This method is time-oriented, which means that the most important decision criterion is the time of realization of particular activities, which is a domain in the exploitation process (Fig. 1).

The process-oriented way of servicing machines is susceptible to apply most exploitation strategies, and hence, measures oriented on the identification, assessment and optimization of the time of the participation of exploitation processes in the production process. It can be mentioned here strategies, that are different forms of PM (preventive maintenance), based on the so-called service life [5].

The data resulting from the realization of exploitation processes, in the context of the process way of servicing are usually continuous in time and oriented to a specific technical system. This means that it is possible and susceptible to the use of CMMs/EAM tools for the purpose of data collection and processing. In this approach, the basis for the operation of such tools os constituted by individually built hierarchical models of the exploited technical systems, based on individual structural connections of components [4]. Exploitation measures are characterized by detailed identification and analysis of individual stages of the realization of exploitation processes. As a result, the use of statistical models is to allow optimization (minimization) of the share of time spent on maintenance works in the production process [2]. The hierarchical arrangement of the components of the technical system allows you to conduct analyzes at particular levels in the complex structure.

♦ Service and assessment of machines in the object-oriented system

The object-oriented way of servicing is determined by the specificity and exploitation characteristics of machines and devices. The implementation of exploitation processes and decision-making processes results from a separate discrete consideration of each of the serviced technical objects. Such facilities are located in various organizational and technical conditions (in various enterprises) and therefore they are treated discreetly by external entities carrying out the maintenance work. This method is object-oriented, which means that the most important decision criterion is the condition of the object in the context of the exploitation process and in the aspect of organizational and technical circumstances in which it operates. An important aspect that distinguishes object-oriented way from process-oriented way of machines servicing is the point of view of service personnel. In the object-oriented way, service covers many technical systems of the same or similar classes operated in different locations. In this context, the use of strategies typical of a process-oriented approach seems unpractical and sometimes even impossible. Each location of machines and devices work must be treated individually and separately, so it is necessary to adapt to the requirements and capabilities of maintenance services by users of technical systems.

Data resulting from the implementation of such processes are usually discrete in time, so they are dispersed and oriented on objects in specific locations,

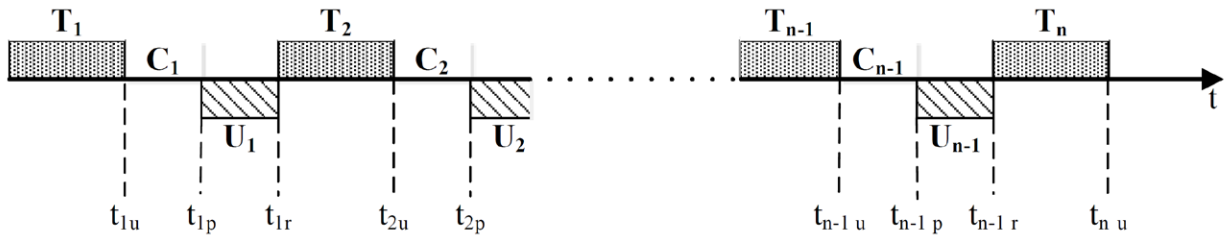

Fig. 1. The scheme of exploitation of the technical object in the conditions of process servicing of machines [5, 12]

as well as on specific classes of technical systems. In addition, industrial practice shows that the scope and the quality of data obtained from particular places of functioning of technical objects are much more limited than in the process-oriented way. It is caused by the lack of possibility of continuous supervision by service staffs over the implemented exploitation process, as well as a significant limitation of the scope of the acquired data on the context of implemented operational processes [11]. It allows carrying out analyzes based on registered values of machine work conditions, as well as exploitation history. Location dispersal of the data also determines a different approach to the use of common tools (CMMS/EAM systems) to support maintenance management tasks. In particular, there are required object-oriented models of technical system components (instead of the hierarchical ones), as well as the as-built way of proceeding maintenance works.

Taxonomic way of assessing machines service in the object-oriented system

On the basis of the specificity of machine servicing presented in the previous point, it can be said that in the object-oriented system, there are limitations on the use of exploitation assessment models typical in industrial practice, such as OEE, KPI or reliability indicators. The problem is mainly the dispersion and diversity of data acquisition sites (data sources), and the consequence is the potential incompleteness of information resources, as well as limited confidence in their credibility. Due to this reason, the assessment of the functioning of the machines may be subject to a significant error, and thus its value for the decision-making process can be reduced.

Therefore, for the purposes of the assessment of the machines exploitation in the object-oriented system, the author proposes the assumption, that the result of the realization of exploitation processes (the exploitation policy) is a function of three characteristics:

$$Y = f(k, c, l) \tag{1}$$

where: k - the cost of the service works, c - the time of the service works, l – the quantity of the service works

The above-mentioned characteristics are identified in the specific periods of time of production processes/exploitation processes (so-called macro times). In this way, it is possible to build models and determined measurement values related to defined groups (types) of machines or entire machine parks, with the simultaneous identification of the value and specificity of the exploitation policy. The use of feature aggregation methods allows to track changes in the exploitation policy in macro time (e.g. in subsequent years), analyze and evaluate its current level, as well as simulate and forecast the changes that may occur in the future [7].

The key aspect to implement the above assumptions is the selection of the method of aggregation of features. The author proposes the use of numerical taxonomy methods, which are traditionally used for linear ordering tasks [3, 9].

In this regard, it is proposed to develop synthetic measures using the features of the exploitation policy, and then using the obtained results in the analysis in a specific exploitation context. In particular, the construction of a synthetic measure using the Hellwig method is carried out according to the following procedure [3]:

A. Identification and ordering the input data, in the form of: the matrix of the features of the exploitation policy, the weight vector of the features of the exploitation policy, the weight vector of categories of the service and repair works:

$$x_{ij} = \begin{bmatrix} x_{11} & \cdots & x_{1n} \\ \vdots & \cdots & \vdots \\ x_{p1} & \cdots & x_{pn} \end{bmatrix}, \quad WW = \begin{bmatrix} ww_1 \\ \vdots \\ ww_n \end{bmatrix}, \quad WK = \begin{bmatrix} wk_1 \\ \vdots \\ wk_p \end{bmatrix} \tag{2}$$

where: x_{ij} - values of features for particular categories of maintenance works, identified over a period of time limited by the number of completed maintenance cycles, $i=(1,...,p)$ - the number of key features included in the model of the assessment of the exploitation policy, $j=(1,...,n)$ - the number of maintenance work categories included in the model of the assessment of the exploitation policy, ww_j - the value that multiplies the importance of individual features in the assessment of exploitation policy, wk_i - the value differentiating the importance of individual categories of maintenance works in the assessment of the exploitation policy.

B. Determination of the matrix of normalized features

$$z_{ij} = \frac{x_{ij} - \overline{x}_j}{S(x_j)} \cdot ww_j \cdot wk_i \tag{3}$$

where: Z_{ij} - normalized feature, $\overline{x}_j$ - mean value of the feature class (column), $S(x_j)$ - standard deviation of the feature class (column).

C. Determination of synthetic measure, as a distance from the reference vector:

$$s_i = 1 - \frac{d_{i0}}{d_0}$$

where: $$d_{i0} = \sqrt{\sum_{j=1}^{m} (z_{ij} - z_{0j})^2}, \qquad z_{0j} = \frac{\overline{z_j}}{s_j} \tag{4}$$

D. Determination of the coordinates of the geometric location of the synthetic measures:

$$x_i = \sqrt{\frac{\sum_{j=1}^{m} w_j \cdot (z_{ij} - \varphi_j)^2}{m \cdot (\overline{d} + 2 \cdot S_d)^2}} \quad ,$$

$$y_i = \sqrt{\frac{\sum_{j=1}^{m} [\![1 - w]\!]_j \cdot (z_{ij} - \varphi_j)^2}{m \cdot (\overline{d} + 2 \cdot S_d)^2}} \qquad (5)$$

where: $w_j = \frac{\omega_j}{\sum_{k=1}^{m} \omega_k}$, $\omega_j = \frac{S_j}{\overline{Z}_j}$

Based on the above procedure (1) – (5), there were determined taxonomic measures describing the exploitation policy.

Taxonomic assessment of machines service in a selected manufacturing company

The proposed way of building a machine service assessment model has been verified based on data from the realization of exploitation processes in a selected manufacturing company in the machines industry. For the purposes of verification, there was selected such an company, whose functioning corresponds to the conditions of object-oriented machine servicing. This company specializes in the production of machines and equipment that are part of automated production lines. In particular, this activity consists of unit and low volume production, sale and subsequent service of robotic palletizing lines, adapted to process almost any type of product and type of packaging, regardless of the weight, shape or material from which these elements were made. Therefore, the exploitation specificity of the discussed company applies simultaneously to two areas:

- servicing production machines and equipment, which are the components of the own machine park,
- servicing production machines and equipment, which are the effects (products) of the company production activity.

The exploitation problems of the first group of machines concern a typical process approach to servicing and will not be the subject of the solution proposed in this article. However, the second group of machines is characterized by object-specific servicing, because it is a set of discrete and locally dispersed technical systems. The exploitation assessment of such machines is less typical but susceptible to the proposed solution. That is why this group of machines of the examined enterprise will be the subject of the proposed taxonomic method of operational assessment.

The identification and analysis of the obtained historical service data allowed to specify the following input conditions:

- data came from the realization of maintenance works for production machines serviced at customer enterprises within one year (2017),
- diagnostic variables were determined based on three features of the exploitation policy: costs, time, quantity of maintenance work,
- diagnostic objects were created based on four categories of maintenance work: inspections, regulations/corrections, repairs, modernizations.

An ordered set of input data is presented in tab. 1.

Based on the data in tab. 1, and also in accordance with the formulas (1) – (5), there were carried out calculations, whose results are summarized in tab 2.

Tab. 1. Input data to the taxonomic method of the exploitation assessment

Diagnostic objects	Weights	Diagnostic features		
		Cost [PLN]	Time [hours]	Quantity of works
	wkj/wwi	1	1	1
Inspections	0,25	151 819,73	38 642	6 328
Regulations/Corrections	0,25	146 773,18	22 965	1 544
Repairs	0,25	192 134,67	8 741	530
Modernizations	0,25	561 928,82	10 908	1 296
Sum		1 052 656,40	81256	9698

Tab. 2. Values of taxonomic measures of the exploitation assessment

Diagnostic objects	Synthetic measure	Taxonomic geometric coordinates		
		x coordinate	y coordinate	Resultant coordinate
Inspections	0,2838	1,4502	2,1088	2,5593
Regulations/Corrections	0,6849	0,2143	0,2996	0,3683
Repairs	0,9742	0,4504	0,6476	0,7888
Modernizations	0,4525	0,6756	0,9372	1,1554

A graphical interpretation of the input data as well as the calculated taxonomic measures is shown in Fig. 2.

Interpretation of the obtained results

As a result of the proposed method, as well as on the basis of calculations, there were obtained values, which may constitute the basis for assessing the way and scope of the exploitation of machines and devices considered in the object service system. However, the method of analysis and interpretation of the results goes beyond the traditional way of using linear ordering methods. In the classic approach, the values of taxonomic measures have a direct impact on the value (position) of each of the assessed objects. In the approach proposed in the article, the complete taxonomic model is analyzed, taking into account the arrangement of all objects, as well as the relative differences in the values of the calculated measures.

The analysis of obtained and graphically summarized results of the development of the taxonomic assessment model consists in isolating the dominant categories of service works for the analyzed machines and devices, and then attempting to interpret the exploitation specificity of servicing procedures and machines. The domination of individual categories of maintenance work should be interpreted as one of two forms [7]:

- the absolute dominance of selected maintenance categories (taxonomic diagnostic objects), expressed in the form of maximizing the value of an appropriate taxonomic synthetic measure, while minimizing the resultant value of the taxonomic geometric distance (distance from the point of origin of the coordinate system),
- the relative dominance of selected categories of maintenance categories (taxonomic diagnostic objects), expressed by minimizing taxonomic geometric distances between particular categories within their clusters.

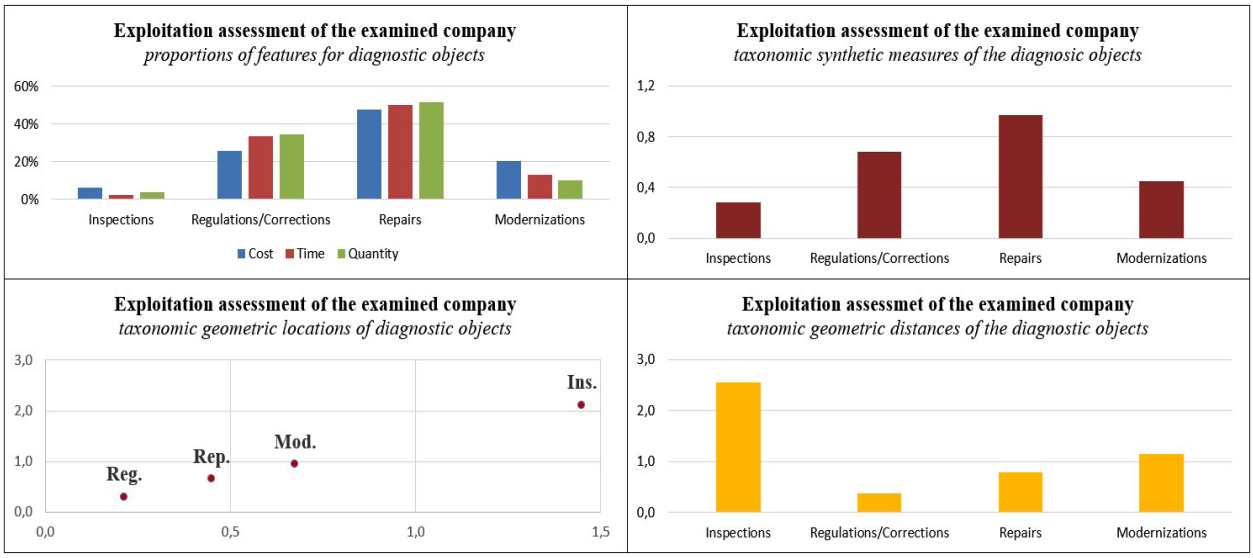

Fig. 2. Graphical interpretation of the results of the exploitation assessment of the examined production company

The exploitation policy realized in relation to the serviced machines and equipment by the analyzed company is characterized by:

- a distinct absolute taxonomic domination of repairs, with the addition of a fairly clear impact on the examined model of regulation/correction works,
- small (smallest in the analyzed case) taxonomic significance of inspections,
- medium mutual taxonomic dispersion of three categories of maintenance work (regulations, repairs, modernizations), with a small distance of the entire cluster from the beginning of the coordinate system, and at the same time a significant distance of the inspections both from the cluster and from the beginning of the coordinate system,
- the lack of distinct dominance of the values of particular features for individual diagnostic objects (categories of maintenance work).

According to the above interpretation, it should be stated that in taxonomic terms, the exploitation policy applied to the serviced machines is the nature of the intervention - of a normative type. This is indicated by the dominant taxonomic impact of repairs, but also a taxonomically balanced and significant system of regulation/corrections and modernization. The frequency and scope of work of these types is mainly based on the results of reliability tests, which corresponds to defining and fulfilling the predetermined norms.

Summary

The development of taxonomic models for the assessment of the exploitation policy allows for conducting the exploitation analyzes in atypical organizational and technical conditions, such as object-oriented machine servicing. In addition to classic analyses and interpretations related to the current time moment, there can be important indications, which are ahead of the current moment. Four concepts are possible and practically justified, in particular:

- linear analysis of the exploitation policy based on developed patterns,
- mutual comparative analysis of the exploitation policy of two or more maintenance organizations with similar business specificity,
- comparative analysis of the exploitation policy of the maintenance organization, carried out in relation to different time periods,
- simulation analysis of the exploitation policy, based on the controlled change in the value of selected features and weights.

From the concepts mentioned above, the first two are static in nature, referring to a specific moment of time, and in this approach they are the subject of interest in the current assessment of the exploitation policy. However, the other two concepts, due to the large time variability, can be used to assess the way and scope of functioning of the maintenance organization in dynamic changes in the environment, both in relation past features - current features, and in relation to the planned, considered or simulated conditions and specificity of the exploitation policy.

References

[1] Antosz K. 2018. Maintenance – identification and analysis of the competency gap. Eksploatacja i niezawodność – Maintenance and Reliability 20(3): 484–49.

[2] Gola A. 2019. Reliability analysis of reconfigurable manufacturing system structures using computer simulation methods. Eksploatacja i Niezawodność – Maintenance and Reliability 21(1): 90–10.

[3] Hellwig Z. 1968. Zastosowanie metody taksonomicznej do typologicznego podziału krajów ze względu na poziom ich rozwoju oraz zasoby i strukturę wykwalifikowanych kadr. Przegląd Statystyczny (4): 307-327.

[4] Jasiulewicz-Kaczmarek M., Wyczółkowski R., Gładysiak V. 2017. Modeling a hierarchical structure of factors influencing exploitation policy for water distribution systems using ISM approach. IOP Conference Series-Materials Science and Engineering, Volume 282, Article Number: UNSP 012014.

[5] Konieczny J. 1975. Sterowanie eksploatacją urządzeń. Warszawa: PWN.

[6] Kozłowski E., Mazurkiewicz D., Żabiński T., Prucnal S., Sęp J. 2019. Assessment model of cutting tool condition for real-time supervision system. Eksploatacja i niezawodność – Maintenance and reliability 21(4): 679–685.

[7] Loska A. 2017. Scenario modeling exploitation decision-making process in technical network systems. Eksploatacja i Niezawodność – Maintenance and Reliability 19(2): 268–278.

[8] Loska A., Paszkowski W. 2018. SmartMaintenance - The Concept of Supporting the Exploitation Decision-Making Process in the Selected Technical Network System. In: Advances in Intelligent Systems and Computing, 54-63. Cham: Springer.

[9] Młodak A. 2006. Analiza taksonomiczna w statystyce regionalnej. Warszawa: Wydawnictwo Difin.

[10] Niebel W.B. 1994. Engineering Maintenance Management. Second edition. New York: Marcel Dekker Inc.

[11] Timofiejczuk A., Brodny J., Loska A. 2018. Exploitation policy in the aspect of Industry 4.0 concept - overview of selected research. XV International Conference Multidisciplinary Aspects of Production Engineering MAPE2018 1(1): 353-359.

[12] Żółtowski B., Niziński S. 2010. Modelowanie procesów eksploatacji. Radom: Wydawnictwo Naukowe Instytutu Technologii Eksploatacji - PIB.

PhD Eng. Andrzej Loska, Assoc. Prof.
Silesian University of Technology
Faculty of Organisation and Management
ul. Roosevelta 26-28, 41-800 Zabrze, Poland
e-mail: Andrzej.Loska@polsl.pl

ROBOTIZATION OF THE PROCESS OF REMOVAL OF THE GATING SYSTEM IN AN ENTERPRISE FROM THE AUTOMOTIVE INDUSTRY

Robotyzacja procesu usuwania układów wlewowych w przedsiębiorstwie z branży motoryzacyjnej

Magdalena BUCIOR ORCID: 0000-0002-1081-5065
Rafał KLUZ ORCID: 0000-0001-6745-294X
Andrzej KUBIT ORCID: 0000-0002-6179-5359

DOI: 10.15199/160.2020.1.2

Abstract: Cleaning and removal of components of the gating system, and finishing of castings are the most labor-consuming and damaging to health foundry processes. This paper presents the results of an analysis of labor consumption of the process of removal of gating systems of aluminium castings, which were carried out in a conventional manner using a band saw and a boring machine, and using an industrial robot. In the final part of this paper the analysis of occupational hazard of work-stands is presented. It has been shown that the use of robotization leads to an increase both the productivity of the process and work safety. The use of an industrial robot allows to reduce the labor consumption of the process of removal of gating systems by 29,5% in relation to the non-robotized stand. Furthermore, on the robotized stand almost all the time needed for the process of removal of the gating system is connected with the machining. It represents 98.7% of the production cycle. In the case of non-robotized stand, the machining takes 79% of the total time required for treatment of one piece of the casting.
Keyword: automation and robotics in foundry, product development, removal of gating systems, work safety

Streszczenie: Oczyszczanie, usuwanie elementów układu wlewowego oraz wykańczanie odlewów należą do najbardziej pracochłonnych, szkodliwych dla zdrowia oraz niebezpiecznych procesów odlewniczych. W pracy przedstawiono analizę pracochłonności procesu usuwania układów wlewowych odlewów aluminiowych, realizowanego w sposób konwencjonalny z zastosowaniem pilarki taśmowej i wytaczarki oraz z zastosowaniem robota przemysłowego. W końcowej części pracy dokonano analizy ryzyka zawodowego stanowisk pracy i wykazano, że wprowadzenie robotyzacji procesu prowadzi do zwiększenia jego wydajności oraz bezpieczeństwa pracy. Zastosowanie robota przemysłowego umożliwia zmniejszenie pracochłonności procesu usuwania układów wlewowych o 29,5% w stosunku do stanowiska niezrobotyzowanego. Na stanowisku zrobotyzowanym, niemalże cały czas potrzebny na realizację procesu usuwania układu wlewowego jest poświęcony na obróbkę właściwą. Stanowi ona 91% cyklu produkcyjnego. W przypadku stanowiska niezrobotyzowanego, obróbka właściwa zajmuje 80% całego czasu potrzebnego na obrobienie jednej sztuki odlewu.
Słowa kluczowe: automatyzacja i robotyzacja w odlewnictwie, projektowanie wyrobów, usuwanie układów wlewowych, bezpieczeństwo pracy

Introduction

Modern industrial robots are very universal. They have been successfully used in such different areas as welding, painting, assembly and casting. The market of industrial robots in Poland and in the world is continuously growing, and the number of robots in production plants is systematically increasing. However, an increase in the use of industrial robots is influenced by a number of advantages, such as its high efficiency, ensuring repeatability of processes, the ability to work in hazardous environments, operating with heavy loads, optimal use of workspace. Furthermore, robots have a number of safeguards to protect the health and life of employees. Due to these advantages, the production plant can increase the variety and quality of manufactured products, and thus it becomes more competitive on the market [1]. The effect of the use of robots in casting processes is an increase of productivity and reduction of the number of defective castings, and reduction of the cost of the product by increasing efficiency [3, 5].

Robots are used both in the pressure die-casting and gravity casting. The use of robots most often is limited to [2, 4, 6, 8, 9]:

- applying of separating medium on the surface of mould joints,
- pouring the pressure casting dies,
- removing the solidified castings from the pressure casting die,
- cooling the castings by immersing them in a cooling tank,
- transfer of the casting from the cooling tank to the automatic edging stand,

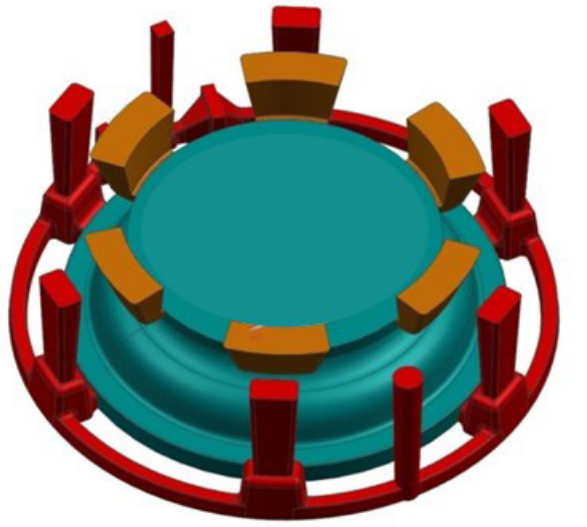

Fig. 1. The casting with the elements of the gating system

– removal of the gating system,
– location of steel inserts inside the pressure casting die,
– inspection of castings dimensions.

Cleaning, removal of components of the gating system and the finishing of castings are the most labour-consuming, harmful and dangerous foundry processes [7]. Estimated duration of cleaning and finishing of casting is from 20 to 50% of the total labour consumption of their manufacturing. Despite the large mechanization, the share of manual work during cleaning, removal of elements of the gating system and finishing of castings is very high and it ranges from 40 to 90%.

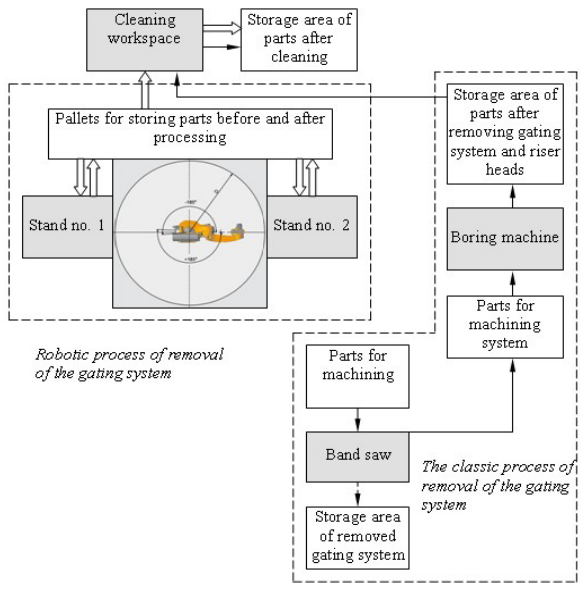

Fig. 2. Scheme of the arrangement of the stands

Despite the existence of beneficial conditions associated with the use of robots in the process of removal of gating systems, many entrepreneurs believe that robotization of their company will not be profitable. As a result, entrepreneur does not see the need to install industrial robots and manipulators in their plants. Therefore, the aim of this paper is to compare the labour consumption and work safety of the process of removal of gating systems realized in the conventional manner using a band saw and boring machines, and by using industrial robots. The obtained results can underlie the decision about robotization of analyzed process.

Analysis of labour consumption

The subject-matter of the analysis was the process of removal of the gating system and process of cleaning of AC-47100 aluminum alloy casting (Fig. 1).

In the process of removing the gating system realized in a conventional manner with the casting with the gating system and riser head is transported from the part store using the foundry crane to the band saw. The removing process is carried out manually. Therefore, the accuracy of the process realization depends on an employee who manipulates cast attached to the foundry crane.

Next the casting with the removed gating system is pushed by using a crane on a manual hand track, which is transported by an employee operating the saw band on the boring machine stand. The distance between the band saw and the boring machine was approximately 30 meters. The casting is clamped by an employee on the boring machine using the foundry crane. On the boring machine the remaining riser heads are removed and one of the flanges is roughened. After that, the casting was transported by the crane to the cleaning stand, where it was subjected to abrasive blasting.

The schematic arrangement of the stands in the present process is shown in Fig. 2. In the case of robotization process, the removal of elements of the gating system (except cleaning) is carried out by using an industrial robot KUKA. The industrial robot KUKA KR 120 R2500 PRO shown in Fig. 3 (workspace graphics) and Fig. 4 (with a mounted circular saw), is an industrial robot with a compact design, high rigidity and high power. It is resistant to high temperatures and impurities. In order to ensure the efficient realization of the process of gating system removal, the robot is equipped with twelve-positional store of tools. Basic technical specifications of the robot are given in Table 1.

In the robotized process of removing the casting gating system, the casting is transported with the foundry crane into the robot's workspace. Then the casting is secured by the employee in the three-jaw chuck located

Table 1. Technical specification of KUKA KR 150 R2700-2 robot

Weight (excluding controller)	1072 kg
Rated payload	150 kg
Maximum reach	2701 mm
Number of axes	6
Positioning repeatability	±0.05 mm
Temperature during operation	+10ºC to +55ºC

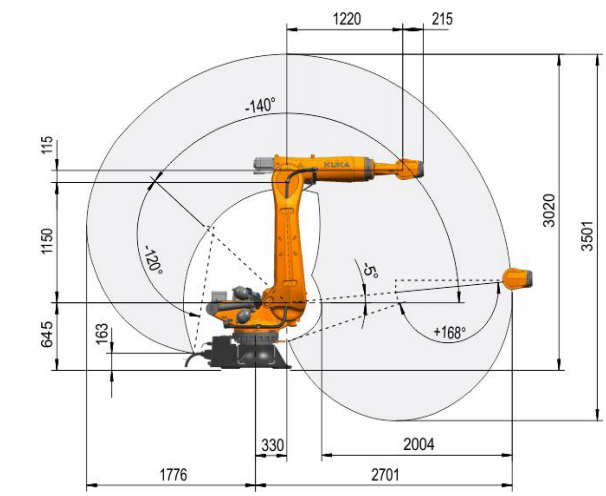

Fig. 3. Workspace graphic

Fig. 4. Industrial robot KUKA KR 150 R2700-2

on the turntable. The following operations are realized on the robotized position:

– removing the gating system using a saw blade with a diameter of Ø 250 mm (Fig. 5),
– cutting off of riser heads with a saw blade Ø 120 mm,
– planning of the flange surface using a faze milling cutter in order to reduce the labor consumption of the process of casting cleaning.

Fig. 5. Cutting off of the gating system by a robot

In order to compare the labour consumption of the process of removing the gating system realized in a conventional manner and using a robot, the chronometrial investigations that involve the measurement of the duration of all operations were carried out within the processes. The measurement was repeated three times, and then the average value of the obtained results was determined. Test results were presented in Tables 2 and 3.

The results of investigations showed that the duration of machining of the casting in the case of robotized stand (40 min 50 s) takes about 1013 seconds (16.88 minutes) shorter than machining without the use of an industrial robot (57 min 13 sec). Assuming that the working shift in the production plant takes 27 000 seconds (7.5 hours - minus 30 minutes break), the plant with the help of an industrial robot can produce 3 casts more per working shift. Assuming a two-shift work per month the usage of robot can increase productivity by 29,5%.

On the robotized stand almost all the time needed for the process of removal of the gating system is connected with the machining. It represents 91% of the production cycle (Fig. 6a). In the case of non-robotized stand, machining takes 80% of the total time required for finishing of one piece of castings. The remaining 20% of the time involved such operations as transport, clamping and unclamping of the casting (Fig. 6b). The use of the robot to process the removal of gating systems allowed a significant reduction in the length of transport paths (Fig. 2) and reducing the handling steps. The time wasted on transport and manipulation was reduced by 58.1%.

Due to the use of an industrial robot, the times of operations such as transport and casting clamping do not extend the casting transition time through the production process. This is because the industrial robot has two workspaces. When the industrial robot is working, the employee has time to prepare the next part for processing in the second workspace. This additionally shortens the production cycle (by 6.8%). Due to the high repeatability of the robot, the surface after the cut off elements of the

Table 2. Removal of the gating system without the help of a robot

Action	Description	Tool	Tavg [s]
1	Casting transport	gantry	52
2	Cutting the gating system	gantry, band sawing machine	514
3	Putting the parts on the trolley	gantry, hand truck	20
4	Cut of the gating system remaining on the band sawing machine	band sawing machine	32
5	Transport to the boring machine	hand truck	141
6	Clamping of the casting	gantry	146
7	Boring	boring machine	753
8	Unclamping of the casting	keys	111
9	Transport to the work-in-progress store	gantry	43
10	Transport of the casting to the cleaning station	gantry	31
11	Casting cleaning	cleaning tools	1 560
12	Transport to the store	gantry	30
			3 433

Table 3. Removal of the gating system using a robot

Action	Description	Tool	Tavg [s]
1	Clamping of the casting	gantry	105
2	Cutting the gating system	industrial robot	416
3	Cutting the feeder	industrial robot	509
4	Milling	industrial robot	315
5	Unclamping of the casting and transport to the work-in-progress store	gantry	76
6	Transport of the casting to the cleaning station	gantry	29
7	Casting cleaning	cleaning tools	1 180
8	Transport to the store	gantry	30
			2 660

gating system is processed more accurately, which allows reducing casting cleaning time by 23.9%.

In the case of machining of the casting without the help of an industrial robot, the setup time (Tpz) and the time necessary for waiting for the foundry crane, which supports several workstations should also be taken into account. The setup time Tpz is the time which occurs when the production plant changes the type of the produced casting. If necessary it is a need to adjust the milling fixture to the new casting. It takes about 420 seconds (7 minutes), which significantly increases the time of the casting flow in the production cycle. In the case of the foundry crane the situation is similar. The foundry crane that operates a few neighbouring workstations can be busy at the given time and the employee must wait to use it. In this case the expected time is in the range of 30 - 240 seconds, what also increases the production cycle. In the case of processing the position of robotic casting, preparation time is virtually unnoticeable, because it takes a few seconds. If it is necessary to process another type of casting, the employee approaches the control panel and selects the appropriate, previously written machining program. For this position, the employee must also wait

Fig. 6. The percentage share of duration of processing on the non-robotized (a) and robotized (b) workstand

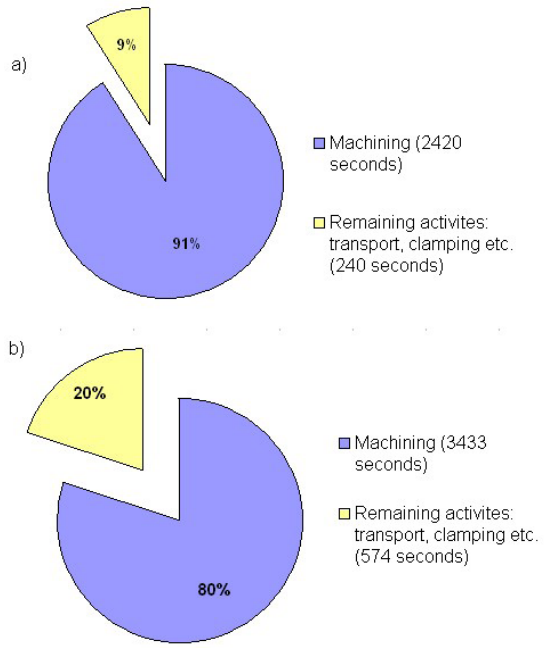

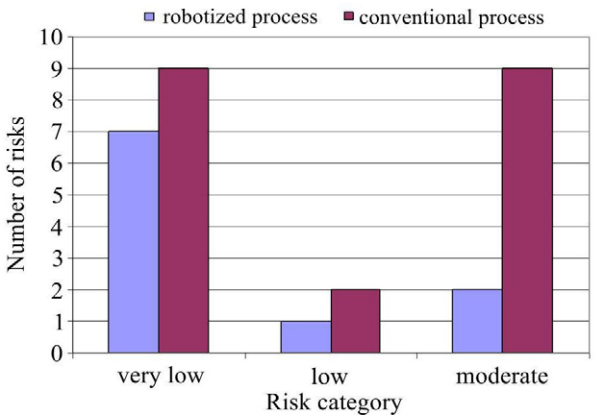

Fig. 7. Types of hazards and their categorization in the process of removing the gating systems

for the gantry to be released, but the industrial robot has two work stations, which allows the employee to perform all auxiliary activities during his work.

Analysis of work safety

When removing elements of the gating system on the non-robotized workstation a number of safeguards located on the machines are used. The main safeguards are warning signs, safety switches or protective casings. However, the safeguards may not be sufficient, because the moment while employee is careless can lead to an accident. The employee that works on a workstation or a random person in the vicinity of the workstation can be injured.

Removing elements of the gating system on the robotized workstation leads to avoiding dangerous situations that occur during its cutting using the saw band or boring machine. However, using an industrial robot we cannot eliminate the possibility of an accident, but its probability is much smaller. To estimate the occupational hazard of workstations the Risk Score indicator method is used.

The assessment of occupational hazard "R" is determined by multiplying three parameters:

$$R = SEP \tag{1}$$

where: S - potential effects of the event,
E - exposure to risk,
P - probability of risk occurrence.

After determination of the R indicator, the results should be interpreted according to Table 4, which contains the degree of occupational hazard in a given workstation and indicates when the appropriate actions should be taken to reduce the risk.

Conducted risk assessment has shown that the use of the industrial robot in the process of removing the gating systems significantly reduces not only the number of types of hazards, but also reduces the risk category (Fig. 7).

In the conventional process, 20 different types of hazards were identified, and 45% of which represent hazards with a moderate risk (70≤R <200). These risks need to take additional actions to increase the occupational safety. Robotization of the process enabled a reduction of 77% of risks characterized by a moderate level of risk. Most of them were shifted to the range in which the value of risk is low (20≤R <70) or very low (R <20). Therefore, it enabled an increase of the level of occupational safety.

Conclusions

The investigations of labour consumption of removal of gating systems of aluminum castings showed that the use of an industrial robot leads to reduction of the labor consumption of the process by 29,5%. In the case of the conventional method of removing the gating systems it should be noted that the transport routes are much longer, and the process required a larger number of workstations.

Table 4. Results of evaluation of occupational hazard using R indicator

R-value	Risk category	Necessary actions	Risk assessment
R<20	Very low	Advisable inspection	Acceptable
20≤R<70	Low	Necessary inspection	Acceptable
70≤R<200	Moderate	Necessary improvement	Tolerated
200≤R<400	High	Necessary immediate improvement	Untolerated
R≥400	Very high	Advisable work stoppage	Untolerated

Additionally, the waiting time for a foundry crane is not constant and employees often need to stop work to wait for the crane. Such stop affects process capability and leads to a significant extension of the duration of casting processing. Robotized stands occupy less space on the production hall, allow shortening the processing time, the time lost in transport and manipulation (about 57%) improve occupational safety and increase the accuracy and repeatability of casting process. The usage of robots in the production plant causes that manufacturer is more flexible to new market requirements.

References

[1] Brogardh T. 2007. „Present and future robot control development — An industrial perspective". Annual Reviews in Control 31(1): 69-79. DOI: 10.1016/j.arcontrol.2007.01.002.

[2] Brussel H.V., Persoons W. 1996. „Robotic deburring of small series of castings". CIRP Ann.-Manuf. Techn. 45(1): 405-410. DOI: 10.1016/S0007-8506(07)63091-1.

[3] Campbell J. 2015. Properties of castings. In J. Campbell (Ed.), Complete casting handbook (2nd ed.). Waltham, MA: Butterworth-Heinemann.

[4] Jaworski J., Kluz R., Trzepieciński T. 2014. „Investigation of stability of fabrication system of casting parts". Arch. Foundry Eng. 14(1): 5-8.

[5] Kluz R. 2012. „Analysis of the repeatability positioning of the assembly robot". Arch. Mech. Techn. Autom. 32(3): 59-68.

[6] Kosler H., Pavlovčič U., Jezeršek M., Možina J. 2016. „Adaptive robotic deburring of die-cast parts with position and orientation measurements using a 3D laser-triangulation sensor". Stroj. Vestn.-J. Mech. Eng. 62(4): 207-212. DOI: 10.5545/sv-jme.2015.3227.

[7] Stefanescu D.M. 2015. Science and Engineering of Casting Solidification. (3rd ed.). Heidelberg: Springer.

[8] Syrcos G.P. 2003. „Die casting process optimization using Taguchi methods". J. Mat. Proc. Technol. 135(1): 68-74. DOI: 10.1016/S0924-0136(02)01036-1.

[9] Trebuna P., Pakarcikowa M., Kronova J. 2018. „Automation of the casting process by the use of simulation software". Management and Production Engineering Review 9(1): 82-89.

Dr. inż. Magdalena Bucior
Rzeszow University of Technology, Department of Manufacturing and Production Engineering
e-mail: magdabucior@prz.edu.pl

Dr. inż. Rafał Kluz
Rzeszow University of Technology , Department of Manufacturing and Production Engineering
e-mail: rkktmiop@prz.edu.pl

Dr inż. Andrzej Kubit
Rzeszow University of Technology , Department of Manufacturing and Production Engineering
e-mail: akubit@prz.edu.pl

Zapraszamy Autorów do współpracy!
www.sigma-not.pl
tiam@sigma-not.pl

ELECTRIC CAR CRASHENERGY ABSORBING STRUCTURE

Struktura pochłaniająca energię zderzenia dla samochodów elektrycznych

Mirosław CHŁOSTA ORCID: 0000-0002-4921-6908
Andrzej BARSZCZ ORCID: 0000-0002-2979-0734

DOI: 10.15199/160.2020.1.3

Abstract: Most of the current electric cars are derived from recreational vehicles; hence, there is a necessity to develop passive safety systems that meet the current traffic requirements. This paper presents passive safety issues and the results of the real model studies.
Keywords: Electric car, safety zones, protecting structures, passive safety, FEM simulation

Streszczenie: Większość użytkowych samochodów elektrycznych produkowanych obecnie w Polsce wywodzi się z elektrycznych pojazdów rekreacyjnych. Stąd konieczność dostosowania ich konstrukcji nośnych do wymagań bezpieczeństwa stawianych pojazdom drogowym. W artykule przedstawiono wymagania prawne w tym zakresie oraz wyniki badań nad obiektami rzeczywistymi.
Słowa kluczowe: pojazd elektryczny, konstrukcje ochronne, strefy bezpieczeństwa, bezpieczeństwo bierne, obliczenia wytrzymałościowe

Introduction

The car's body structure depends on many factors; it is a truism, but having far-reaching implications for electro-mobility programs in Poland. The question arises whether and in what scale the Polish electric car will be produced. This issue is crucial in a view of the necessity to adopt a proper technology, adequate to the economic aspect of the investment and, at the same time, optimum due to the vehicle manufacturing and maintenance. Protection, and in particular, the degree of passive safety that a modern car must provide should play the key role, irrespectively of the adopted technology. It is the main reason that the authors focused on the passive safety structures' parts of the e-cars.

Active safety is another problem which is solved by mechatronic systems. Advanced Driver Assistance Systems (ADAS) are electronic systems that aid a vehicle driver. Designed with a human-machine interface, they are intended to increase car safety and more generally road safety by avoiding collisions. ADAS relies on inputs from multiple data sources, including automotive imaging, LiDAR, radar, image processing, computer vision, and in-car networking. The additional inputs are possible from other sources separate from the primary vehicle platform, such as other vehicles, referred to as Vehicle-to-vehicle (V2V), or Vehicle-to-Infrastructure (V2X), such as mobile telephony or WiFi data network systems. The advanced driver-assistance systems are one of the fastest-growing segments in automotive electronics with steadily increasing rates of adoption of industry-wide quality standards, in vehicular safety systems, developing technology specific standards, such as IEEE 2020 for Image Sensor quality and communications protocols such as the Vehicle Information API. Next-generation ADAS will increasingly leverage wireless network connectivity to offer improved value by using car-to-car (also known as Vehicle to Vehicle, or V2V) and car-to-infrastructure (also known as Vehicle to Infrastructure, or V2X) data.

State of art in Poland

At the present moment, there is no big native car manufacturer in Poland. With regards to the government promoted projects, it is a big opportunity to initiate the car electric drive and control production. This is a huge challenge for the Polish industry due to its current technologies and funds. For example, it is not possible to start-up the modern car platform manufacturing with the deep stamping technology without the billions € investments. On the other side, there is no opportunity to acquire the main e-cars parts made by worldwide manufacturers, due to share a big development cost.

The usage of the modern modular frames, design for the system platforms, is their alternative. The tailored tubes, with the different material characteristic, are commonly used in the modern frame e-car bodies (Fig. 1).

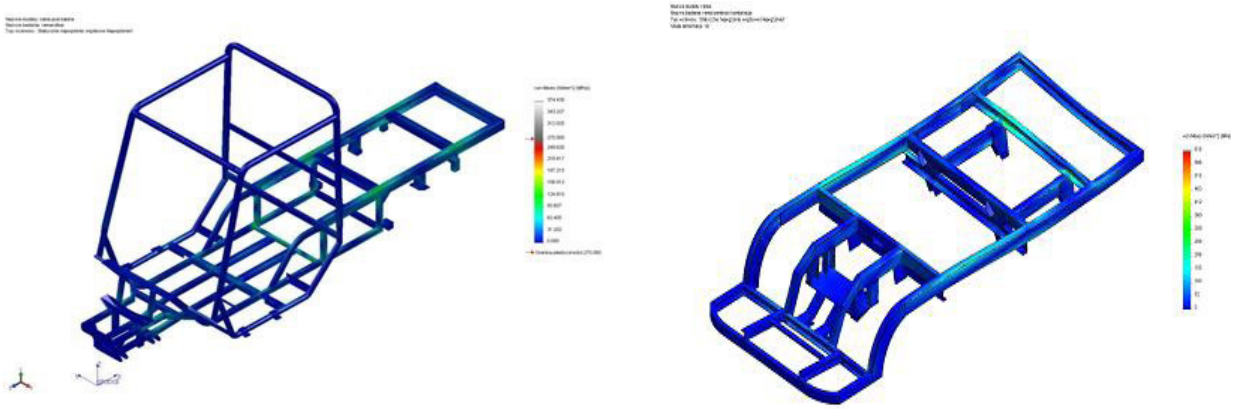

Fig.1. Body structures of the e-car manufactured in Poland

Fig. 2. Modern LEV manufactured in Poland

Fig.3. Crash accident with LEV participation (USA)

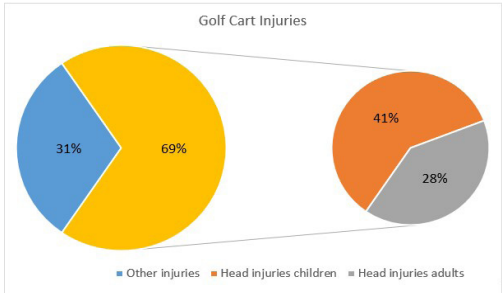

Fig. 4. The main injuries as the effects of accidents with LEV

It should be therefore assumed that it will be a Polish e-car body structure, because the manufacturing technology is well-known in the SMEs.

Nowadays, there are two companies, manufacturing varying-purpose electric vehicles in Poland.

MELEX S.A, with the headquarters situated in Mielec, has the most abundant offer. The industrial electric vehicles for utilization in the industrial areas as well as those ones for typical road traffic are produced. PW BARTESKO Koźmin Wielkopolski focuses mainly on industrial applications but also produces different vehicles intended for urban application (Fig. 2). Although their common usage is relatively rare now, the number of the applications is expected to be increased, especially in relation to the “last mile” delivery vehicles idea spreading out in Europe.

So, the question is: what is the level of passive safety offered by the current constructions and their possible directions of development.

The available information suggests that the introduction the recreational origin vehicles to the road traffic results in a significant increase of the passenger danger in the case of an accident (Fig. 3, 4).

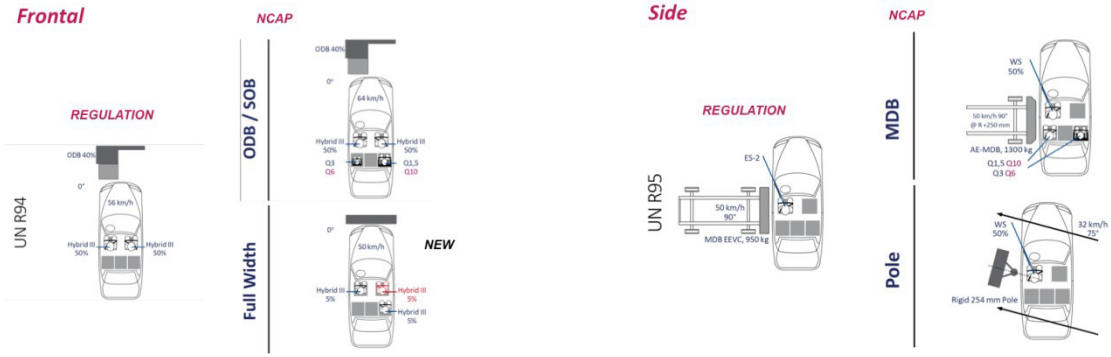

Fig. 5. ECE-R94, 95 and E-NCAP requirements at frontal and side impact of the car

Passive safety requirements

The requirements for passive protection are several dozen – all of them are classified in the relevant approval documents and regulations. These are mainly EURO NCAP requirements and UN/ECE protocol requirements and approval regulations. However, it must be pointed out that these requirements are very limited, in the case of vehicles located in category N1 and lower (Fig. 5).

Due to the continuous development of manufacturing processes, as well as changes in the technical consciousness of the recipients, the mentioned requirements are undergoing modifications. A new directive that imposes the commercial vehicles and trucks manufacturers the necessity of a new type of the energy-absorbing crumple zones that increase drivers' safety during the crash accident.

In the modern solutions, a big attention is also paid to the protection of the pedestrian as a frequent participant of the accidents.

Research work undertaken

Passenger cars passive safety has been one of the main goals for automotive corporations – with protective structures currently being mainly under the requirements of the European and US testing rules for the passenger cars. In this area, each of the automotive corporations has conducted many studies, but they relate to the modern superstructures based on the modern modular floorboards and self-supporting structures. However, there is no information available on the scope of activities relating to LEV with frame structures.

The studies of protection systems mainly in the field of military vehicles, due to meet the different, non-civilian, requirements, were carried out in Poland. The vast majority of self-supporting bodyshell structures are therefore considered and the results of the frame support structures relate to a very narrow group of military cars and elite sports cars.

IMBiGS Protective structure for the frame structure car

During the years 2013 – 2016, Institute of Mechanization of Construction and Rock Mining (IMBiGS) participated in the PLUS-MOBY international project on the development of electric car. The challenge has been undertaken to ensure the proper passive protection for the driver and passengers. As a result of the research work, a framework structure has been developed, which incorporates solutions to meet the current requirements (Fig. 6).

In the successive years, IMBiGS has undertaken its own work on the development of a protective structure for commercial electric vehicles with a GVWR of up to 3.5 tones. Protective structure computer models, including a bumper and shock absorbent assemblies, have been

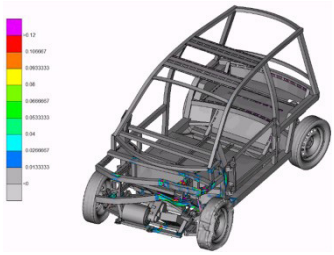

Fig. 6. Results of the PLUS-MOBY car safety zones simulations (courtesy of consortium)

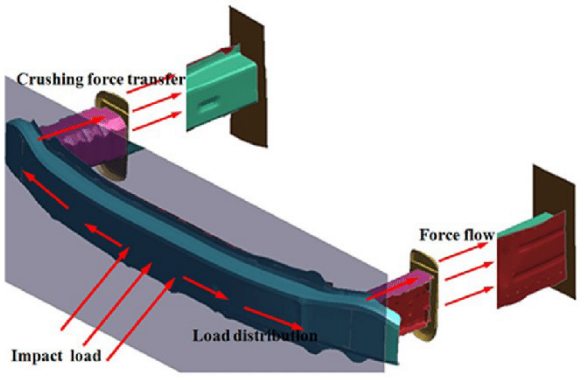

Fig. 7. Force distribution in the passive safety car's part

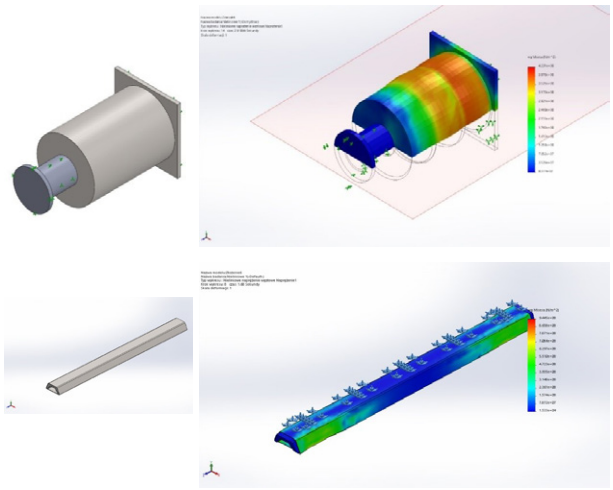

Fig. 8. Crash-box elements design in IMBiGS

Fig. 9. IMBiGS bumper with crash-box for LEV

Fig. 10. Bumper test preparation on the test bed

developed as the results of this work. It was based on the US pick-up cars, which are largely built on frame chassis and partly modeled on the solutions used in the rail industry (Fig. 7, 8).

The main project assumption was to provide multiple actions in low loads conditions following relatively long periods of time, contrary to the protective parts used in the automotive industry. This was achieved by applying of the appropriately shaped rod movable relative to the external element running with the elastomer plies.

Protective structure testing in IMBiGS

The developed bumper design with shock absorbent units was subjected to impact resistance test with defined energy value (Fig. 9). The applied test was the same test object used in the FOPS (Falling Object Protective Structure) test procedure (Fig. 10). Three main test cycles were carried out: the central point impact and side, near the absorbing energy unit, impact (Fig. 11, 12).

The conclusions of the test results show that the designed protective unit behaves as expected. The inner element moves in and the elastomers were compressed at the first phase of impact. In the second phase, the main parts work and the destruction of metal structures began. Values of the real and FEM calculated deformation are very similar (Fig. 13).

The deformation concerned both the internal and the external element of the "crashbox" (Fig. 14).

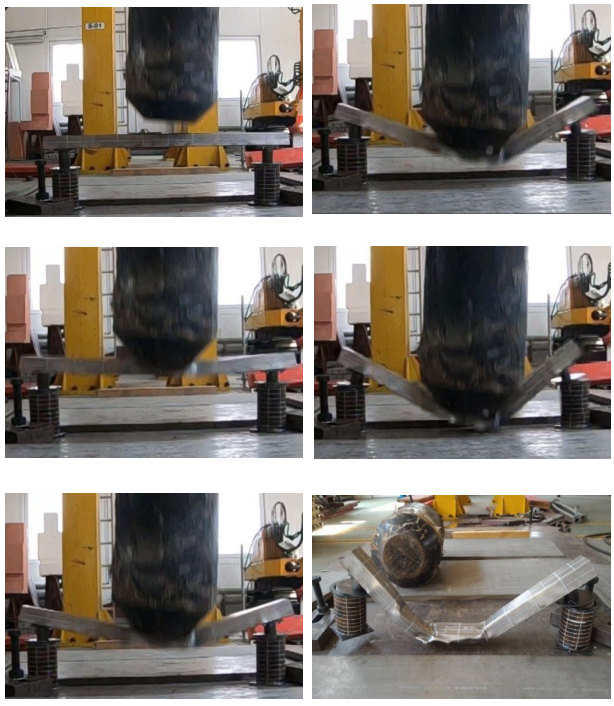

Fig. 11. Bumper with crash-boxes frame-by-frame shots – center point test.

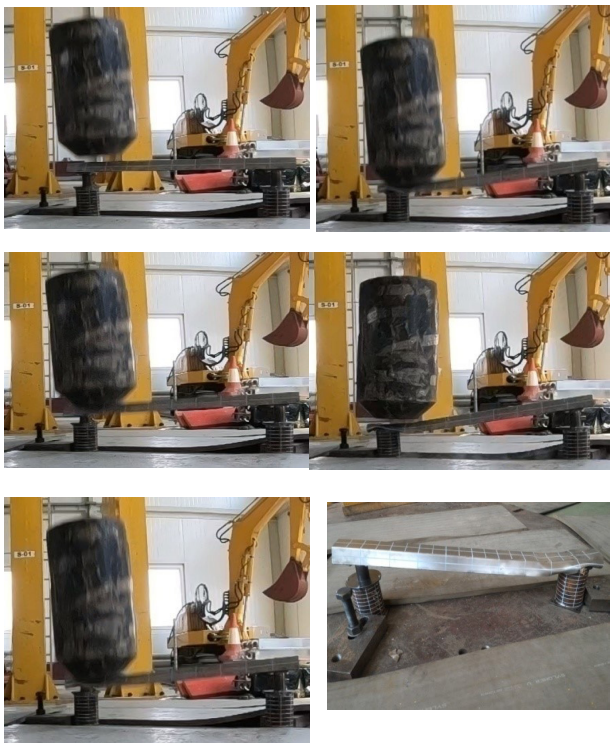

Fig. 12. Bumper with crash-boxes frame-by-frame shots – 25% side movement test.

Fig. 13. Passive safety assembly with crash box–FEM simulation and site test results comparison

Fig. 14. Car beam with crashboxes – automotive manufacturing example

Fig. 15. Crash box elements – before and after the impact test. Modification #1

Fig. 16. Crash box elements – modification #2

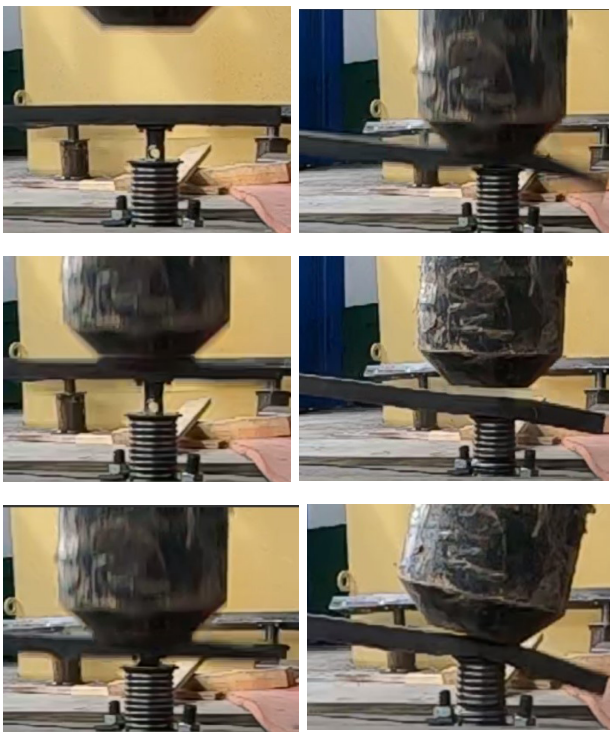

Fig. 17. Bumper with modified crash boxes – frame-by-frame impact test shots.

The design bumper bar was deformed as modeled the deflections, and the entire structure was finally behaved in a similar way of the protective structures used in the automotive industry. The analysis found, however, that the strength of the structure was too high, and the visual inspection and deformation measurements allowed determining the potential section weakening zones. The changes were already introduced at the third stage of the research model.

The modifications included the weakening of the external body's strength by milling grooves with a depth of 1.5 mm and a width of 6 mm at distances of 11 mm from each other, with the unchanged interior elements (for one component - marked "I M") and the addition with the holes in the internal element (for the second component, the marked "M II"). The real object tests have been performed after the modifications (Fig. 15, 16, 17).

Designed in IMBiGS the modification in the form of alternately arranged holes made the near axial element's deformation. The total length of the element after impact was 58 mm to the bottom surface of the backing plate, versus 126 mm before the impact (Fig. 17 – 20)).

The test carried out allowed setting up the following hypothesis concerning the mechanism of destruction:

Fig. 18. Modified crash box elements deformation after the impact test

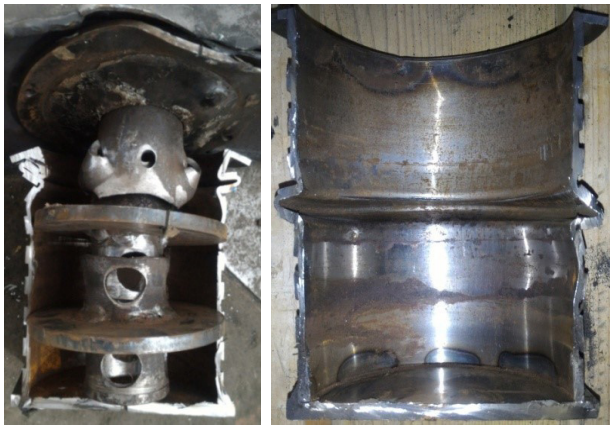

Fig. 19. Modified crash box elements deformation after the impact test (next)

Fig. 20. Comparison of the modified crash box elements before and after the impact test

1. In the first phase of the impact, the inner element is pushed into the outer body of the crashbox components, while the elastomer shock absorbers of section I and section II are crushed. The internal subassemblies clearances are erased at the same time.
2. When the resistance of the spacers is reached, the deflection of the bumper beam begins. It leads to the inner element and guide sleeve deformation and next to the crashbox body component deformation.
3. Deformation of the inner element is significant and mainly concentrated in the upper part, adjacent to the bumper beam. The outer diameter of the piston tube increase with an initial value of ϕ = 44 mm to the end value ϕ = 46 mm on the entire length and ϕ = 60 mm at the shortening the length of the active part by 48 mm – the initial value h_1 = 115 mm to h_2 = 67 mm.
4. At the same time there was a deformation of the inner sleeve in the upper part, integrated with the damping piston. These strains are symmetrical and gradual changing on the sleeve tube diameter and its shortening. Longitudinal deformation amounted to 2 mm and a diameter change of 5 mm – from the initial ϕ = 44 mm to the end value ϕ = 49 mm.
5. In this case, the deformation of the body is irregular and includes a breakdown in its upper part, leading to a shortening of the active height from h_1 = 149 mm to h_2 = 138 mm, the change by 11 mm.

Conclusions

1. The results obtained through impact tests of the real protective structure showed a significant compliance with the expectations for correlation with the computational method (FEM). The deformation of the external and the internal components are in match with the initial assumptions adopted at the preliminary stage. It should be noted that there is a satisfactory accuracy of the location of the largest deformation locations. Studies have shown that

it is possible to obtain a controlled deformation of crashbox assemblies by using commercially available materials.

2. Functional optimization of the developed components is possible through the CAD models calculation, allowing the most favorable mechanism of destruction of the structure. The real models that optimize the construction of the crashbox components have shown that by their proper shaping, they can lead to a controlled and repetitive deformation of the components.
3. The characteristics of the deformation elements can be developed by appropriately shaping the sections of the metal elements and the selection of a structure dedicated to the total weight of the vehicle in the range to GVWR (max) of 3.5 tones.

References

[1] ECE standards and regulations: FMVSS 216 (USA), (Roof strength), FMVSS 301 (USA) (Rear impact)

[2] Ibrahim, H. K. 2009. Design optimization of vehicle structures for crashworthiness improvement. Department of Mechanical and Industrial Engineering, Concordia University.

[3] Khattab, A., El Rahman A. 2011. Investigation of an adaptable crash energy management system to enhance vehicle crashworthiness. Doctoral dissertation, Concordia University.

[4] Koora, R., Suman R., S. A. P. 2014.“Quadri Design Optimization of Crush Beams of SUV Chassis for Crashworthiness”. International Journal of Science and Research (IJSR): 327–332.

[5] Kopczyński A., Rusiński E. 2010. Bezpieczeństwo bierne. Pochłanianie energii przez profile cienkościenne. Wrocław: Oficyna Wydawnicza Politechniki Wrocławskiej.

[6] PLUS-MOBY. Project papers.

[7] UE directives: 96/27/EC, 98/79/EC, ECE R 32 (Collision Structure Performance - Rear-end.), ECE R 33 (Uderzenie czołowe w sztywną barierę), ECE R 42 (Zderzaki), ECE R 94 (Offset frontal impact), ECE R 95 (Occupant Protection in Lateral Collisions),

[8] https://en.wikipedia.org/wiki/Advanced_driver-assistance_systems - cite_note-6 (2.12.2019)

[9] http://web.iitd.ac.in/~achawla/public_html/736/7-Design_of_Vehicle_Structures_for_crash_energy_management_v6.pdf (2.12.2019)

Mgr inż. Andrzej Barszcz
Sieć Badawcza Łukasiewicz – Instytut Mechanizacji Budownictwa i Górnictwa Skalnego; Racjonalizacji 6/8, 02-673 Warszawa, e-mail: a.barszcz@imbigs.pl

Dr inż. Mirosław Chłosta
Sieć Badawcza Łukasiewicz - Instytut Mechanizacji Budownictwa i Górnictwa Skalnego;
e-mail: m.chlosta@imbigs.pl

PORTAL INFORMACJI TECHNICZNEJ
WIRTUALNA CZYTELNIA
DOSTĘP DO PRASY FACHOWEJ W KAŻDEJ CHWILI
www.sigma-not.pl

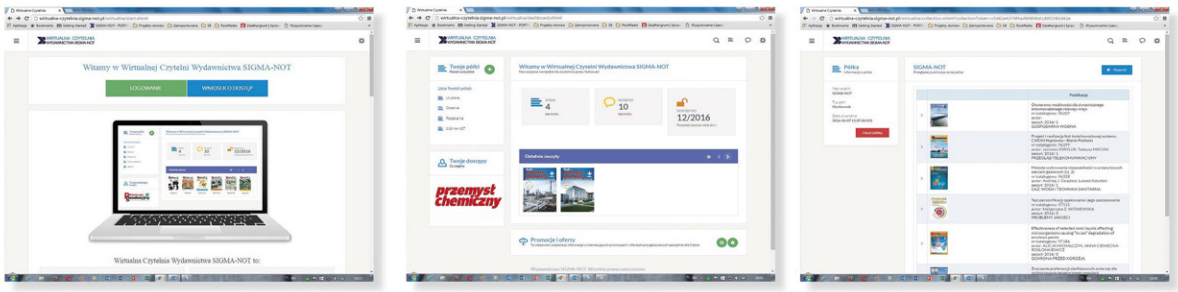

więcej informacji: 22 840 30 86, prenumerata@sigma-not.pl
22 827 43 65, reklama@sigma-not.pl
WYDAWNICTWO SIGMA-NOT

APPLICATION OF SELECTED BALANCING METHODS FOR ANALYSIS AND EVALUATION OF THE WORKING EFFICIENCY OF THE ASSEMBLY LINE ON THE EXAMPLE OF A SELECTED PRODUCT

Zastosowanie wybranych metod balansowania do analizy i oceny wydajności pracy linii montażowej na przykładzie wybranego produktu

Katarzyna ANTOSZ ORCID: 0000-0001-6048-5220
Rafał KLUZ ORCID: 0000-0001-6745-294X

DOI: 10.15199/160.2020.1.4

Abstract: Economic development requires from production companies to use more and more effective production methods. The growing demand for goods requires from them to reduce the lead time and to produce products of the best quality and competitive price. One of the problems of production lines is their proper balance. Balancing the production line consists in finding the optimal order of performed operations and assigning operations to individual operations in such a way, that work on positions is comparable. In this way, it is strive to minimize machine downtime and to distribute the work evenly between them. In the work, the performance analysis of the assembly line was made on the example of a selected product using three methods of balancing: the experimental method, the RPW (Ranked Positional Weight) heuristic method and SPT (Shortest Processing Time) method. The obtained results were analyzed and solutions were proposed to improve the work of the line.
Keywords: assembly line performance, RPW (Ranked Positional Weight) method, SPT (Shortest Processing Time) method, balancing the production line

Streszczenie: Rozwój gospodarczy wymaga od przedsiębiorstw produkcyjnych stosowania coraz to bardziej efektywnych metod produkcyjnych. Rosnący popyt na towary wymaga od nich zmniejszenia czasu potrzebnego na produkcję wyrobów o jak najlepszej, jakości i konkurencyjnej cenie. Jednym z problemów linii produkcyjnych jest ich prawidłowe zbalansowanie. Balansowanie linii produkcyjnej polega na znalezieniu optymalnej kolejności wykonywanych operacji oraz przypisaniu czynności poszczególnym operacjom w taki sposób, aby praca na stanowiskach była porównywalna. Dąży się w ten sposób do zminimalizowania czasów przestoju maszyn oraz do jak najbardziej równomiernego rozłożenia pracy pomiędzy nimi. W pracy wykonano analizę wydajności pracy linii montażowej na przykładzie wybranego wyrobu z wykorzystanie trzech metod balansowania: metody doświadczalnej, metody heurystycznej RPW (ang. Ranked Positional Weight) oraz metody SPT (ang. Shortest Processing Time). Dokonano analizy uzyskanych wyników i zaproponowano rozwiązania pozwalające na usprawnienie pracy linii.
Słowa kluczowe: wydajność linii montażu, metoda RPW (ang. Ranked Positional Weight), metoda SPT (ang. Shortest Processing Time), balansowanie linii produkcyjnej

Introduction

Constant economic development requires manufacturers to use more and more effective production methods. The growing demand for goods requires producers to drastically reduce the time needed to produce the best quality and competitive price. This allowed a significant reduction in production cycle time and an almost two-fold reduction in production costs. Ford's success, as the first in history to adapt the production line to the production of cars, initiated the dynamic development of line production in almost all branches of industry, from agriculture to the defense industry. This allowed a significant reduction in production cycle time and an almost two-fold reduction in production costs. The biggest problem of production lines is their proper balancing. It strives to minimize machine downtime and to distribute work as evenly as possible between them. In the rest of the work, it will focus on presenting the methods of balancing production lines and carry out performance analysis for the assembly line of the chosen product.

Characteristics and analysis of selected methods of balancing assembly lines

Balancing of the production line consists in minimizing machine downtime and the most even distribution of work between them. In order for the balancing process to be completed, each operation should be assigned once and

only to one workstation (Fig. 1) [1-8]. The basis of the balancing problem is to assign a set of tasks to an ordered set of workstations so that the order relations are met and the quality indicators optimized. The assembly line is properly balanced if all operations have been carried out, without prejudice to production assumptions on the line [5, 13, 15]. Due to the optimality criterion, two basic types of assembly line balancing problems are distinguished:

- type 1, minimizing the number of assembly stations at a constant cycle value, the goal is to minimize station downtime, which is equivalent to minimizing the number of work stations [9-12, 13]. The estimated number of workstations is calculated according to formula (1).

$$K_s = \left\lceil \frac{\sum_{i=1}^{N} t_i}{c} \right\rceil \quad (1)$$

where: K_s - estimated number of workstations, c - cycle value, N - number of tasks, t_i - task completion time i.

- type 2, minimizing the production cycle with a constant number of workstations, the goal is to minimize the cycle line balanced, which is equivalent to maximizing production [9, 14]. The estimated number of workstations is calculated according to the formula (2).

$$c_s = \left\lceil \frac{\sum_{i=1}^{N} t_i}{K} \right\rceil \quad (2)$$

where: c_s - estimated cycle value, K - number of workstations, N - number of tasks, t_i - time of task implementation i.

Balancing the production line consists in reducing machine downtime and for even distribution of work between workstations. There are many values that allow you to compare assembly line balancing methods.

The most commonly used quantities allowing for comparison of balancing results are [13]: assembly line efficiency, smoothness factor and line time.

The efficiency of the assembly line is calculated according to the formula (3):

$$LE = \frac{\sum_{i=1}^{K} ST_i}{c \cdot K} \cdot 100\% \quad (3)$$

where: c - cycle time, K - number of assembly stations, LE - line efectiveness, ST_i - time of use of every (i) station.

The line smoothness factor expresses a value representing the relative smoothness of a balanced assembly line. The better balanced the line, the closer to zero the smoothness factor will be. The smoothness coefficient is described by the formula (4):

$$SI = \sqrt{\sum_{i=1}^{K} (ST_{\max} - ST_i)^2} \quad (4)$$

where: SI - smoothness factor, ST_i - time of use of i - this station, ST_{max} - maximum time of use of the workstation.

The value that allows comparison of balancing results is the time of the line. This ratio is strictly dependent on the number of workstations. The shorter the line time, the better balanced the line will be. The line time is calculated according to the formula (5):

$$LT = (K-1) \cdot c + ST_K \quad (5)$$

where: c - cycle time, K - number of workstations, LT - line time, ST_k - time of the last workstation.

Various types of algorithms are used to solve the problem of assembly line balancing. Generally, these algorithms were divided into two groups [9, 13]: exact algorithms and heuristic algorithms. Accurate algorithms are those that are able to provide a clear solution to the problem or no solution to it. Accurate algorithms are mainly based on methods [10, 13]: linear discrete programming, network programming, dynamic programming as well as division and constraints. Heuristic algorithms allow finding an approximate solution to the problem. They make it possible to indicate an acceptable or even optimal solution in a relatively short time. Heuristic algorithms are characterized by great diversity. In general, it was divided into algorithms [9]: scheduling and allocation. Examples of heuristic methods include the RPW- Ranked Positional Weight, RRPW - Reversed Ranked Positional Weight, K&W (Kilbridge & Wester), Hoffman order matrix, and IUFF-Immediate Update First - Fit method.

Analysis and assessment of the working efficiency of the assembly line for the production of the automotive industry

- **Collecting data on the process and preliminary analysis of the line's operation**

The assembly line, which will be rebalanced in this work, produces products for the automotive industry. This line is a serial construction, which means that all operations are carried out in a strictly defined order between workstations. The parts are transported through a conveyor belt. The assembly line consists of eight assembly stations and one finished product testing station. The number of operators envisaged for all machines is six people. Currently, production is envisaged in a three-shift system five days a week. The working time is seven and a half hours. The weekly demand for the product is

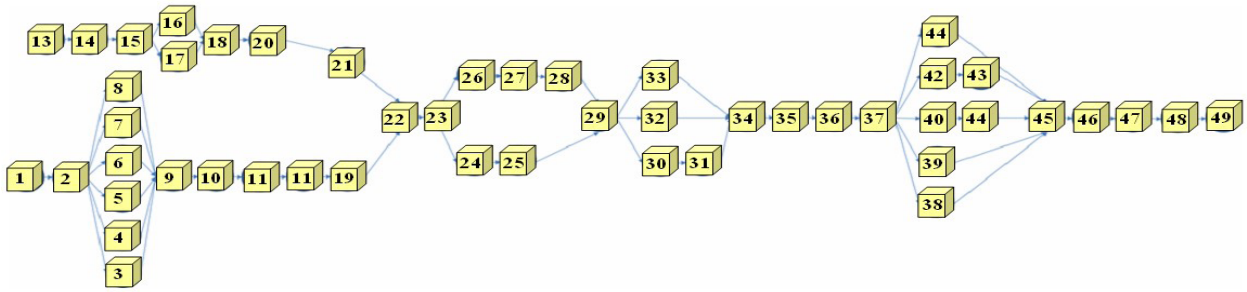

Fig.1. Graph of the relationship of the consequences of individual tasks of the product assembly process

2780 pieces.The total working time on the line is 24,07 hours a day. The minimum number of working days in a month is 24 days.

The technological process of product assembly consists of 9 operations divided into 49 assembly tasks. Each assembly task is assigned to individual assembly stations, taking into account their duration. Based on the collected information, a graph of the consequences of individual tasks was created (Fig. 1). This graph is designed to clearly show all the relationships between production stages.

Then, for the analyzed assembly line, cycle time was measured for each task included in the process. Based on the results obtaineddetermined the production time, cycle time and theoretical minimum number of workstations were [12].

The production time allowed was determined from formula (6).

$$Tp = npr \cdot z \cdot nh \tag{6}$$

where: Tp - production time allowed, npr - number of working days per week, z - weekly number of shifts, nh - number of working hours per shift.

The production line cycle was determined from formula (7).

$$T = Tp / P \tag{7}$$

where: T - production line cycle, Tp - production time allowed, P - weekly production demand pcs / week.

The theoretical minimum number of workstations from formula (8).

$$LS_{min} = \frac{\sum_{i=1}^{I} T_i}{T} \tag{8}$$

where: LS_min- theoretical minimum number of workstations T - production line cycle, $\sum_{i=1}^{I} T_i$- total execution time and - these tasks.

The following results were obtained: the allowable production time was Tp= 120s, the tact time T= 150s and the theoretical minimum number of work stations: LS= min 6.94≈7. Calculations indicate that seven positions are enough to ensure optimal performance on the assembly line. Currently, the analyzed assembly line has as many as nine stations, which indicates that it has not been thoroughly analyzed at the modeling stage.

In addition, the results of the measurement of cycle times of individual tasks allowed assigning tasks to workstations, thanks to which it will show to what extent they are used (Fig. 2).

The analysis of the results obtained indicates that the big problem of the analyzed assembly line is the lack of even loading of work stations. In addition, too many assembly stations are another problem. The assembly line rebalancing process was carried out to eliminate the identified problems. The experimental method, RPW *(Ranked Positional Weight)* method and SPT *(Shortest Processing Time)* method were used for the analysis.

Development and analysis of new models - experimental method

The first method used was the experimental method. Its first element was the reduction of the number of assembly stations from 9 to 7, and then the reassignment of tasks to individual positions based on the obtained cycle times. Figure 3 presents the load diagram of individual assembly stations after modification.

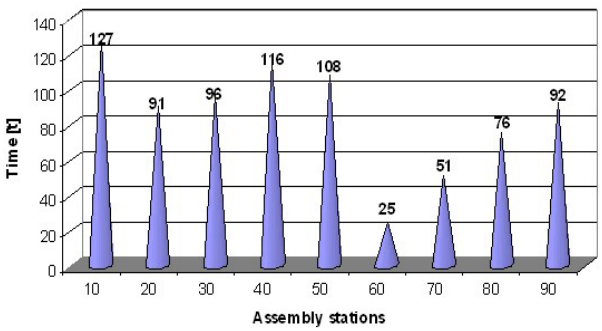

Fig. 2. Graph of current loads of individual assembly stations

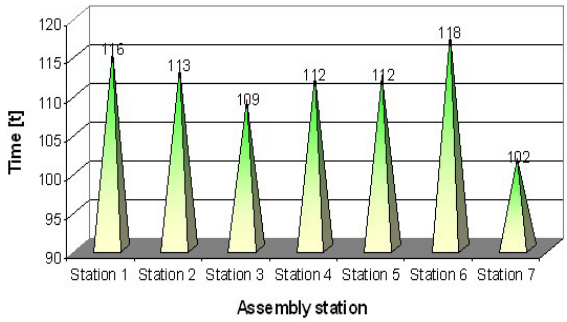

Fig. 3. Load diagram of individual assembly stations after modification

The results obtained after the modification indicate that earlier disparities between cycle times of individual stations have been reduced.

Development and analysis of new models - the RPW method

The second method used to rebalance the line was the heuristic method RPW (Ranked Positional Weight). The steps to follow when using this method are as follows:

- Specify the weight position for each task. (The longest path time from the beginning of the operation to the rest of the network).
- Then organize the network tasks based on weight positions. The task with the highest weight position takes first place.
- Match tasks to work stations. Priority is given to elements of the highest weight.
- If there is time remaining on any workstation after assigning the task, assign the tasks until the order of sequence order is exceeded or the cycle is exceeded.
- Repeat steps 3 and 4 until all items are assigned to workstations.

The use of this method requires determination of the weight position for each task. Starting from task number 1 up to task 49. The weight relationship graph was used to determine the results of individual tasks (Fig. 1.)

The weight position for task number1 is 564. It is calculated by adding together the next longest lasting tasks up to task number 49 according to Table 1. Table 1 presents the values and components of weight items for tasks from 1 to 13.

Table 1. Values and components of weight items for tasks from 1 to 13

no.	1	2	3	4	5	6	7	8	9	10	11	12	13
Time Ti [s]	11	5	6	3	3	5	3	5	66	6	12	91	11
	11	5	6	3	3	5	3	5	66	6	11	91	11
	5	6	66	66	66	66	66	66	6	12	91	6	16
	6	66	6	6	6	6	6	6	12	91	6	6	4
	66	6	12	12	12	12	12	12	91	6	6	52	17
	6	12	91	91	91	91	91	91	6	6	52	7	18
	12	91	6	6	6	6	6	6	6	52	7	15	9
	91	6	6	6	6	6	6	6	52	7	15	32	7
	6	6	52	52	52	52	52	52	7	15	32	13	6
	6	52	7	7	7	7	7	7	15	32	14	39	52
	52	7	15	15	15	15	15	15	32	14	39	25	7
	7	15	32	32	32	32	32	32	14	39	25	51	15
	15	32	13	13	13	13	13	13	39	25	51	5	32
	32	14	39	39	39	39	39	39	25	51	5	16	13
	13	39	25	25	25	25	25	25	51	5	16	5	39
	39	25	51	51	51	51	51	51	5	16	5	5	25
	25	51	5	5	5	5	5	5	16	5	5	17	51
	51	5	16	16	16	16	16	16	5	5	17	43	5
	5	16	5	5	5	5	5	5	5	17	42	25	16
	15	5	5	5	5	5	5	5	16	41	24		5
	5	5	17	17	17	17	17	17	43 43	25			5
	5	17	43	43	43	43	43	43	26 26				17
	17	43	26	26	26	26	26	26					43
	43	26											26
	26												
Weigh	564	553	548	545	545	547	545	547	541	475	469	457	442

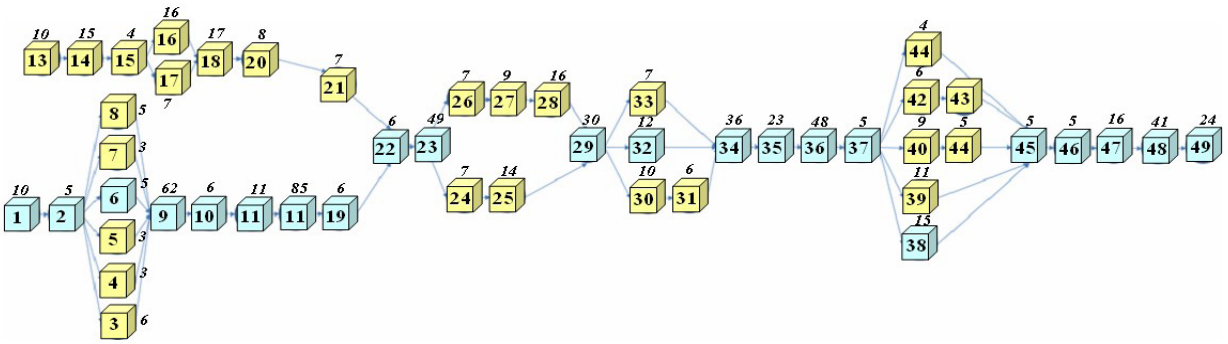

Fig. 4. Graph of the relationship of the consequences of individual tasks of the product assembly process with the longest path marked in green for task number 1

Figure 4 shows the longest possible path for task number 1 in green.

Having calculated weight position values for all events of the production process, events were assigned to workstations, taking into account operations of the highest importance first. If there is free time left in the open position after assigning the task, assign the next until the measure is not exceeded or the order of the order is disturbed. Figure 5 presents a graph of loads of individual assembly stations after applying the RPW method.

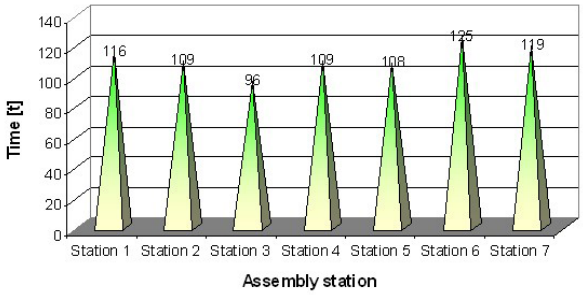

Fig. 5. Load diagram of individual assembly stations after using the RPW method

Development and analysis of new models - the SPT method

The SPT (Shortest Processing Time) method consists in determining the shortest path needed for a given event to achieve the last task. The methodology for using this method is very similar to the RPW method, but with the difference that using the graph of the consequences of individual tasks is determined not the longest, but the shortest path to overcome for each task. Fig. 6 in orange shows the shortest path for task number 13.

Then, similarly to the RPW method, weights were calculated for each task of the production process. This time the basic difference will be the way events are selected. The RPW method should aim to find the event with the longest possible duration, remembering not to violate the order of order tasks. In the SPT method, however, you need to find the shortest possible way to overcome subsequent events. Having calculated weight position values for all events of the production process, events were assigned to workstations, taking into account operations with the lowest weight first. Figure 7 presents a graph of loads of individual assembly stations after the SPT method.

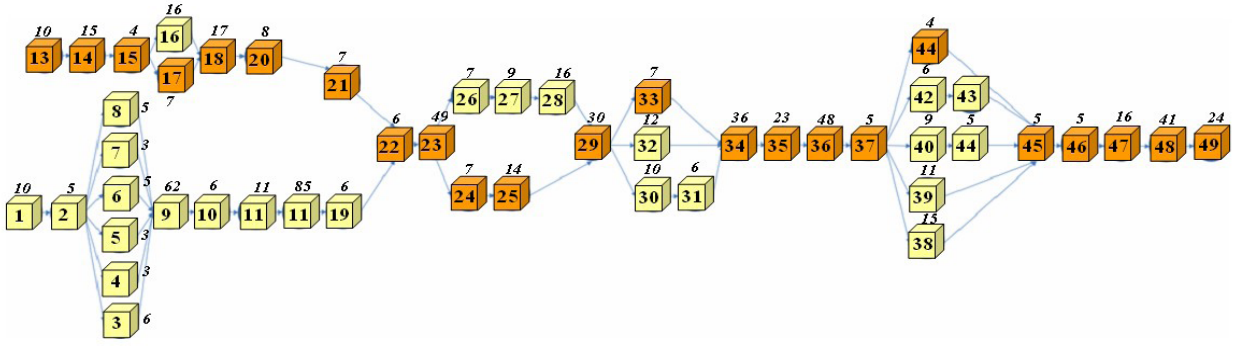

Fig. 6. Graph of relations between the consequences of individual tasks of the product assembly process and the shortest path for task number 13

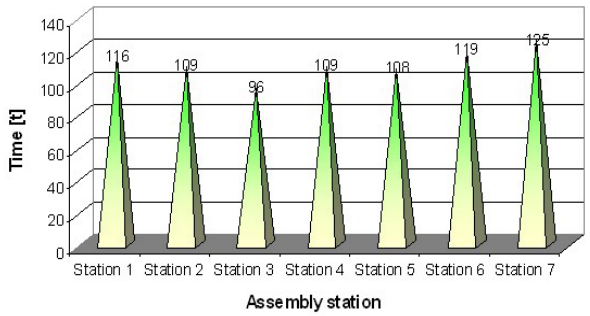

Fig. 7. Load diagram of individual assembly stations after applying the SPT method

Analysis of the obtained results

The analysis of the obtained results was carried out by comparing the balancing results for each developed model: assembly line efficiency (LE), smoothness factor (SI) and line time (LT). Fig. 8 presents the values of coefficients characterizing the line's work efficiency. The ideal solution is one in which the value of the assembly efficiency factor will be as high as possible. It should be noted that for the current state it is only 68.3%, which makes it the lowest. The results obtained for the SPT and RPW methods are 89.2% each. The experimental method gave the best result, for which the efficiency ratio is equal to 95%.

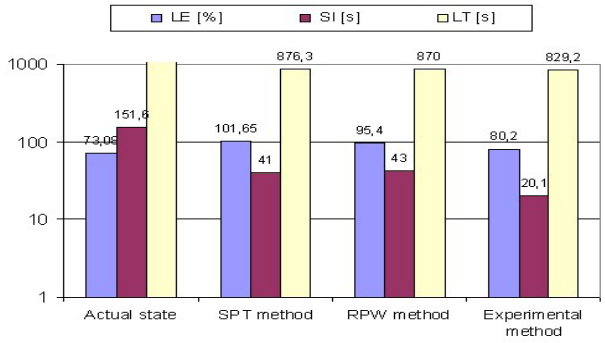

Fig. 7. Load diagram of individual assembly stations after applying the SPT method

The higher the SI value, the worse the line will be balanced. The obtained results clearly show that the best result was obtained by the experimental method 20.1 s. The SPT and RPW methods achieved 41 and 43 equally. The initial parameter was as much as 151,6 s. The results show that the assembly line time significantly decreased, which before modification it was as much as 1110 s. The SPT method reduced this time to 876.3 s. The RPW method proved to be slightly better giving 870 s. Again, as in previous cases, the best result was obtained thanks to the experimental method. It amounts to 829.2 s.

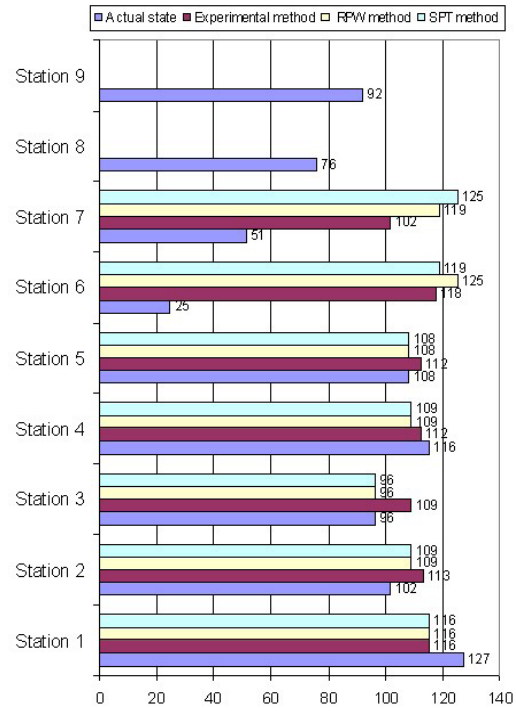

Fig. 8. List of coefficients describing the efficiency of the module assembly line before and after modifications

Figure 9 presents a load diagram of individual assembly stations before and after the proposed modifications.

On fig. 9 the load on assembly stations is before applying modifications is presented. The biggest difference was noticed between stations number 1 and number 6, whose working time was only 25 seconds. Initially, the number of stands was nine, where in reality only seven are needed to meet production requirements. After reducing the number of stations, operations were assigned to other stations. This allowed for balancing the loads on individual assembly stations.

Conclusion

The purpose of this work was to analyze the performance of the product assembly line for the automotive industry. In order to identify the problems of assembly line operation, a performance analysis was carried out for the current condition of the line. Then methods were used to balance it. Conducting a detailed analysis of the results obtained showed that the methods proposed have obtained a measurable effect. The best results were obtained after applying the experimental method. A very comparable effect was obtained using RPW and SPT methods. To sum up, by using the right ones, significant improvement was achieved in the basic factors determining work efficiency on the line.

References

[1] Adil B., Türkay D. 2009. “Simple and u-type assembly line balancing by using an ant colony based algorithm”. Mathematical and Computational Applications 14(1): 1-12.
[2] Grzechca W. 2015. “Balancing of the bilateral assembly line taking into account costs”. Logistyka (02): 211 - 220.
[3] Grzechca W. 2007. “Balancing the assembly line including costs”. PAK (08): 10 - 12.
[4] Grzechca W. 2012. “JUST IN TIME strategy in the problem of assembly line balancing”. Logistyka (02): 623 - 632.
[5] Grzechca W. 2014. “Method of selecting and assessing assembly line structure”. Mechanik (07): 209 - 216.
[6] Grzechca W. 2014. “Method of selecting and assessing the structure of the assembly line”. Mechanik (07): 209 - 216.
[7] Ismail N., Hamedi M., Esmaeilian G. R., Hamedi M. 2011. Balancing of parallel assembly lines with mixed-model product. International Conference on Management and Artificial Intelligence IPEDR, vol.6. Bali, Indonesia: IACSIT Press.
[8] Kowalski T. 2006. Technology and automation of machine assembly. Warszawa: Oficyna Wydaw. Politechniki Warszawskiej.
[9] Marecki F. 1986. Mathematical models and algorithms for the allocation of operations and resources on the assembly line. Gliwice: Department of Publications of the Silesian University of Technology.
[10] Scholl A. 1999. Balancing and Sequencing of Assembly Lines. Heidelberg: Physica-Verlag.
[11] Sharma P., Thakar G., Gupta R.C. 2014. “Evaluation of multi criteria assembly line balancing by mcdm approaches: A conceptual review”. International Journal for Quality Research 8(1) 87-106.
[12] Sivasankaran P., Shahabudeen P. 2017. “Comparison of Single Model and Multi-Model Assembly Line Balancing Solutions”. International Journal of Computational Intelligence Research 13(8): 1829-1850.
[13] Thomopoulos N. T. 2014. Assembly Line Planning and Control. Switzerland: Springer International Publishing.
[14] Vishnu Raj A. S., Jeeno Mathew, Peter Jose, Gishnu Sivan. 2016. “Optimization of Cycle Time in an Assembly Line Balancing Problem”. Global Colloquium in Recent Advancement and Effectual Researches in Engineering, Science and Technology (RAEREST 2016), Procedia Technology 25: 1146 – 1153.
[15] Yazdanparast V., Hajihosseini H., Bahalke A. 2011. “Cost Oriented Assembly Line Balancing Problem with Sequence Dependent Setup Times”. Australian Journal of Basic and Applied Sciences 5(9): 878-884.

Katarzyna Antosz, PhD., D. Sc. Eng.
Rzeszow University of Technology
Faculty of Mechanical Engineering and Aeronautics
Department of Manufacturing and Production Engineering Technology and Production Engineering, Al. Powstańców Warszawy 12, 35-959 Rzeszów, Poland, e-mail: katarzyna.antosz@prz.edu.pl

Rafał Kluz, PhD
Rzeszow University of Technology
Faculty of Mechanical Engineering and Aeronautics
Department of Manufacturing and Production Engineering, Al. Powstańców Warszawy 12, 35-959 Rzeszów, Poland, e-mail: rkktmiop@prz.edu.pl

EFFECT OF TEMPERATURE ON THE SHEAR STRENGTH OF GFRP-ALUMINIUM ALLOY 2024-T3 SINGLE LAP JOINT

Wpływ temperatury na wytrzymałość na ścinanie połączenia adhezyjnego pomiędzy kompozytem GFRP a blachą ze stopu aluminium 2024-T3

Andrzej KUBIT ORCID: 0000-0002-6179-5359
Magdalena BUCIOR ORCID: 0000-0002-1081-5065
Rafał KLUZ ORCID: 0000-0001-6745-294X

DOI: 10.15199/160.2020.1.5

Abstract: The paper presents the results of experimental studies determining the effect of temperature on the shear strength of the adhesive joint between the layers of the fiber metal laminate (FML). The tests were carried out for composites being a combination of 2024-T3 aluminum alloy sheet and Glass Fiber-Reinforced Polymer (GFRP) made in the autoclave process. The key factor determining the quality of layered composites is the high strength adhesive joint between the layers. Due to the possibility of extreme temperature conditions during utilization of the composite structure, tests were carried out at reduced temperatures, i.e. -60°C, as well as elevated temperatures, i.e. 80°C. The obtained results were related to the results obtained at a room temperature (RT). The study showed that at the elevated temperature the shear strength increased by approx. 10% compared to the result obtained at room temperature. There is also a significant reduction in the stiffness of the joint as the temperature increases. In turn, a slight increase in joint stiffness was demonstrated for the reduced temperature.
Keywords: FML composites, adhesive joints, shear strength, 2024-T3 aluminium alloy, GFRP composites

Streszczenie: W pracy przedstawiono wyniki badań eksperymentalnych określających wpływ temperatury na wytrzymałość na ścinanie połączenia adhezyjnego pomiędzy warstwami składowymi hybrydowego kompozytu metalowo-włóknistego (FML). Próby przeprowadzono dla kompozytów będących połączeniem blachy ze stopu aluminium 2024-T3 oraz kompozytu szklanego polimerowo-włóknistego (ang. Glass Fiber-Reinforced Polymer - GFRP) wykonanych w procesie autoklawowym. Kluczowym czynnikiem determinującym jakość kompozytów warstwowych jest wysokiej wytrzymałości połączenie adhezyjne pomiędzy warstwami. Ze względu na możliwość występowania różnych warunków temperaturowych w procesie eksploatacyjnym struktury kompozytowej, zrealizowano badania w temperaturach obniżonej tj. -60°C, a także podwyższonej tj. 80°C. Uzyskane rezultaty odniesiono do wyników uzyskanych w temperaturze pokojowej. W pracy wykazano, że w podwyższonej temperaturze dochodzi do wzrostu wytrzymałości na ścinanie o ok. 10% w stosunku do rezultatu uzyskanego w temperaturze pokojowej. Dochodzi tu także do znacznego obniżenia sztywności połączenia wraz ze wzrostem temperatury. Dla obniżonej temperatury wykazano z kolei nieznaczny wzrost sztywności połączenia.
Słowa kluczowe: kompozyty warstwowe FML, połączenia adhezyjne, wytrzymałość na ścinanie, stop aluminium 2024-T3, kompozyty GFRP

Introduction

Composite materials, which are more and more widely used, especially in aviation constructions, despite many obvious advantages, have some limitations that make them impossible to appear in the whole aircraft structure. This limitation applies especially to the places in the structure where the temperature is high. Therefore, there is a frequent need to combine polymer-fiber composites with other materials, mainly metals such as aluminum alloys or titanium [27]. Adhesive joints have the advantage over the riveting technique, popular in aircraft construction, that they do not require holes, which are often the cause of stress concentrators, and do not affect the weight of the structure as much as rivets [27], hence the adhesive joints are widely used in the aviation industry.

Due to the growing interest in FML composites, recently there has been an intensive increase in the number of publications in the field of strength analysis of adhesive joints between fiber composites and light metals. For analysis of cracking the connection between the layers of FML composites, samples in the form of a double cantilever beam are most often used. The purpose of such research is to determine the behavior of crack propagation and obtain energy data for numerical analysis of the fracture mechanism [10, 14]. In turn, for determining the shear strength of the considered joints, usually one or two-fold metal-composite joints

Table 1. Chemical composition (wt. %) of 2024-T3 aluminum alloy

Alloy	Cu	Mg	Fe	Si	Mn	Zn	Ti	Cr	Other
2024-T3	4.35	1.50	0.50	0.50	0.30	0.25	0.15	0.10	0.20

Table 2. The basic mechanical parameters of 2024-T3 aluminium alloy sheet

Thickness *t*, mm	Young's modulus *E*, GPa	Poisson's ratio	Yield stress $R_{p0,2}$, MPa	Ultimate tensile stress R_m, MPa
0.4	72,874	0.33	302	449

are tested [7, 12, 17, 22]. Many authors also address the issue of analytical and numerical analysis related to the shear strength of glued joints of various materials [2, 9,16]. Fatigue strength of adhesive joints is also a very important issue.

The interlaminar shear strength (ILSS) is mainly used for the assessment of bond strength between fibres and the matrix resin in FML. ILSS may be determined in many shear tests [18, 21], including the short-beam shear test which is the simplest and most feasible [8, 19]. Naik et al. [5] observed that the interlaminar shear strength increases with increasing shear strain rate. The differences in the thermal expansion coefficients of the matrix and fibre and cure shrinkage in thermosetting matrices result in the development of residual stresses at the fibre/matrix interface [13]. The aircraft structure is subjected to multiple rapid changes in temperature. So, it is important to assess the degradative effect of thermal fatigue on conditioning times during exposure to above-zero and sub-zero temperatures [20].

When considering the issue of adhesive bonding of materials with significantly different coefficients of thermal expansion, one should take into account the stresses in the plane of connection of these materials that are the cause of the variable operating temperature, which may contribute to reducing the strength of the connection. Hence, many studies focus on the possibility of minimizing the negative effects resulting from different properties of materials joined by proper selection of the bonding layer [23, 24].

It can be stated that a properly made adhesive connection in the composite manufacturing process determines the later operational quality of the layered composite structure. FML composites based on prepregs based on epoxy resins are produced in such a way that the adhesive connection between the layers is formed by an epoxy resin which is the resin of the prepreg [25].

It is very important to know the strength of the adhesive joint between the layers of the FML composite depending on the temperature conditions. The issue of adhesive joints based on epoxy resins has been described in the work [3]. The authors presented the effect of temperature on both strength and stiffness of the joint.

This paper presents the effect of temperature on the shear strength of the GFRP-Aluminum alloy adhesive joint made according to the technology of producing FML composites in an autoclave process.

Materials and methods

A 2024-T3 aluminum alloy sheet with a thickness of 2 mm was used in this study for the fabrication of layered specimens. This aluminum was selected because it is widely used to manufacture adhesively bonded aircraft structures due to its excellent specific strength and fatigue performance, good conformability and surface finishing capabilities [5, 13]. 2024-T3 aluminum alloy is commonly used to manufacturing FML composites [14]. The chemical composition is listed in Table 1, and the mechanical properties determined in the uniaxial tensile test according to ISO 6892-1 standard [11] is listed in Table 2.

The preparation of the surface of the sheets before adhesive bonding with the fibre layers was carried out according to the technology used in the aviation industry [28]. First, the sheets were anodized.

The oxide coatings were produced onto the alclad substrate in the anodizing process. The specimens were abraded with sand paper of grade 320, rinsed with water and degreased in the NaOH aqueous solution (100 $g \cdot dm^{-3}$) for 1 minute at 25°C, rinsed with deionised water, pickled in the 400 $g \cdot dm^{-3}$ for 1 minute at 25°C$g \cdot dm^{-3}$) at 15°C. The constant current density equal to 1 $A \cdot dm^{-2}$ was applied. When the anodizing process was completed, the

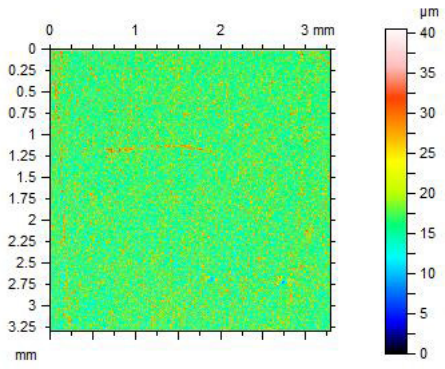

Fig. 1. Three-dimensional structure of the sheet surface

Fig. 2. Configurations of FML composite (2/1 lay-up) considered

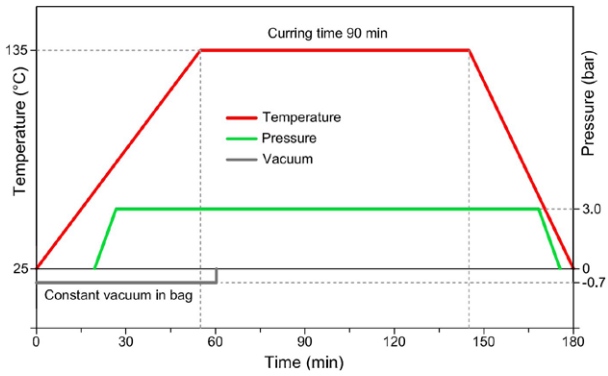

Fig. 3. The autoclave cure cycle

Table 3. Sheet surface roughness parameters for three-dimensional analysis

Roughness parameter	Value for the sheet used
S_q [µm]	4.32
S_{sk} [µm]	1.39
S_{ku} [µm]	3.75
S_p [µm]	22.9
S_v [µm]	17.6
S_z [µm]	40.5
S_a [µm]	3.36
S_{al} [µm]	0.00726
S_{tr} [µm]	0.756
S_{td} [µm]	84.5

coatings obtained were rinsed with deionised water and dried in air. Their thickness was determined by using the eddy-current method (Dualscope FMP100, Fischer). For substrate thickness equal to 2 mm the thickness of the coating was 10 ± 1 *µm*.

After anodizing, the surfaces of the sheets were measured by white light interferometer Talysurf CCI Lite using objective 5x. Parameters of surface textures were calculated using TalyMap software. The measured areas of 3.3 mm x 3.3 mm contained 1024 x 1024 points. Textures of surfaces were only levelled, digital filtration was not used.

Fig. 1 shows the three-dimensional structure of a fragment of the surface of sheets joined with a GFRP layer. Table 3 summarizes the sheet surface roughness parameters for three-dimensional analysis.

Immediately after anodizing the surfaces were primed with EC3924B (3MTM, Maplewood, Minnesota, USA) primer. As a polymer-fibrous layer, a prepreg based on glass fibres with a thermosetting epoxy matrix was used. The prepreg was supplied from HEXCEL, its trade symbol is HexPly 916G-1581-53.5%.

The composites were prepared in a 'clean room' by placing complex layers (Fig. 2) in a vacuum bag, and then cured in an autoclave according to the parameters shown in Fig. 3.

The composite was made in the form of a panel with the dimensions of 360×200 mm (Fig. 4a).

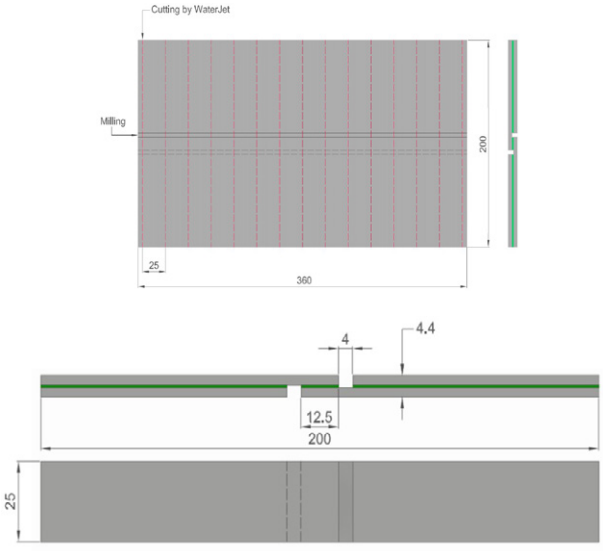

Fig. 4. Dimensions of sample sheets with the cutting path for the shear test (a); geometry and dimensions of specimens for shear strength test (b)

Fig. 5. Specimen view in a temperature chamber at -60°C

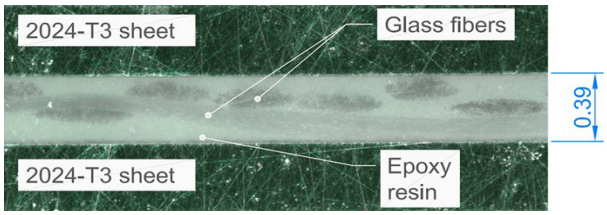

Fig. 6. Structure of the composites studied showing the direction of the fibers and the thickness of the GFRP

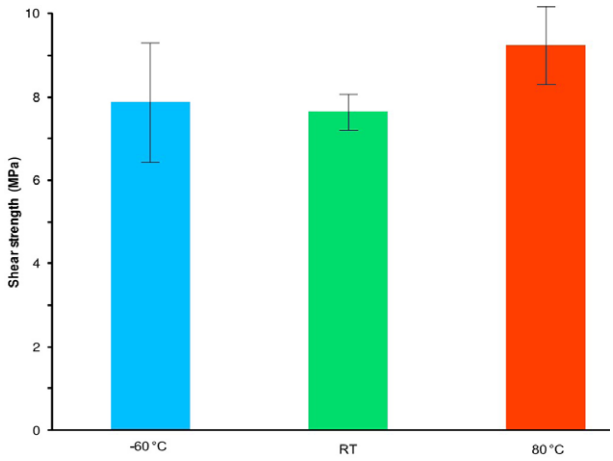

Fig. 7. Average values of shear strength for the samples tested at considered temperatures

Samples for individual strength tests were cut from these sheets (Fig. 4b). Before cutting the sheet, it was milled along its entire length on both sides to obtain an overlap (Fig. 4a).

The samples were cut using a high-pressure water jet technique. The treatment was carried out at a water pressure of p = 350 MPa, an abrasive mass flow rate of ma = 300 g min^{-1} and a speed of cutting head v_f = 250 mm min^{-1}.

The endurance test was carried out on a Zwick/Roell Z030 testing machine with a temperature chamber, a jaw feed speed of 2 mm/min was used. Extensometers were used to measure sample deformation during the test.

In order to obtain a reduced test temperature of -60°C, the temperature chamber was cooled with liquid nitrogen; the view of the chamber during tests at this temperature is shown in Fig. 5.

Results and discussion

After curing the samples in the autoclave process, the thickness of the GFRP layer was measured and the fiber direction was determined. Fig. 6 shows a view of the microsection the structure of the resulting composite as a combination of three layers. The thickness of the GFRP has been shown to be 0.39 mm. The fibers were obtained evenly parallel and perpendicular to the direction of load of the sample.

Fig. 7 shows the average values of shear strength together with the standard deviation for individual temperature levels at which the tests were carried out.

The study showed that at elevated temperature, i.e. 80°C, there was a significant increase in strength. The average value in this case was 9.24 MPa, which is almost by 11% higher compared to the average value of the strength obtained at a room temperature, which was 7.65 MPa. At the reduced temperature, i.e. -60°C, the average shear strength increased slightly, i.e. by less than 2%, to the value of 7.96 MPa.

It should be noted that in the case of tests at the reduced temperature, the largest spread of results occurred. The most reproducible test results were obtained for the samples tested at a room temperature.

Fig. 8 presents stress-displacement curves for the samples tested. Based on the nature of the course of individual curves, significant differences can be observed in the way the samples are destroyed at the considered temperature levels. In the case of samples at a room temperature and reduced temperature, i.e. -60°C, the course of stretching curves is generally similar in nature, with a clear increase in stiffness of samples tested

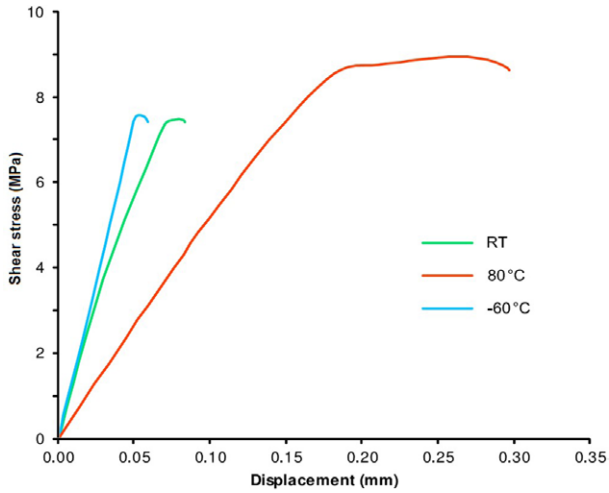

Fig. 8. Typical tensile/shear test curves of the FML composites studied.

at reduced temperature. The increase in the rigidity of adhesive joints based primarily on epoxy resins at reduced temperatures is also confirmed by the authors of the papers [1, 4, 6, 12, 26].

Turning to the test variant at an elevated temperature of 80°C, the distinct nature of the stretching curve is clearly seen here. First of all, there is a significant decrease in stiffness, which coincides with the results of the research presented by the authors of work [3]. In the same work, the authors noticed, that at elevated temperature, the strength of the adhesive connection made on the basis of epoxy resin increases to the glass transition temperature Tg of the adhesive, while after exceeding this temperature it decreases markedly. This tendency was confirmed by showing an increase in shear strength of the joint at 80°C, thus below the glass transition temperature of the epoxy resin used, which is about 150°C [29].

Conclusions

The purpose of the work was to determine, by the experimental method, the properties of the adhesive joint between GFRP and metal layers in the FML composite. The research showed that the extreme temperature conditions that may occur in the operation process do not lead to a reduction in the shear strength of the joint between the layers of the composite. At the elevated temperature, i.e. 80°C, an increase in shear strength of almost 11% was observed compared to the result obtained at room temperature. Importantly and in line with the observations of the authors of other papers [3], it has been shown that there is a close relationship between the stiffness of the connection and the temperature. As the temperature increases, the stiffness of the connection decreases, while at -60°C, the stiffness is higher than that recorded at room temperature.

Attention should also be paid to the distribution of strength results at individual test temperature values. At negative temperature the largest spread of results was recorded, while at a room temperature the highest repeatability was obtained.

To ensure the required properties of FML composites, it is necessary to obtain a high-strength joint between layers, the properties of which do not change significantly in the expected operating conditions. The study confirms that in the presented temperature range, layered composites can be safely exploited, as no significant decrease in the strength of the connection has been demonstrated.

The presented test results propose a methodology for testing the strength of the interlayer joint in FML composites.

The research results presented in the work are part of a series of the tests conducted by the authors in the field of the influence of temperatures on the properties of FML composites. The work [15] presents the influence of temperature gradient thermal shock cycles on the interlaminar shear strength of FML composite determined by the short beam test.

References

[1] Adams R.D., Coppendale J., Mallick V., Al-Hamdan H. 1992. “The effect of temperature on the strength of adhesive joints”. International Journal of Adhesion and Adhesives 12:185–90.
[2] Adams R.D., Mallick V. 1993. “The effect of temperature on the strength of adhesively-bonded composite-aluminium joints”. J. Adhes. 43: 17–33.
[3] Banea M.D., da Silva L.F.M., Campilho R.D.S.G. 2014. “Effect of temperature on the shear strength of aluminium single lap bonded joints for high temperature applications”. Journal of Adhesion Science and Technology 28(14-15): 1367-1381.
[4] Banea M.D., da Silva L.F.M. 2009. “Mechanical characterization of flexible adhesives”. Journal of Adhesion 85:261–85.
[5] Critchlow G.W., Brewis D.M. 1996. “Review of surface pretreatments for aluminium alloys”. International Journal of Adhesion and Adhesives 16(4): 255–275.
[6] Deb A., Malvade I., Biswas P., Schroeder J. 2008. “An experimental and analytical study of the mechanical behaviour of adhesively bonded joints for variable extension rates and temperatures”. International Journal of Adhesion and Adhesives 28: 1–15.
[7] Giannis S., Hansen K. 2010. Investigation on the Joining of CFRP-to-CFRP and CFRP-to-Aluminium for a Small Aircraft Structural Application. 25th Technical Conference of the American Society for Composites and 14th US-Japan Conference on Composite Materials.
[8] Heidenwolf G. 2005. GLARE - Industrialization of an Advanced Light Weight Material, Airbus Deutschland GmbH A380 Programme.

[9] Hua Y., Gu L., Trogdon M. 2012. “Three-dimensional modeling of carbon/epoxy to titanium single-lap joints with variable adhesive recess length”. International Journal of Adhesion and Adhesives 38: 25–30.
[10] Ishii K., Imanaka M., Nakayama H.J. 2007. “Fatigue crack propagation behavior of adhesively-bonded CFRP/aluminum joints”. Adhes. Sci. Technol. 21: 153–167.
[11] ISO 6892-1:2016. Metallic Materials - Tensile Testing - Part 1: Method of Test at Room Temperature. Geneva: International Organization for Standardization.
[12] Kang S.G., Kim M.G., Kim C.G. 2007. “Evaluation of cryogenic performance of adhesives using composite-aluminum double-lap joints”. Composite Structures 78:440–6.
[13] Khalili S.M.R., Mittal R.K., Kalibar G.S. 2005. “A study of the mechanical properties of steel/aluminium/grp laminates”. Materials Science and Engineering 412(1-2): 137–140.
[14] Khoshravan M., Mehrabadi F.A. 2012. “Fracture analysis in adhesive compositematerial/aluminum joints under mode-I loading; experimental and numerical approaches. International Journal of Adhesion and Adhesives 39: 8–14.
[15] Kubit A., Trzepiecinski T., Kłonica M., Hebda M., Pytel M. “The influence of temperature gradient thermal shock cycles on the interlaminar shear strength of fibre metal laminate composite determined by the short beam test”. Composites Part B 176: 107217.
[16] Narasimhan S., Shenoi R. A., Jeong, H. K. 2004. “Three-dimensional stresses in adhesively bonded lap joints with non-identical adherends”. Proceedings of the Institution of Mechanical Engineers Part L Journal of Materials Design and Applications 218(4): 283–298.
[17] Owens J., Lee-Sullivan P. 2000. “Stiffness behavior due to fracture in adhesively bonded composite-to-aluminum joints II”. International Journal of Adhesion and Adhesives 20: 47–58.
[18] Pahr D.H., Rammerstorfer F.G., Rosenkranz P., Humer K., Weber H. W. 2002. “A study of short-beam-shear and double-lap-shear specimens of glass fabric/epoxy composites”. Composites Part B: Engineering 33(2): 125-132.
[19] Park S.Y., Choi W.J., Choi H.S., Kwon H. 2010. “Effects of surface pre-treatment and void content on GLARE laminate process characteristics”. Journal of Materials Processing Technology 210(8):1008-1016.
[20] Ray B. C. 2005. “Thermal shock and thermal fatigue on delamination of glass fiber reinforced polymeric composites”. Journal of Reinforced Plastics and Composites 24(1): 111-16.
[21] Schneider K., Lauke B., Beckert W. 2001. “Compression shear test (CST) - a convenient apparatus for the estimation of apparent shear strength of composite materials”. Applied Composite Materials 8(1):43-62.
[22] Seong M., Kim T., Nguyen K., Kweon J., Choi J. 2008. “A parametric study on the failure of bonded single-lap joints of carbon composite and aluminum”. Composite Structure 86(1-3): 135–145. Schneider K., Lauke B., Beckert W. 2001. “Compression shear test (CST) - a convenient apparatus for the estimation of apparent shear strength of composite materials”. Applied Composite Materials 8(1):43-62.
[23] da Silva L.F.M., Adams R.D. 2006. “Stress-free temperature in a mixed-adhesive joint”. Journal of Adhesion Science and Technology 20(15):1705-1726.
[24] da Silva L.F.M., Adams R. 2007. „Techniques to reduce the peel stresses in adhesive joints with composites”. International Journal of Adhesion and Adhesives 27: 216–226.
[25] Sinmazcelik T., Avcu E., Ozgur Bora M., Coban O. 2003. “A review: Fibre metal laminates, background, bonding types and applied test methods”. Materials and Design 32: 3671–3685.
[26] Srivastava V.K. 2003. “Characterization of adhesive bonded lap joints of C/C-SiC composite and Ti-6Al4V alloy under varying conditions”. International Journal of Adhesion and Adhesives 23:59–67.
[27] Teixeira de Freitas S., Sinke J. 2014. “Adhesion Properties of Bonded Composite-to-Aluminium Joints Using Peel Tests”. The Journal of Adhesion 90(5-6): 511–525.
[28] Trzepiecinski T., Kubit A., Kudelski R., Kwolek P, Obłój A. 2018. „ Strength properties of aluminium/glass-fiber-reinforced laminate with additional epoxy adhesive film interlayer”. International Journal of Adhesion and Adhesives 85:29-36.
[29] https://www.hexcel.com/Resources/DataSheets/Prepreg

Dr inż. Andrzej Kubit
Rzeszow University of Technology, Faculty of Mechanical Engineering and Aeronautics, al. Powstańców Warszawy 8, 35-959 Rzeszów, Poland
e-mail: akubit@prz.edu.pl

Dr inż. Magdalena Bucior
Rzeszow University of Technology, Faculty of Mechanical Engineering and Aeronautics, al. Powstańców Warszawy 8, 35-959 Rzeszów, Poland
e-mail: magdabucior@prz.edu.pl

Dr inż. Rafał Kluz
Rzeszow University of Technology, Faculty of Mechanical Engineering and Aeronautics, al. Powstańców Warszawy 8, 35-959 Rzeszów, Poland
e-mail: rkluz@prz.edu.pl

PORTAL INFORMACJI TECHNICZNEJ
największa baza publikazji on-line
www.sigma-not.pl

VALUE STREAM MAPPING OF A UNIQUE COMPLEX PRODUCT MANUFACTURING PROCESS

Mapowanie strumienia wartości procesu produkcji niepowtarzalnego wyrobu złożonego

Barbara BUKOWSKA
Dorota STADNICKA **ORCID: 0000-0002-4516-7926**

DOI: 10.15199/160.2020.1.6

Abstract: Value stream mapping is a method used for wastes' identification in manufacturing systems as well as in other processes realized in the companies. The method is well known and applied in different areas and industries. However, as each process is different, every time when the method is used, some unexpected problems in its implementation can appear or the method has to be applied in a specific way. In this paper, the value stream mapping method is applied in order to analyse a manufacturing system in which unique complex products are manufactured. The paper discusses important issues which have to be taken into consideration while the method is applied in the circumstances similar to these presented in the analysed case study. In the work, on the basis of the collected data, the current state of a value stream map was developed. Then, the problems existing in the manufacturing system were identified and analysed. Finally, on the basis of the suggested solutions for the problems, the future state of a value stream map was proposed. The paper emphasizes the aspects important in the value stream mapping of a unique complex product manufacturing process.
Keywords: Value stream mapping, unique complex product, problems analysis, pull system

Streszczenie: Mapowanie strumienia wartości jest metodą stosowaną do identyfikacji strat w systemach produkcyjnych, a także w innych procesach realizowanych w przedsiębiorstwach. Metoda ta jest dobrze znana i stosowana w różnych obszarach i branżach przemysłu. Ponieważ jednak każdy proces jest inny, za każdym razem, gdy stosowana jest metoda mapowania strumienia wartości, mogą pojawić się nieoczekiwane problemy z jej implementacją lub metoda musi być zastosowana w określony sposób. W niniejszym artykule zastosowano metodę mapowania strumienia wartości do analizy systemu produkcyjnego, w którym wytwarzane są niepowtarzalne produkty złożone. W artykule omówiono ważne kwestie, które należy wziąć pod uwagę, gdy metoda jest stosowana w okolicznościach podobnych do przedstawionych w analizowanym studium przypadku. W pracy, na podstawie zebranych danych, opracowano mapę strumienia wartości stanu aktualnego, a następnie zidentyfikowano i przeanalizowano problemy występujące w systemie produkcyjnym. Następnie, na podstawie zaproponowanych rozwiązań problemów zaproponowano mapę strumienia wartości stanu przyszłego. W artykule podkreślono aspekty ważne w mapowaniu strumienia wartości procesu wytwarzania niepowtarzalnego produktu złożonego.
Słowa kluczowe: Mapowanie strumienia wartości, niepowtarzalny produkt złożony, analiza problemów, system ssania

Introduction

The organization of a manufacturing process of a complex product is challenging. Especially, if the product changes in time and if it is a little bit different with every new customer's order. The situation is better when a product is composed with standard components and has a modular structure. However, there are cases in which it is impossible. Thus, the components are a little bit different every time. This makes the work organization more difficult and the production must be realized on the basis of a received order. A manufacturing process cannot begin in advance. If, in this case the lead time *(LT)* of a manufacturing process is longer than the delivery time *(DT)*, a company has problems. In consequence, it has to work on additional shift(s), has to work overtime if possible, or has to find other solutions in order to prevent delivery delays.

Therefore, the company must ensure that the lead time is shorter than the delivery time *(LT < DT)*. Hence, the lead time that is too long is the biggest problem in the company which manufactures unique complex products. In order to analyse the organization of manufacturing processes, the literature proposes a value stream mapping *(VSM)* method. Although in the work [2] the authors claim that there is no significant correlation between VSM and the defined by them operational performance measures such as e.g. quality, speed, flexibility, cost etc., other publications prove the usefulness of this method [8]. For example, in the work [9] the authors present how it was possible to decrease *LT* in manufacturing processes with the use of VSM. In the analysed lock manufacturing process *LT* was decreased by 62.74%. In the work [6], which analyses the process of car parts manufacturing, *LT* was decreased by 140%. In the work [7] the authors obtained the improvement of a manufacturing process

productivity by almost 11%. Moreover, the literature also presents a positive and significant influence of the VSM implementation on the OEE indicator [5]. Furthermore, in the papers [4, 12] the way of the implementation of VSM, improving process efficiency and decreasing the costs was presented.

In the work [11], it is shown how the VSM method can be applied in complex product manufacturing processes. However, the VSM methodology is usually applied for repetitive production. In this work the problem is not only connected to the product complexity but also with to the product uniqueness. In the work [1] the authors apply VSM in a low volume production. Therefore, the mentioned studies are a good starting point for the analyses.

Research problem and goal

The problem which is analysed in this paper concerns long *LT* of the manufacturing process of a unique complex product. A unique complex product is defined as a product which is unique and complex. The uniqueness of the product means that each product (which can be still ordered by a customer in a small batch) is a little bit different from the previous one ordered by a customer. Consequently, the manufacturer never knows in advance what will change. Therefore, *LT* cannot be longer than the delivery time. The product complexity is connected to a large number of parts which have to be manufactured and then assembled into a ready product. The complexity also concerns a manufacturing process in which the product components can be manufactured in parallel. In the analysed case study the situation is even more complicated because there is a necessity of using subcontractors' services. This creates an additional risk of delivery delays. To summarize, the following factors influence difficulties with the VSM implementation: product uniqueness, product complexity, parallel manufacturing of components and engagement of subcontractors. The goal of this paper is to analyse a case study manufacturing process organization and propose solutions to decrease *LT* to an acceptable value. The project presented in the case study was initiated because the company had a problem with on time deliveries and the employees had to work on additional shifts or overtime in order to prevent delivery delays. However, it was not always possible.

Work methodology

The work methodology, which was applied in this paper, is based on the value stream mapping (VSM) method presented in [10]. However, the VSM application for a complex product is not so simple as presented in the mentioned work. Therefore, the VSM adapted to a complex products manufacturing system analysis, presented in the work [11], was taken into consideration in the analyses and calculations. Nevertheless, in the cited work, a collaboration with external service providers was not investigated. In the case study, presented later in this work, it is necessary to include external service providers in a value stream map. This is a novelty, in relation to the aforementioned work. Moreover, the uniqueness of a product requires additional attention when setting value stream mapping targets. Therefore, the following main steps of the work methodology are realised:

Step 1. Identifying a product family and choosing a representative of the product family. In the presented case study the analysis was performed for a product family representative that is an expansion tank. For the product, which is a complex product, a product structure was developed.

Step 2. Setting the value stream mapping goals which take into consideration customer's requirements connected to the delivery time, bearing in mind that the manufacturing process concerns the production of unique products.

Step 3. Identifying the material and information flow and data collection. The data were collected with the use of a time study and discussion with the employees engaged in the process.

Step 4. Developing the current state of a value stream map (CS-VSM). The value stream maps were developed with the use of Visio Professional software. The lead time *(LT)* for the current state was calculated.

Step 5. Identifying and analysing problems. The problems were analysed and the suggestions for the problem elimination were presented.

Step. 6. Developing the future state of a value stream map (FS-VSM). The FS-VSM presents the proposals which can improve the flow. The *LT* for the future state was calculated. The obtained results were assessed.

Step. 7. Assessing the improvements. The improvements were assessed with the use of the *LT* improvement *(LTI)* and of value-added activities improvement *(VAI)* indicators.

The listed steps were applied. That is presented later in this work.

Description of the product

The product which is manufactured on the analysed manufacturing line is an expansion tank used in vehicles, and it is considered as a complex product [3]. Figure 1 shows ready products. The structure of the product is presented in Figure 2. The product consists of the components which are manufactured in the company, delivered by a customer or bought. In order

Figure 1. A photo of ready products

to manufacture the components, the company uses the following materials, i.e. round bars, stainless steel and seamless pipes. Table 1 presents a list of components, units and materials indicating their origin and quantity.

The structure of the product shows its complexity. The uniqueness is not presented here. The products are differentiated by size or number of certain product components. This can influence the processing time.

Communication with customer and suppliers and working time

A customer orders 32 pcs of ready products which have to be delivered in 6 weeks. The products have to be delivered in containers. One container includes 4 pcs of ready products. 32 pcs of ready products are delivered to a customer every 6 weeks. The next order will concern a product of a different structure. The client orders products 8 weeks before the planned shipment. Therefore, the lead time cannot be longer than 8 weeks.

Materials are delivered by the suppliers every 2 weeks. Additionally, the customer delivers some parts which are assembled to a ready product.

The company works 20 days in a month on two shifts (Production Department, Quality Department) and one shift (Design and Technology Department, Logistics Department and Marketing Department). One shift lasts 8 hours with a 30-min-break. Therefore, the available working time per shift is 27,000 seconds.

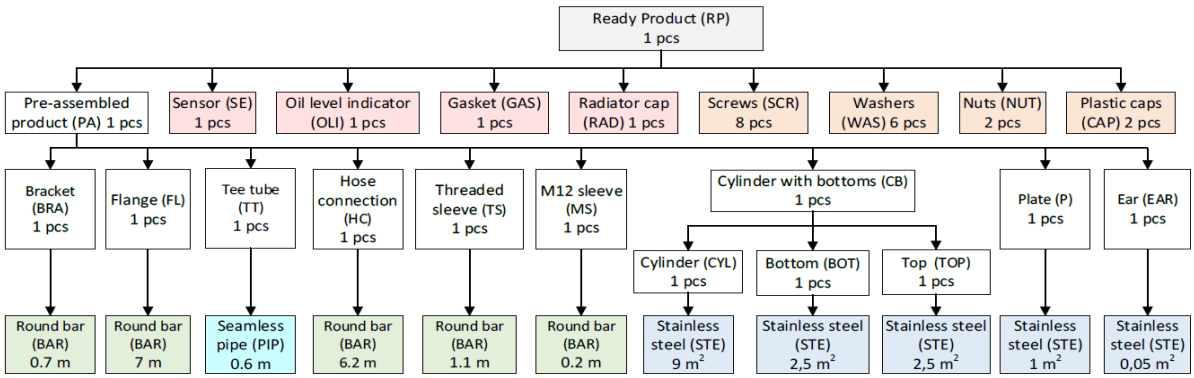

Figure 2. The structure of the product

Table 1. Components and materials needed to manufacture one expansion tank; MB – material bought, DC – delivered by customer, M – manufactured in the company, RP – ready parts bought

No	Component/material	Origin	Symbol	Qty	No	Component/material	Origin	Symbol	Qty
1	Bracket	M	BRA	1 pcs	13	Pre-assembled Product	M	PAP	1 pcs
2	Tee Tube	M	TTU	1 pcs	14	Round bar	MB	BAR	15.2 m
3	M12 sleeve	M	MSL	1 pcs	15	Stainless steel	MB	STE	15.05 m2
4	Threaded Sleeve	M	TSL	1 pcs	16	Seamless pipe	MB	PIP	0.6 m
5	Hose connection	M	HC	1 pcs	17	Sensor	DC	SE	1 pcs
6	Flange	M	FL	1 pcs	18	Oil level indicator	DC	OLI	1 pcs
7	Cylinder	M	CYL	1 pcs	19	Gasket	DC	GAS	1 pcs
8	Bottom	M	BOT	1 pcs	20	Radiator cap	DC	RAD	1 pcs
9	Top	M	TOP	1 pcs	21	Screws	RP	SCR	8 pcs
10	Ear	M	EAR	1 pcs	22	Washers	RP	WAS	6 pcs
11	Cylinder with bottoms	M	CB	1 pcs	23	Nuts	RP	NUT	2 pcs
12	Plate	M	PLA	1 pcs	24	Plastic caps	RP	CAP	2 pcs

Table 2. Manufacturing processes; CT – cycle time, CO – changeover time, AVA - Availability

No	Input	Process	Output	CT [s]	CO [s]	AVA [%]
1	BAR	Deburring I	BRA	180	0	80
2	BRA	Bending	BRA	60	480	90
3E	BRA	External service I: Hot dip galvanizing	BRA	Batch size: 4 pcs Lead time: 1 day		
4	BRA	Deburring II – after galvanizing	BRA	120	0	100
5	PIP	Shipment to a subcontractor	TTU	3 600	0	80
6E	TTU	External service II: 3D laser burning	TTU	Batch size: 4 pcs Lead time: 1 day		
7	TTU	Turning I – universal lathe	TTU	360	600	90
8	BAR	Cutting I – band saw (33 pcs)	MSL TSL	78	1 800	70
9	MSL TSL	Turning II – CNC lathe (33 pcs)	MSL TSL	2 073	7 860	80
10	BAR	Cutting II – cut-off machines	HC FL	2 040	0	100
11	HC FL	Turning III – CNC lathe	HC FL	2 190	4 140	80
12	HC	Turning IV – universal lathe	HC	90	1 800	100
13	FL	Milling – Centrum VZ-700	FL	960	2 160	80
14	STE	Deburring III	EAR PLA CYL BOT TOP	510	0	80
15E	CYL	External service III: Coiling	CYL	Batch size: 4 pcs Lead time: 1 day		
16	CYL BOT TOP	Welding	CBT	2 100	0	90
17	TTU MSL TSL HC FL EAR PLA CBT	Assembly of components	PAP	7 500	0	100
18E	PAP	External service IV: Passivation	PAP	Batch size: 4 pcs Lead time: 1 day		
19	BRA PAP SCR WAS NUT CAP	Final assembly + Pressure test	RP	6 300	7 200	100

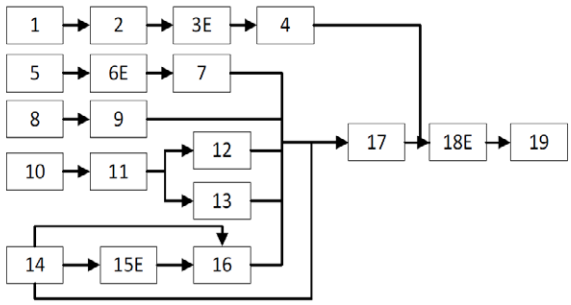

Figure 3. The structure of the manufacturing process

Manufacturing process description

Manufacturing is implemented within the processes presented in Table 2. One operator works in each process. Some processes are realized in co-operation and these are: Hot dip galvanizing (3E), 3D laser burning (6E), coiling (15E) and passivation (18E). Table 2 presents the data concerning the processes i.e. cycle time (CT), changeover time (CO), workstation/machine availability (AVA). Moreover, the information concerning inputs and outputs for each process is presented. In two processes (8 and 9) one additional piece is manufactured. This is due to the poor quality of the processes. Therefore, the need to produce one additional piece is determined in advance. The structure of the manufacturing process is presented in Figure 3.

On the basis of the present manufacturing process structure (Fig. 3) and the data presented in Table 2, CS-VSM was developed and it is presented in the next part of this work.

Current state of the value stream map development and problems identification

The current state of a value stream map (CS-VSM) is presented in Figure 4. The scheme shows that some components are delivered from the outside of the company, directly to the assembly process, and some of them are manufactured in the company. Manufacturing processes of different components are realized in parallel. In the presented case study a time line is divided into a few parts. That is different from what was presented in the work [11]. The time line is situated directly under the processes. The authors consider that the map is easier to read this way.

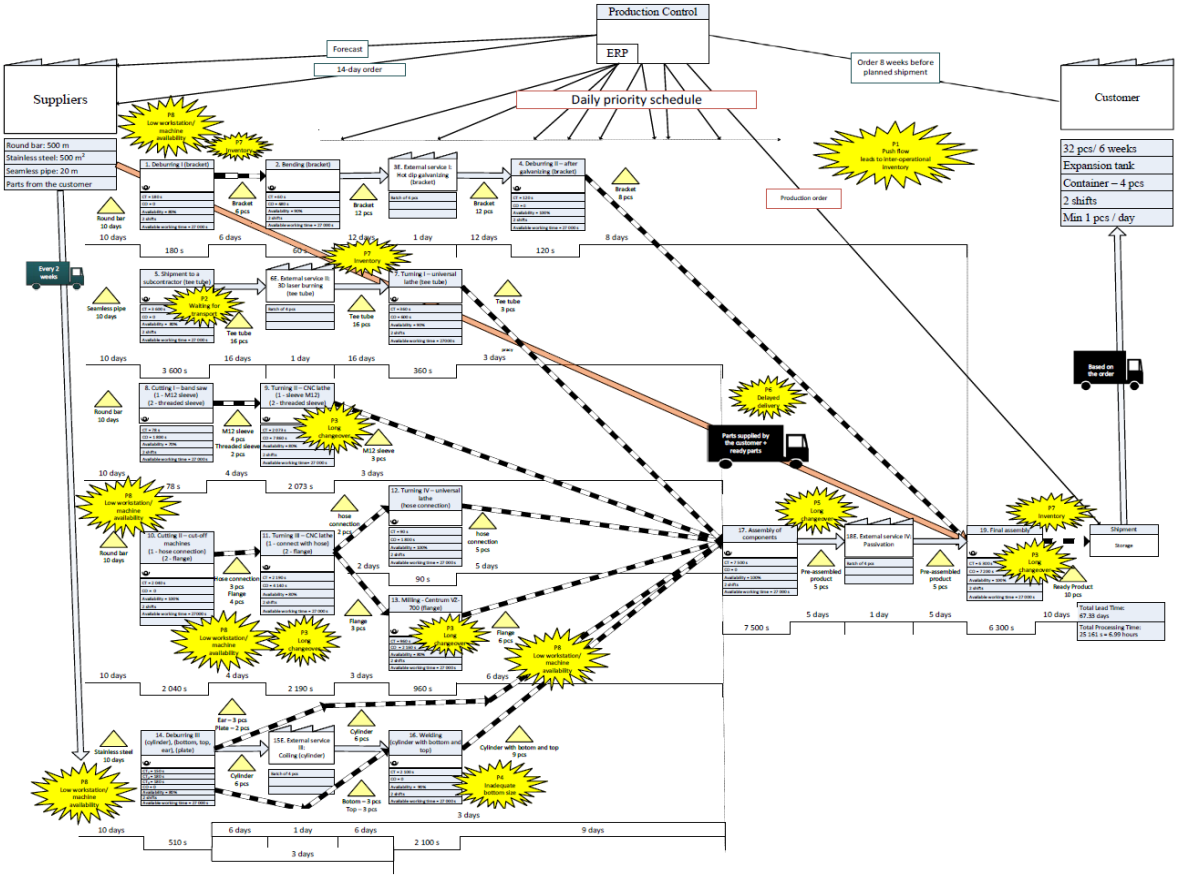

Figure 4. CS-VSM of an expansion tank manufacturing process

The lead time was calculated based on a time line (Fig. 5). For each parallel manufacturing process the lead time (*LTP*) was calculated (equation 1). A critical path defines the length of *LT*, and it was calculated with the use of equation (2).

In the presented case study, in the current state, the lead time LT_{CS} equals 67.33 days. The processing time equals to 28 161 s (469.35 min = 7.82 h). It is too long for *LT* considering that the processes are realized in parallel. Moreover, 67.33 days is too long taking into account that the company has 8 weeks to manufacture the products, i.e. it can start production at the earliest 40 days before delivery. Therefore, it is impossible to deliver the products on time without any problems despite the fact that the takt time (*TT*) equals to 15 hours and CT_s of all processes are shorter than 15 hours.

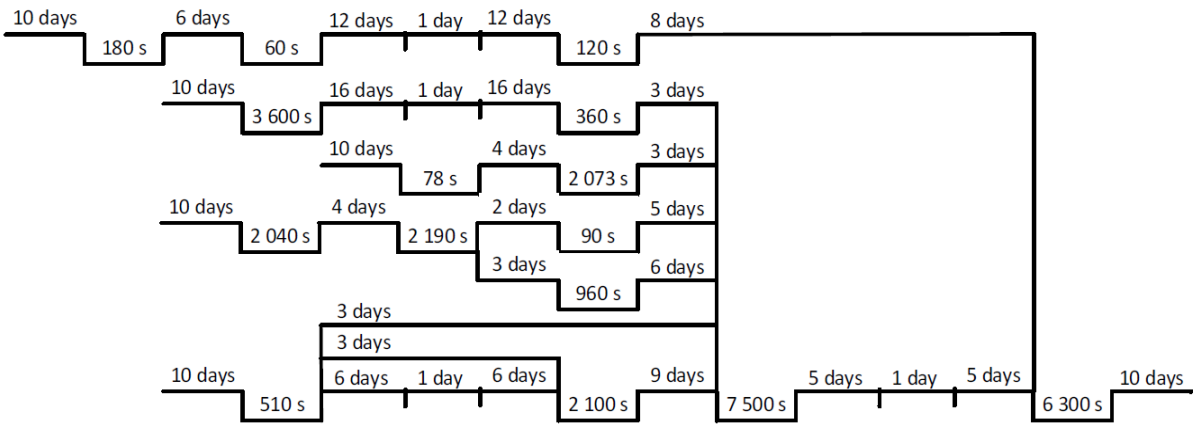

Figure 5. CS-VSM of an expansion tank manufacturing process time line

$$LT_{P-CS} = \begin{bmatrix} \sum_{l=1}^{r} ILT_{1l} + \sum_{l=1}^{v} CT_{1l} \\ \sum_{l=1}^{m} ILT_{2l} + \sum_{l=1}^{s} CT_{2l} \\ \dots \\ \sum_{l=1}^{p} ILT_{kl} + \sum_{l=1}^{q} CT_{kl} \end{bmatrix} = \begin{bmatrix} LT_{P1} \\ LT_{P2} \\ \dots \\ LT_{Pk} \end{bmatrix} = \begin{bmatrix} 59\ days + 6\,660\ s \\ 67\ days + 17\,760\ s \\ 38\ days + 15\,951\ s \\ 42\ days + 18\,120\ s \\ 44\ days + 18\,990\ s \\ 34\ days + 14\,310\ s \\ 43\ days + 16\,410\ s \\ 53\ days + 16\,410\ s \end{bmatrix} = \begin{bmatrix} 59.12\ days \\ 67.33\ days \\ 38.29\ days \\ 42.33\ days \\ 44.35\ days \\ 34.27\ days \\ 43.30\ days \\ 53.30\ days \end{bmatrix} \quad (1)$$

where: *ILT* – inventory lead time, *CT* – cycle time, *LTP* – lead time for a path, *l* – a number of process steps, *k* – a number of paths

$$LT_{CS} = \max\{LT_{CS1}, LT_{CS2}, \dots, LT_{CSn}\} = 67.33\ days \quad (2)$$

The current state was studied and the following problems were discovered. The problems were analysed and proposals for improvement were offered.

Problem 1. Push system. In the current state the push system was applied. It was because different kinds of tanks being in the same product family were ordered by customers in different time periods. This way, in one period of time only one kind of expansion tanks was manufactured. Therefore, the company decided to push production to obtain this product which was ordered first to be ready. This way, the Lead Time (*LT*) was long. The implementation of a pull system with the introduction of FIFO lanes and supermarkets with kanbans can be the solution then.

Problem 2. Waiting for transport to collaborators and long preparation time. The manufacturing process cannot be realized fully in the company. Therefore, the company uses external services. This concerns four processes (3E-Hot dip galvanizing, 6E-3D laser burning, 15E-Coiling and 18E-Passivation). Components and products have to be sent to collaborators. Sometimes it causes problems of waiting for transport and this, in turn, increases the inventory of the products waiting to be sent to collaborators who are currently responsible for the transport process. The solution proposed is that the company takes the responsibility for the transport process and an additional training for the employees who prepare transport in order to decrease the preparation time. The training additionally decreased the processing time of process 5 from 3 600 s to 600 s.

Problem 3. Long changeover time. The next problem concerns a long changeover time in the processes: Bending (2), Turning (7, 9, 11, 12), Cutting (8), Milling (13) and Final assembly (19). In order to decrease a changeover time the SMED method was recommended for the implementation.

Problem 4. Inadequate components waiting for a process. Another problem which was discovered was connected to inadequate components (e.g. bottoms) which were waiting for an assembly process. In order to solve this problem, 5S method is the best solution to be introduced. Other solutions of this problem include visualization or Poka Yoke implementation.

Problem 5. Long processing time. Long processing times (*PT*) in the last processes (17). Assembly of components – 2.1 hours and 19. Final assembly – 1.75 hours) are much longer than PT_s of other processes, what additionally increases *LT*. In these processes two operators could possibly work. That might shorten the processing times by half.

Problem 6. Component delivery delays. Delayed deliveries of components from the customer were another problem. The customer does not deliver the components together with an order but later, not always on time. Therefore, the company has to wait with the assembly process for the delivery. The implementation of supermarkets for the components from the customer should solve this problem.

Problem 7. High inventories. The problem is caused by the existing push system and the lack of the implementation of inventory limits. The solution is to introduce a pull system, supermarkets, and/or FIFO lanes.

Problem 8. Low workstations/machines availability. The last identified problem concerns workstations/machines availability. However, because the takt time (*TT*) is much longer than CT_s. Currently, this problem does not influence the manufacturing process. The problem can become serious if the production volume increases. Therefore,

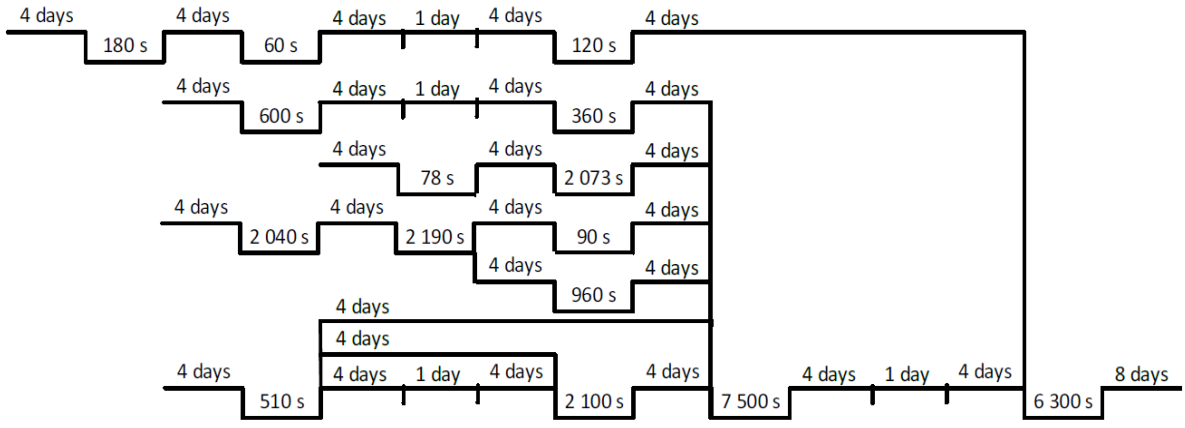

Figure 6. FS-VSM of an expansion tank manufacturing process time line

Figure 7. FS-VSM of an expansion tank manufacturing process

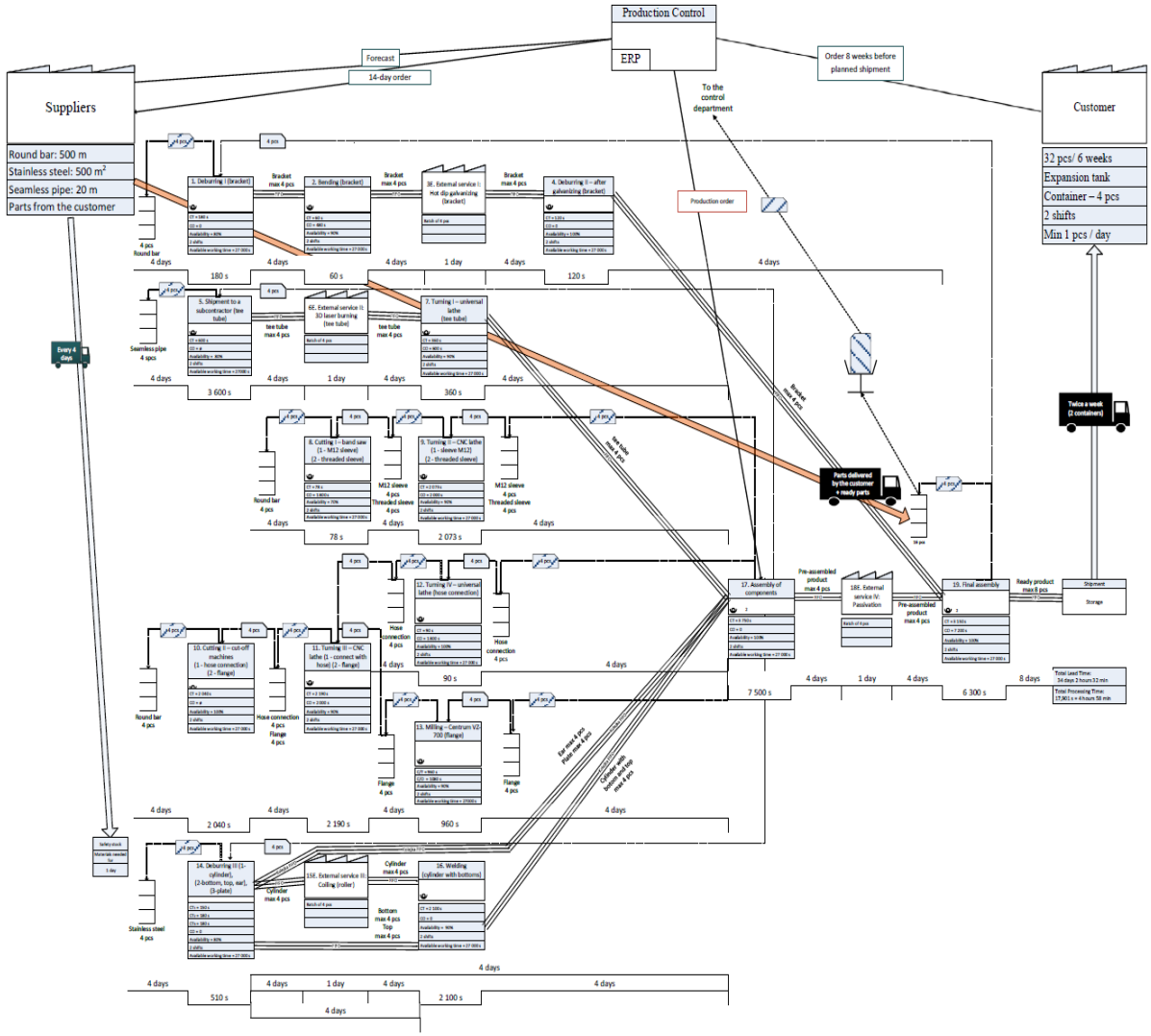

the problem was not analysed in this work. Moreover, in the current calculations some simplifications were made. Namely, an available working time for each process was assumed as 27 000 s.

Future state of the value stream map

The presented solutions allowed proposing the future state of a value stream map (FS-VSM).The implementation of the FIFO lanes and supermarkets allowed to decrease *LT*. A lead time for the future state was calculated based on a time line (Fig. 6). FS-VSM is presented in Figure 7.

For each parallel manufacturing process a lead time (*LTP*) was calculated (equation 3). The critical path defines the length of *LT*. It was calculated with the use of equation (4).

$$LT_{P-FS} = \begin{bmatrix} 29\ days + 6\,660\ s \\ 34\ days + 14\,760\ s \\ 29\ days + 15\,951\ s \\ 33\ days + 18\,120\ s \\ 33\ days + 18\,990\ s \\ 25\ days + 14\,310\ s \\ 29\ days + 16\,410\ s \\ 34\ days + 16\,410\ s \end{bmatrix} = \begin{bmatrix} 29.12\ days \\ 34.27\ days \\ 29.29\ days \\ 33.33\ days \\ 33.35\ days \\ 25.27\ days \\ 29.30\ days \\ 34.30\ days \end{bmatrix} \quad (3)$$

$$LT_{FS} = \max\{LT_{Cs1}, LT_{Cs2}, \ldots, LT_{Csn}\} = 34.30\ days \quad (4)$$

The pull system with kanbans, supermarkets and FIFO lanes, proposed in FS-VSM, allowed decreasing *LT* to LT_{FC} that equalled 34.3 days. Since the customer is asked to make an order 8 weeks (40 working days) before the shipment of a product, it is enough time to deliver the products on time. Finally, the improvements were assessed with the use of *LTI* (equation 5) and *VAI* (equation 6).

$$LTI = (LT_{CS} - LT_{FS})/LT_{CS} = (67.33\ days - 34.3\ days)/67.33\ days = 0.49 \quad (5)$$

$$VAI = (PT_{CS} - PT_{FS})/PT_{CS} = (28\ 161\ s - 25\ 161)/28\ 161\ s = 0.1 \quad (6)$$

On the basis of *LTI* and *VAI* it can be concluded that *LT* decreased by 49% and the processing time decreased by 10%. It is known that the processing time of the current state (PT_{CS}) equals to 28 161 s and the processing time of the future state (PT_{FS}) equals to 25 161 s. In order to achieve this improvement, the presented proposals for the problem elimination have to be implemented. If not, the achievement might not be obtained or it might be smaller.

Summary

In the presented case study the manufacturing process of an expansion tank was analysed. On the basis of the collected data, the current state of a value stream map was developed and then analysed. The identified problems were discussed and some solutions were proposed. Next, the future state of a value stream map was created taking into account the proposed solutions. The lead times for CS-VSM and FS-VSM were calculated. The goals set for the work have been achieved. *LT* for the future state equals to 38.52 days and it is lower than the maximal (40 days).

The presented work has some limitations. In the calculations, the workstations/machines availability was assumed as 100%. It means that the time of 27,000s was taken as an available working time for each process. However, in reality the availability was lower and equalled, in the presented case study to 100%, 90%, 80% to even 70% in case of a cutting process (7). The availability reduction was not taken into consideration because in the analysed case study *TT* was much higher than CTs of the manufacturing processes. However, in other cases the decreased availability has to be considered and it will be discussed in the future studies.

References

[1] Balaji M., Manivel Muralidharan V., Victor Prathaban, N., & Vinoth, D. 2019. "Productivity enhancement using lean tools in low volume production". International Journal of Mechanical and Production Engineering Research and Development 8(Special Issue 7): 77-86. DOI:10.24247/ijmperdoct201810.

[2] Belekoukias I., Garza-Reyes J. A., Kumar V. 2014. „The impact of lean methods and tools on the operational performance of manufacturing organisations". International Journal of Production Research 52(18): 5346-5366. DOI:10.1080/00207543.2014.903348

[3] Bukowska B. 2019. "Mapping the value stream of the tank production process". Diploma thesis under supervision of Dorota Stadnicka. Rzeszow.

[4] Carvalho C. P., Carvalho D. S., Silva M. B. 2019. "Value stream mapping as a lean manufacturing tool: A new account approach for cost saving in a textile company". International Journal of Production Management and Engineering 7(1): 1-12.

[5] Dadashnejad A-A., Valmohammadi C. 2019. "Investigating the effect of value stream mapping on overall equipment effectiveness: a case study". Total Quality Management & Business Excellence 30:(3-4): 466-482. DOI: 10.1080/14783363.2017.1308821.

[6] Kale S. V., & Parikh R. H. 2019. "Lean implementation in a manufacturing industry through value stream mapping". International Journal of Engineering and Advanced Technology 8(6 Special issue): 908-913. DOI:10.35940/ijeat.F1172.0886S19.

[7] Manikandaprabu S., Anbuudayasankar S. P. 2019. "Productivity improvement through lean manufacturing". International Journal of Engineering and Advanced Technology 8(5): 2657-2660.

[8] Masuti P. M., & Dabade U. A. 2019. „Lean manufacturing implementation using value stream mapping at excavator manufacturing company". Materials Today: Proceedings 19: 606-610.

[9] Parab P. A., & Shirodkar V. A. 2019. „Value stream mapping: A case study of lock industry". Paper presented at the AIP Conference Proceedings 2148. DOI:10.1063/1.5123963.

[10] Rother M., Shook J. 2003. "Learning to see: value stream mapping to add value and eliminate muda". Lean Enterprise Institute.

[11] Stadnicka D., Ratnayake R. C. 2017. „A VSM and VSA methodology for performance assessment of complex product manufacturing processes: an industrial case study". International Journal of Product Development 22(2): 104-134.

[12] Wicaksono S. R., Setiawan R. 2019 March. "Lean Manufacturing Machine using Value Stream Mapping". Journal of Physics: Conference Series 1175(1): 012118. IOP Publishing.

Barbara Bukowska, M.Sc.
Faculty of Mechanical Engineering and Aeronautics
Rzeszow University of Technology, Poland

Dorota Stadnicka, Ph.D., D.Sc.,
Faculty of Mechanical Engineering and Aeronautics
Rzeszow University of Technology, Poland
e-mail: dorota.stadnicka@prz.edu.pl

TiAM TECHNOLOGIA I AUTOMATYZACJA MONTAŻU kwartalnik naukowo-techniczny ZESPOŁÓW • MASZYN • URZĄDZEŃ

www.tiam.pl
tiam@sigma-not.pl
tel. 22 853 81 13

ANALYSIS OF THE GRINDING FORCE COMPONENTS AND SURFACE ROUGHNESS IN GRINDING WITH THE USE OF A GLASS-CRYSTALLINE BONDED GRINDING WHEEL

Analiza składowych siły szlifowania oraz chropowatości powierzchni podczas szlifowania z użyciem ściernicy ze spoiwem szklanokrystalicznym

Marcin ŻÓŁKOŚ **ORCID: 0000-0003-0377-1428**

DOI: 10.15199/160.2020.1.7

Abstract: The article concerns an investigation of 100Cr6 steel surface peripheral grinding process with glass-crystalline bonded grinding wheels. More precisely the investigation of surface roughness parameters and grinding force components in relation to different dressing overlap ratio, feed rate and grinding depths values. Seven different values of dressing overlap ratio have been used to determine influence of dressing overlap ratio to grinding force and surface roughness. After determining the stable range of dressing overlap ratio, other tests were conducted with eleven different values of feed rate and two values of grinding depth to determine how they shape the grinding force components and surface roughness parameters. The machining has been performed using a CNC surface grinding machine, together with a surface grinding wheel and up grinding strategy. Additional NI equipment was used for grinding force data acquisition. The surface roughness was assessed using two parameters (*Ra, Rz*). The contact measurements of surface roughness were carried out using the MarSurf PS 10 profilometer. The dresser effective width was measured with the use of AM7515MZT Dino-Lite microscope to ensure consistent values of dressing overlap ratio throughout the entire experiment. Significant impact of the dressing overlap ratios, feed rate and grinding depths on the grinding force components F_n and F_t*as* well as the roughness parameters *Ra* and *Rz* were obtained.
Keywords: grinding, grinding force components, surface roughness, dressing overlap ratio, glass-crystalline bond

Streszczenie: Artykuł dotyczy badań procesu szlifowania obwodowego stali 100Cr6 za pomocą ściernic o spoiwie szklanokrystalicznym. Dokładniej dotyczy badań parametrów chropowatości powierzchni i składowych siły szlifowania w odniesieniu do różnych wartości wskaźnika pokrycia przy obciąganiu, posuwu i głębokości szlifowania. Siedem różnych wartości wskaźnika pokrycia przy obciąganiu zostało wykorzystanych do określenia wpływu wskaźnika pokrycia na siłę szlifowania i chropowatość powierzchni. Po określeniu stabilnego zakresu wskaźnika pokrycia przy obciąganiu przeprowadzono kolejne badania z jedenastoma różnymi wartościami posuwu i dwiema wartościami głębokości szlifowania, aby określić ich wpływ na składowe siły szlifowania i parametry chropowatości powierzchni. Obróbka została wykonana przy użyciu szlifierki CNC do płaszczyzn wraz ze ściernicą obwodową i strategią szlifowania przeciwbieżnego. Dodatkowo do pomiarów siły szlifowania zostało wykorzystane oprzyrządowanie NI. Chropowatość powierzchni została oceniona za pomocą dwóch parametrów (*Ra, Rz*). Pomiary stykowe chropowatości powierzchni przeprowadzono przy użyciu profilometru MarSurf PS 10. Czynna szerokość obciągacza była mierzona przy użyciu mikroskopu Dino-Lite AM7515MZT, aby zapewnić stałe wartości wskaźnika pokrycia przy obciąganiu w trakcie wszystkich wykonywanych badań. W efekcie uzyskano istotny wpływ wskaźnika pokrycia przy obciąganiu, posuwu i głębokości szlifowania na składowe siły szlifowania F_n i F_t oraz na parametry chropowatości *Ra* i *Rz*.
Słowa kluczowe: szlifowanie, składowe siły szlifowania, chropowatość powierzchni, wskaźnik pokrycia przy obciąganiu, spoiwo szklanokrystaliczne

Introduction

Grinding is a process of subtractive machining, which may have the character of a precise finishing machining or highly efficient subtractive machining [22, 23]. There are many types of grinding, such as, among others, surface peripheral and face grinding, longitudinal shafts grinding, hole grinding [23, 26]. In order to carry out the grinding process, it is necessary to use appropriate machine tools and grinding wheels.

Grinding is still one of the basic processes for finishing operations, where peripheral grinding is widely used for precise surface grinding. Grinding wheel wear, geometric accuracy and surface quality of workpiece are greatly influenced by grinding forces [25]. The ability to predict grinding force components is important in many aspects of grinding process optimization, monitoring and control [4]. In this context, research into the modeling and calculation of grinding forces is current, necessary and constantly being developed.

The main directions of the development of grinding processes can be divided into three main groups, such as hybrid processes, new kinematic varieties and modifications of grinding wheel structure. The development of abrasive tools is a complex issue including, among others, works on new abrasive materials and binders,

which together define the structure of grinding wheels. The possibility of influencing on the structure of a grinding wheel is also a modification of the existing types of binders or abrasive materials [15, 17, 18].

The basic task of the binder is to bond the abrasive grains in the abrasive tool. It determines the properties of the tool, proper maintenance of the abrasive grains, proper porosity, maintaining the shape accuracy of the grinding wheel and determines the dressing method [13, 26]. The bond therefore has a decisive influence on the grinding wheel active surface (GWAS), which is shaped both in the dressing process and in the grinding wheel self-sharpening process. One of the most widely used types of binders in tools with conventional abrasives are ceramic bonds [13, 15]. One of the variations of these binders is glass-crystalline binders, which are characterized by a different mechanism of propagation of cracks in the bridges of the binder in relation to glass binders. That characteristic translates into the ability of the binder to micro-chipping in a similar manner as it takes place in grains of microcrystalline sintered corundum [7, 9, 19].

Herman [5] and Herman et al. [6, 8] conducts research on the construction, production and physical proper-ties of glass-crystalline binders and the manufacturing of new varieties of glass-crystalline binders. Nadolny et al. [16, 19 ─ 21] conducts technological research on grinding wheels with glass-crystalline bond and grains of microcrystalline sintered alumina in the process of holes grinding. Other research on the production of different varieties of glass-crystalline binders [2, 10, 11, 14, 24] do not include extended and accurate technological research of abrasive tools with such binders in the process of peripheral surface grinding. This state of affairs determines the necessity of conducting research on glass-crystalline binders in the process of peripheral grinding of surfaces and their improvement.

Conducted experimental tests concerned the 100Cr6 surface peripheral grinding process with the use of innovative grinding wheels with glass-crystalline bond. Their goal was to determine the influence of dressing overlap ratio, feed rate, grinding depth on grinding force components and surface roughness parameters. So it would be possible to specify the dressing overlap value. Also to select feed rate and grinding depth values ranges for further more extended experiments.

Research methodology and experimental conditions

To accomplish that goal samples in the form of cuboids (length of 50 mm and width of 30 mm), made of 100Cr6 steel, were prepared and used as the workpieces in the conducted experiments. The samples were through hardened and tempered to 60 ±2 HRC hardness. The workpieces were machined on the test stand described in the subsection „The grinding process" and shown in Figure 1.

As the machining tool the Andre Abrasive Articles grinding wheel (type 7), was used, with a two-sided cylindrical recess A. The tested grinding wheel with designation M3X60H8VTHE-35 had medium sized abrasive grains (average grain size - 275 μm) made of monocrystalline corundum, with a 30% share of microcrystalline electro-corundum. The tool that was used for research was bonded with modified vitrified binder that has glass-crystalline structure.

The abovementioned material samples were machined and measured using the machining and measurement parameters, which are presented in Table 1. As the results of conducted experiments the grinding force components (normal *Fn* and tangential *Ft*) and surface roughness parameters (*Ra* and *Rz*) were acquired. Based on that results correlations between grinding force components/surface roughness parameters and dressing overlap ratio/feed rate/grinding depth were obtained.

• The grinding process

The experimental part of the research (mechanical machining) was carried out using the CNC test stand. The test stand (see Figure 1) was developed for the needs of the research revolved around grinding wheels with modified vitrified binders [3, 27]. The Geibel & Hotz GmbH FS 640 Z surface grinding machine was the main part of this test stand. The stand has been equipped with Kistler type 9121 piezoelectric dynamometer, Kistler Type 5019 A amplifier, NI CompactDAQ system and LabVIEW SignalExpress software that together allowed the measurement of grinding force components.

The stand was also equipped with a high pressure cooling system, in which a coolant in the form of a 5% synthetic emulsion was fed into the grinding zone, over the entire width of the grinding wheel, by means of a needle nozzle at a pressure of 1 MPa, which corresponded to a volumetric flow rate of 22 l/min [1, 12]. For coolant pressure readout and control there was pressure sensor installed and DC power supply with desktop multimeter added to the test stand.

The tests were carried out in the surface peripheral up grinding setup with constant grinding speed value and varying values of feed rate, grinding depth and dressing overlap ratio (refer to Table 1). Before each measurement pass, the dressing of the grinding wheel with single grain diamond dresser was performed with specific set of parameters, which are presented in Table 1. After dressing one machining pass was made with grinding depth 0.002 mm and feed rate 20000 mm/min to remove loose grains remaining after the sharpening process of

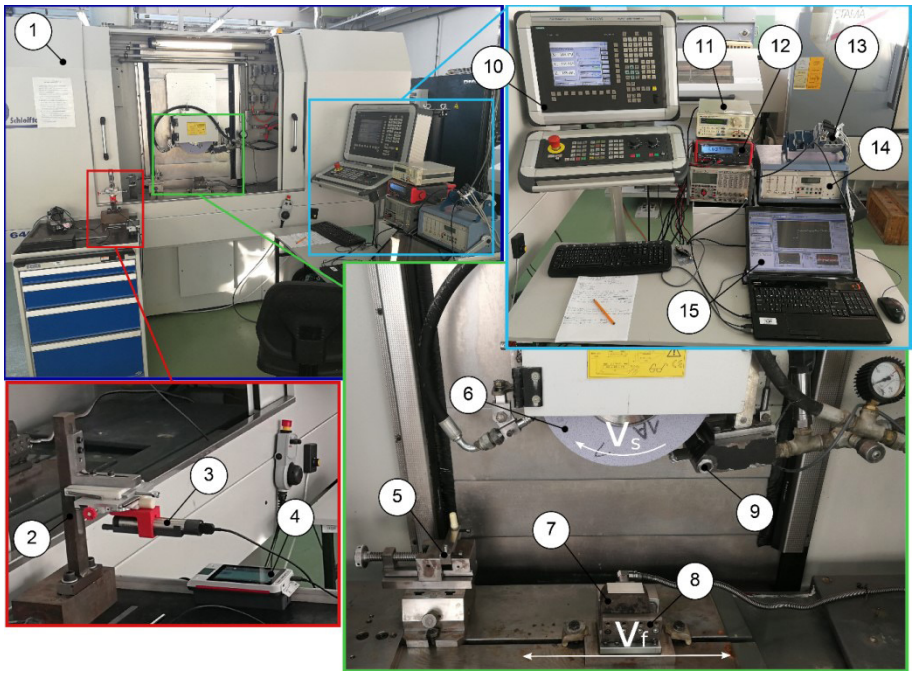

Fig. 1. Configuration of the test stand: 1 – G+H FS 640 Z surface grinding machine, 2 – mounting holder for profilometer drive unit,3 - MarSurf PS 10 profilometer drive unit, 4 - main unit of MarSurf PS 10 profilometer, 5 – diamond dresser, 6 – grinding wheel, 7 – workpiece, 8 – dynamometer, 9 – needle nozzle for coolant distribution, 10 – machine control panel, 11 – DC power supply, 12 – desktop multimeter for coolant pressure readout, 13 – NI CompactDAQ system, 14 – Kistler 5019 A amplifier, 15 – computer with LabVIEW SignalExpress software

the grinding wheel. Afterwards a machining pass took place, for which values of the normal and tangential component of the grinding force were recorded. After the measurement pass, ten sparking passes were made to provide a constant machining allowance for the next pass. Grinding was performed with specific technological parameters whose values are shown in the Table 1. Values of the grinding force components were recorded for each machining pass, which were repeated three times for one set of technological parameters.

- **Measurements of surface roughness parameters**

The measurements of surface roughness parameters were performed with the use of the MarSurf PS 10 profilometer directly at the surface grinding machine without removing workpieces from dynamometer (refer to Figure 1). Measurements were performed for all 18 different combinations of technological parameters values. Parameters of every roughness measurement are listed in Table 1. Three measurements replications of the analyzed surface roughness parameters *Ra* and *Rz* were carried out. They were done after every repetition of the machining pass with different set of technological parameters values. The surface roughness measurements were executed in perpendicular direction to the feed rate. A total number of 162 single surface roughness measurements were made for all the investigated technological parameters values combinations.

Table 1. Parameters of machining and measurement processes

Parameters of grinding process	Parameters of dressing process	Parameters of surface roughness measurement
Andre Abrasives Articles surface grinding wheel- 7-300x50x76.2 P150;F10;G10 M3X60H8VTHE-35 5% synthetic coolant mixed with water cutting fluid pressure, p = 1 MPa cutting fluid volumetric flow, q = 22 l/min grinding speed, v_c = 40 m/s feedrate, v_f = 4000 / 7000÷35000 mm/min grinding depth, a_e = 0.02 / 0.03 m	single-grain diamond dresser dressing peripheral speed, v_d = 25 m/s dressing depth, a_{ed} = 0.02 mm dressing overlap ratio, u_d = 1.5÷10 /4 dressing passes - 5	traversing length, l_t = 4.8 mm evaluation length, l_n = 4.0 mm max. probe tip radius, r_{tip} = 2 µm sampling length, lr = 0.8 mm scanning speed, v_t = 1.0 mm/s measurement resolution - 8 nm number of repetition - 3

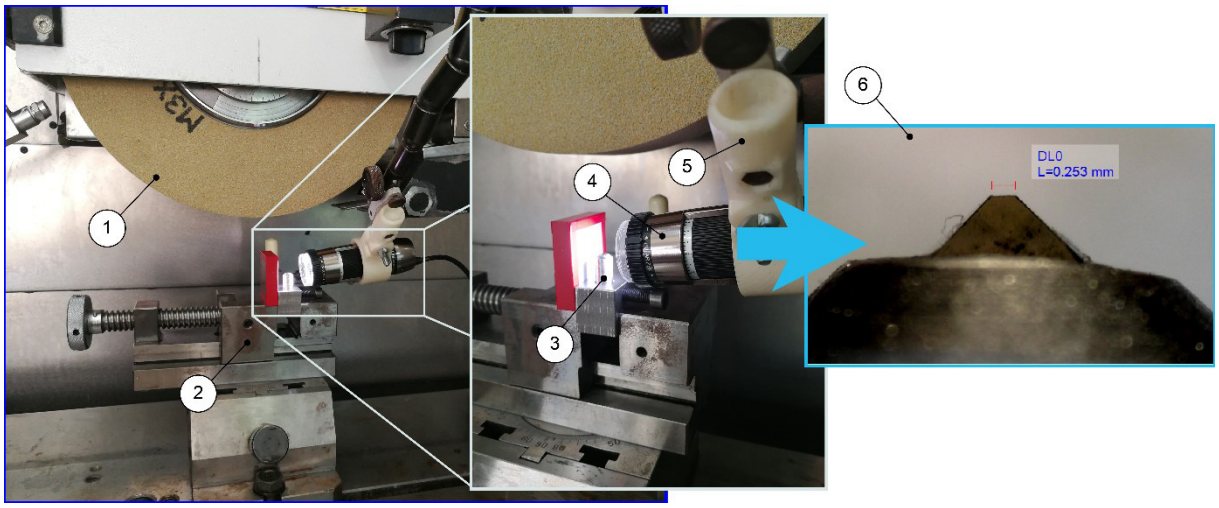

Fig. 2. Test stand configuration for diamond dresser measurements: 1 – grinding wheel, 2 – grinding vise, 3 – diamond dresser, 4 – AM7515MZT Dino-Lite portable microscope, 5 – adjustable holder, 6 – microscope diamond dresser view with width measurement result

- **Measurements of dresser effective contact width**

In order to achieve the specified U_d values, the width of the dresser was measured before each dressing process to adjust the feed rate of the grinding wheel at dressing to maintain the specified U_d value. Also, in some tests, where the U_d parameter remained constant, it was necessary to continuously check the width of the dresser. This was required to keep the value of this ratio constant. Therefore, the AM7515MZT Dino-Lite portable microscope was used to measure the width of the dresser before each dressing pass. The microscope was calibrated to read the correct width values before the measurements were taken. The microscope, when properly placed in the holder attached to the grinding wheel housing, allowed the evaluation of the condition of the dresser and measurements of the active dresser width in the grinding machine working area (see Figure 2). This eliminated the need to remove the dresser from the machine and to repeat after each measurement the setup steps on the machine.

The results and discussion

On figure 3 there are presented average values of the normal F_n and tangential F_t grinding force components in relation to dressing overlap ratio U_d.

Calculated confidence intervals for 3 measurement repetitions (per each of the grinding force component) executed at each different dressing overlap ratio value are shown on the graph. The applied significance level was 0.05. The obtained values of the F_n and F_t components indicate significant differences in grinding force components among different values of dressing overlap ratio. The lowest values were obtained for the smallest U_d value, which were 68 N for normal component and 31 N for tangential component. The highest values were obtained for the largest value of U_d ratio: 197 N and 83 N respectively. This corresponds to 190% increase for F_n component and 168% increase for F_t component. In both cases for normal and tangential components the positive correlation to dressing overlap ratio can be seen on the graph below. In addition, the local minimum of the force component values for a dressing overlap ratio of 3 can be observed.

For the smallest U_d ratio the lowest forces occur, because we get the most aggressive GWAS due to higher pulling forces in the dressing process. They are caused by the higher dressing feed rate (the lower the U_d ratio, the higher the dressing feed rate v_d). This results in a smaller contact area between the grains and the workpiece surface during cutting. While the dressing overlap ratio increases the dresser smoothes the grain surface by blunting rather than pulling it out or chipping. This translates into increased forces due to the increased contact area between the grains and the machined surface. For U_d ratio, we can indicate a stable

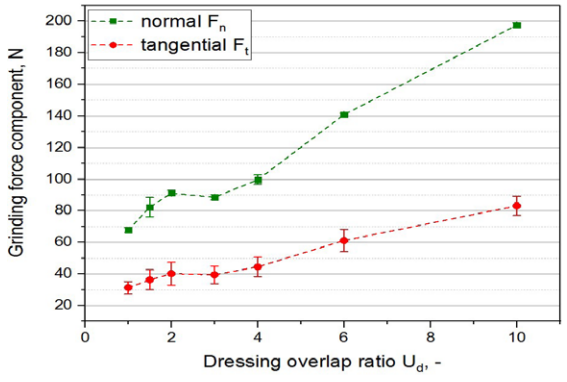

Fig. 3. The results of F_n/ F_t grinding force component measurements vs. dressing overlap ratio

range of values from 2 to 4. Smaller values should be ignored, as it will be difficult to maintain its exact value in this range (inaccuracy in measuring the width of the dresser), which can translate into cutting a helix line into a GWAS that will affect the quality of the grinded surface. In addition, in the range below 2 there is definitely the fastest wear of the dresser. On the other hand, values above 4 contribute to higher forces in the process, which can cause surface damage. Larger values of U_d ratio also increase significantly the time of the dressing process, which results in a longer total machining time.

Figure 4 indicates average values of the grinding force components in relation to feed rate v_f.

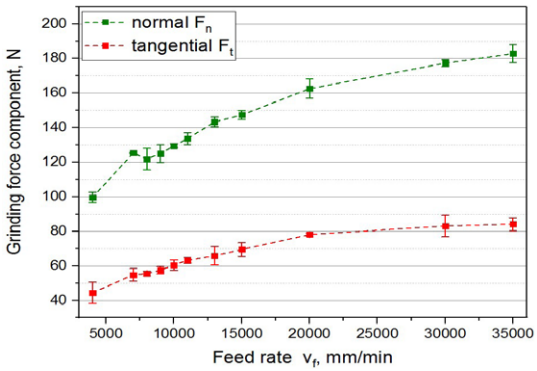

Fig. 4. The results of Fn / Ft grinding force component measurements vs. feed rate

This may be caused by the higher strength of the glass-crystalline bond compared to the traditional ceramic bond. The glass-crystalline bond requires higher forces to tear out and chip out the blunted grain. Therefore, in the range of v_f up to 20000 mm/min, dulled grains are kept in the binder all the time, causing an increase in forces. On the other hand, above v_f 20000 mm/min there are enough large forces that allow to occur the grinding wheel selfsharpening process and reduction of the forces value gradient for higher feed rates.

Figure 5 presents average values of the normal F_n and tangential F_t grinding force components in relation to grinding depth a_e.

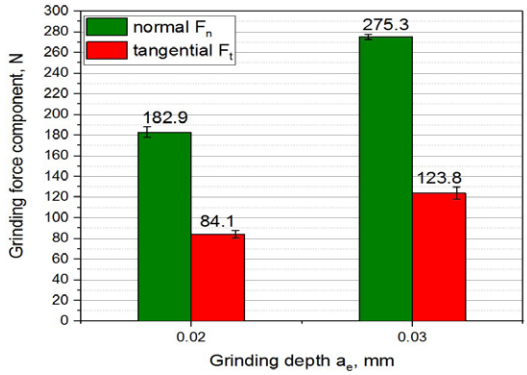

Fig. 5. The results of Fn and Ft grinding force component measurements vs. grinding depth

In the case of measurements of the impact of feed rate on the components of grinding forces, the conditions were adopted as for previous tests. The obtained values of the F_n and F_t components indicate significant differences in grinding force components among different values of feed rate. The lowest values were obtained for the feed rate of 4000 mm/min and the highest for the 35000 mm/min feed rate. The lowest values of F_n component and F_t component were 100 N and 44 N. The highest values were 183 N and 84 N accordingly. That corresponded to 83% increase for normal component and 91% for tangential component. As in figure 3, the above graph shows a small break of the normal grinding force component for a feed rate of 8000 mm/min. For both grinding force components the positive correlation to feed rate can be observed on the Figure 4.

The obtained graph of dependence of the grinding force component values confirms their dependence on the feed rate in grinding processes - increase of the forces values together with the feed rate increase. What is interesting, however, above the feed rate value of 20000 mm/min there does not occur a significant increase in grinding forces, which takes place in the range from 4000 to 20000 mm/min. This indicates that grinding wheels with this bond perform better in tougher conditions.

On the graph are also marked the calculated confidence intervals for 3 measurement repetitions (per each of the grinding force component) executed at two grinding depth values. The applied significance level was the same as in previous tests. The obtained values of the F_n and F_t components indicate significant differences in grinding force components among different values of grinding depth. The lower values were obtained for the ae equal to 0.02 mm, which were 183 N for normal component and 84 N for tangential component. The higher values were obtained for the 0.03 mm value of ae: 275 N and 124 N respectively. This corresponds to 50% increase for F_n component and 48% increase for F_t component. In both cases for normal and tangential components their values are bigger while grinding depth increases.

The graph above thus confirms the same dependence of forces from the grinding depth for grinding wheels with glass-crystalline bond and ceramic bond. However, in order to fully confirm this statement, additional research will be required in a wider range of grinding depth values.

Figure 6 presents average values of the *Ra* and *Rz* parameters in relation to overlap dressing ratio U_d.

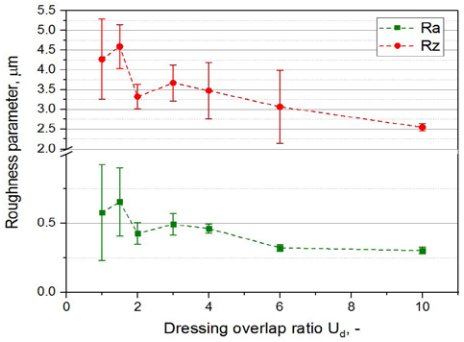

Fig. 6. The results of *Ra* / *Rz* parameter measurements vs. dressing overlap ratio

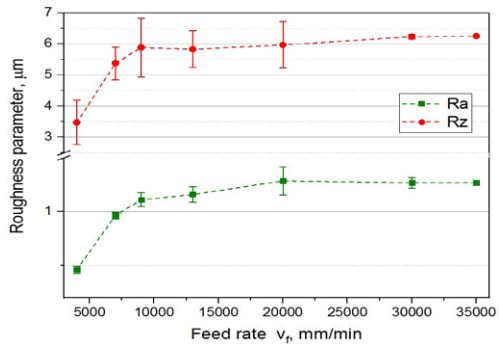

Fig. 7. The results of *Ra* / *Rz* parameter measurements vs. feed rate

The calculated confidence intervals for 7 different dressing overlap values (3 machining passes per each Ud value and 3 measurement repetitions per each machining pass) are shown on the graph. The applied significance level was 0.05. The obtained values of the *Ra* and *Rz* parameters indicate significant differences in surface roughness among different dressing overlap ratio values. The lowest roughness parameters values were obtained for the biggest U_d values, and the highest ones for the lowest U_d values.

On the above chart it can be observed that for smaller values of the dressing overlap ratio there are larger confidence intervals. It is especially visible for the obtained values of the roughness parameter *Ra*. For the results of the parameter *Rz*, the spread of results values is greater for the vast majority of measurement points. Due to the characteristics of this roughness parameter, the *Rz* parameter is more sensitive to single defects in the measured profile that interfere with the final result. This is confirmed by the previously determined stable U_d ratio range for the dressing overlap ratio dependence on the grinding force components. Of course, the surface roughness for higher values of the dressing overlap ratio is lower, but this results in a significant increase in the grinding force value. The obtained roughness dependence on the dressing overlap ratio allows us to determine the best value for further research. For value 4 we obtain the smallest spread of values for a given stable range of dressing overlap ratio. This may indicate a more stable process of dresser wear and reduced wear value for this exact value U_d.

Figure 7 presents average values of the *Ra* and *Rz* parameters in relation to feed rate v_f.

On the graph are also marked the calculated confidence intervals in the same way as in previous tests. The obtained values of the *Ra* and *Rz* parameters indicate significant differences in surface roughness among different feed rate values. The lowest roughness parameters values were obtained for the lowest v_f values, and the highest ones for the biggest v_f values.

In the graph above it can be observed that for *Ra* and *Rz* parameters from 9000 mm/min, the gradient of change of *Ra* and Rz values depending on the change of the feed rate is significantly reduced. This leads to very similar results for surface roughness parameters above the feed rate thresholds values given above. It may be associated with the phenomenon of micro-chipping of abrasive grains and glass-crystalline binder, which ensures stabilization of the GWAS profile, translating into stabilization of the roughness parameters *Ra* and *Rz*. Similarly as in the graph 6 for the results of the parameter *Rz* confidence intervals are larger for the vast majority of measurement points, compared to the results of the *Ra* parameter.

Figure 8 presents average values of the *Ra* and *Rz* parameters in relation to grinding depth a_e.

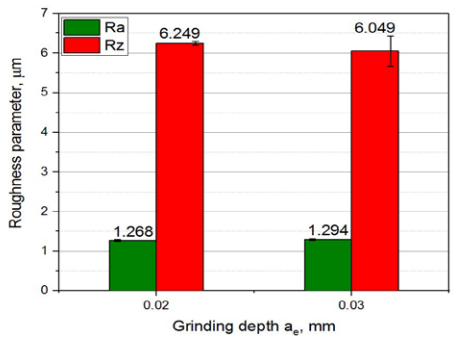

Fig. 8. The results of *Ra* / *Rz* parameter measurements vs. grinding depth

The calculated confidence intervals (the same significance level as stated before) for 3 measurements executed for each machining pass repetition at two grinding depth values are marked on the graph. The obtained values of the *Ra* and *Rz* parameters indicate no significant differences in surface roughness among different grinding depth values. The *Ra* roughness parameter values were practically the same for both grinding depth values. It was similar in the case of *Rz* parameter, but for grinding depth equal to 0.03 mm there was bigger confidence interval.

From the above obtained dependence of roughness parameters on grinding depth for grinding wheels with glass-crystalline bond it can be concluded that the grinding depth does not influence the roughness value. However, in order to confirm this thesis, it is necessary to perform more thorough research for a larger number of measuring points.

Conclusions

As the results of the study, the impact of the dressing overlap ratios, feed rate and grinding depths on the grinding force components F_n and F_t, as well as the roughness parameters *Ra* and *Rz* were obtained. The obtained results allow stating the following conclusions:

- For investigated grinding process the stable range for dressing overlap ratio is U_d = 2.0÷4.0.
- For further research, the ratio U_d = 4.0 have been selected due to the more stable process of dresser wear and smaller wear value during the grinding wheel sharpening process, which manifests itself in a smaller spread of *Ra* and *Rz* surface roughness parameter values as well as comparable grinding force components values compared to U_d values 2 or 3.
- Increase of dressing overlap ratio U_d from the lowest to the highest considered value results in 190% increase of normal force F_n and a 168% increase of tangential force F_t. In addition dressing overlap ratio increase results in increasing the surface roughness parameters *Ra* and *Rz*.
- Increase of feed rate from the lowest to the highest value results in 83% increase of normal force F_n and a 91% increase of tangential force F_t. For *Ra* and *Rz* parameters the increase of feed rate results in an initial increase in their value, but later on the stabilization of the surface parameters values occur.
- Increase of grinding depth by 0.01 mm results in 50% increase of normal grinding force component F_n and a 48% increase of tangential component F_t. Grinding depth increase does not significantly affect the change of surface roughness parameters.
- The selected overlap dressing value, for all the analyzed feed rates and grinding depths values, allowed *Ra* parameter values below 1.4 *μm*, *Rz* below 6.8 *μm* and normal grinding force components F_n values below 278 N, tangential component F_t below 130 N, to be obtained.

References

[1] Babiarz R., Żyłka Ł., Płodzień M. 2014. "Concept design of the high-pressure cooling system for the grinding of air alloys". Mechanik (87): 4–7.

[2] Chainikova A.S., Orlova L.A., Popovich N.V., Grashchenkov D.V., Lebedeva Y.E., Solntsev S.S. 2015. "Sr-anorthite glass ceramic with enhanced crack resistance, reinforced with silicon nitride particles". Russ. J. Appl. Chem. (88): 18–26.

[3] Habrat W., Żółkoś M., Świder J., Socha E. 2018. "Forces modeling in a surface peripheral grinding process with the use of various design of experiment (DoE)". Mechanik (91): 929–931.

[4] Hecker R.L., Liang S.Y., Wu X.J., Xia P., Jin D.G.W. 2007. "Grinding force and power modeling based on chip thickness analysis". Int J Adv Manuf Technol (33): 449–459.

[5] Herman D. 2006. "New generation of CBN grinding wheels bonded with glass-ceramic". Advances in Science and Technology (45): 1515–1519.

[6] Herman D., Okupski T., Walkowiak W. 2011. "Wear resistance glass-ceramics with a gahnite phase obtained in CaO-MgO-ZnO-Al2O3-B2O3-SiO2 system". Journal of the European Ceramic Society (31): 485–492.

[7] Herman D., Plichta J., Karpiński T. 1997. "Effect of glass-crystalline and amorphous binder application to abrasive tools made of microcrystalline alumina grains type SG". Wear (209): 213–218.

[8] Herman D., Pobol T., Walkowiak W. 2015. "Wpływ właściwości termicznych i mechanicznych spoiw szklanokrysta-licznych na mechanizm zużycia ściernic z pcBN". Mechanik (88): 126–131.

[9] Höland W., Beall G.H. 2012. "Glass-ceramic technology". John Wiley & Sons, Inc.

[10] Iordanova R.S., Milanova M.K., Aleksandrov L.I., Khanna A., Georgiev N. 2016. "Optical characterization of glass and glass- crystalline materials in the B2O3-Bi2O3-La2O3 system doped with Eu3+ ions". Bulg. Chem. Commun. (48): 11–16.

[11] Karamanov A., Kamusheva A., Karashanova D., Ranguelov B., Avdeev G. 2018. "Structure of glass--ceramic from Fe-Ni wastes". Materials Letters (223): 86–89.

[12] Kieraś S., Nadolny K., Wójcik R. 2015. "State in the art of cooling and lubrication of the machining zone in grind-ing processes". Mechanik (88): 204–211.

[13] Marinescu I.D., Rowe W.B., Dimitrov B., Ohmori H. 2013.Abrasives and abrasive tools. In Tribology of Abrasive Machining Processes (Second Edition), 243–311.William Andrew Publishing.

[14] Moreno M.B.P., Murillo-Gómez F., De Goes M. 2018. "Effect of different ceramic-primers and silanization--protocols on glass-ceramic bond strength". Dental Materials (34): e80–e81.

[15] Nadolny K. 2014. "State of the art in production, properties and applications of the microcrystalline sintered corun-dum abrasive grains". Int J Adv Manuf Technol (74): 1445–1457.

[16] Nadolny K. 2016. "Shaping the cutting ability of grinding wheels with zone-diversified structure". Proceedings of the Institution of Mechanical Engineers, Part B: Journal of Engineering Manufacture (230): 254–266.

[17] Nadolny K., Habrat W. 2017. "Potential for improving efficiency of the internal cylindrical grinding process by mod-ification of the grinding wheel structure—Part I: Grinding wheels made of conventional abrasive grains:". Proceed-ings of the Institution of Mechanical Engineers, Part E: Journal of Process Mechanical Engineering (231): 621–632.

[18] Nadolny K., Habrat W. 2017. "Potential for improving efficiency of the internal cylindrical grinding process by mod-ification of the grinding wheel structure—Part II: Grinding wheels made of superabrasive grains:". Proceedings of the Institution of Mechanical Engineers, Part E: Journal of Process Mechanical Engineering (231): 813–823.
[19] Nadolny K., Herman D. 2015. "Effect of vitrified bond microstructure and volume fraction in the grinding wheel on traverse internal cylindrical grinding of Inconel® alloy 600". The International Journal of Advanced Manufacturing Technology (81): 905–915.
[20] Nadolny K., Kapłonek W. 2015. "Identification of the tribological processes on the grinding wheel surface during the internal cylindrical grinding of 100Cr6 steel, based on SEM-EDS analysis". International Journal of Surface Sci-ence and Engineering (9): 298–313.
[21] Nadolny K., Kapłonek W., Ungureanu N. 2017. "Effect of macro-geometry of the grinding wheel active surface on traverse internal cylindrical grinding process". Journal of Mechanical and Energy Engineering (1): 15–22.
[22] Oczoś K.E., Habrat W. 2010. "Doskonalenie procesów obróbki ściernej. Cz. I. Quo vadis szlifowanie?". Mechanik (83): 449–452.
[23] Oczoś K.E., Habrat W. 2010. "Doskonalenie procesów obróbki ściernej. Cz. II. Wysokoefektywne ściernice i procesy szlifowania.". Mechanik (83): 517–529.
[24] Shi J., He F., Xie J., Liu X., Yang H. 2019. "Effect of heat treatments on the Li2O-Al2O3-SiO2-B2O3-BaO glass-ceramic bond and the glass-ceramic bond cBN grinding tools". International Journal of Refractory Metals and Hard Materials (78): 201–209.
[25] Tang J., Du J., Chen Y. 2009. "Modeling and experimental study of grinding forces in surface grinding". Journal of Materials Processing Technology (209): 2847–2854.
[26] Toenshoff H.K., Denkena B. 2013. "Basics of Cutting and Abrasive Processes". Springer.
[27] Żółkoś M., Habrat W., Świder J., Socha E. 2018. "Analysis of influence of the mono-crystalline corundum grinding wheel wear on grinding forces and roughness parameters in peripheral surface grinding of 100Cr6 steel". Mechanik (91): 702–704.

Mgr inż. Marcin Żółkoś

Rzeszow University of Technology, The Faculty of Mechanical Engineering and Aeronautics, al. Powstańców Warszawy 8, 35-959 Rzeszów, Poland

e-mail: markos@prz.edu.pl

THE POSSIBILITIES TO REDUCE SURFACE ROUGHNESS IN PRE-ASSEMBLY FACE MILLING WITH WIPER INSERTS

Możliwości obniżenia chropowatości powierzchni w przedmontażowym frezowaniu czołowym z wykorzystaniem płytek typu Wiper

Adam FRĄCZYK ORCID: 0000-0002-3056-3141
DOI: 10.15199/160.2020.1.8

Abstract: In the paper, the results of the comparative studies of the surface roughness, as obtained after face milling, with the application of standard cutting inserts and Wiper inserts, have been discussed. The presented results of the studies show in what technological conditions it is possible to obtain the best effects of reducing the surface roughness.
Keywords: face milling, surface roughness, cutting plates, Wiper inserts

Streszczenie: W artykule przedstawiono wyniki badań porównawczych chropowatości powierzchni, uzyskanych po obróbce frezowania czołowego, przy wykorzystaniu standardowych płytek skrawających oraz płytek typu Wiper. Zaprezentowane rezultaty badań pokazują, w jakich warunkach technologicznych obróbki można uzyskać najlepsze efekty obniżenia chropowatości powierzchni.
Słowa kluczowe: frezowanie czołowe, chropowatość powierzchni, płytki skrawające, Wiper

Introduction

Milling is one of the most frequently employed methods of machining. Nowadays, owing to a wide application of CNC machine tools and modern too materials, we may replace grinding with milling as a finishing in technological process of manufacture. To this end, we should optimally choose the technological machining parameters to the applied tool and the treated material. On the grounds of, *inter alia*, literature analysis [4, 6, 7, 9, 16] it may be observed that there are many studies concerning the effect and optimization of the technological machining parameters on the quality of the treated surface in the case of different metal alloys.

The utilization of smoothing Wiper inserts in the machining process, recommended by tool producers, is another method for improvement of the treated surface quality.

The mentioned aspect inclined the author of the paper to check to what degree the application of Wiper inserts affects the lowering of the surface roughness parameters in the case of treatment of two different species of steel.

The methodology of the studies

To examine the advantages resulting from the application of Wiper inserts, two types of steel were subjected to treatment: low-alloy steel S355JR (acc. to PN-18G2A) and tool alloy steel for hot work X40CrMoV511 (acc. to PN-WCLV).

The machining was carried out in 3-axial vertical milling machine CNC Mori Seiki DURA VERTICAL 5080.

Face milling cutter by Mitsubishi Materials marked as ASX445-063A05R, with number of edges=5, was used as a tool. The mentioned device employs cutting inserts with a positive geometry and rake angle 20°; the major cutting-edge angle is 45°. According to the producer's information, the mentioned head has a universal application – it is intended for rough and finishing (end) face milling of the alloys of light metals, cast iron, carbon steel and alloy steel, stainless steel and hardened steels [11].

On the conducted experiment, two types of inserts produced by Mitsubishi were used. The standard cutting inserts marked as SEMT13T3AGSN-JM, VP15TF type and the smoothing inserts of WIPER type – WEEW13T3AGER8C were applied. The both types of the inserts had a coverage (Al, Ti) N [12]. In the case of smoothing Wiper inserts, it is sufficient to install one insert in the milling head on order to improve the quality of the treated surface. It is important to ensure that the feed per revolution is not greater than the width of the smoothing edge of the insert [10].

The treatment was performed in two variants of technological parameters:

- Variable feed per tooth f_z, constant cutting speed V_c, constant depth of cutting α_p,
- Variable cutting speed V_c, constant minute feed f, constant depth of cutting α_p.

Tab.1. Variants and technological parameters of machining

Variant I of the machining			Variant II of the machining		
a_p [mm]	f_z [mm/z]	V_c [m/min]	a_p [mm]	f [mm/min]	V_c [m/min]
0,4	0.05	160	0,4	606	80
	0.1				120
	0.15				160
	0.2				200
	0.3				240

For the needs of the experiment, it was decided to extend the range of the feed by value of f_z =0.05 mm/tooth in relation to the parameters, recommended by the producer. The comparison of the parameters, employed in the studies has been presented in Table 1.

Additionally, the following assumptions were adopted for each treatment:

- Down milling operations,
- Incomplete milling at the width a_e =0.6 D,
- Cooling of the tool with the compressed air.

The measurements of the roughness were carried out using the contact profilometer Mitutoyo SJ-210 (Fig.1). The conditions of the measurements were based, *inter alia*, on the recommendations of standards PN-ISO 4288 and PN-ISO 3274:

- The employed filter – ISO 11562,
- Length of travel – l_t = 4.8 mm
- Sample length (Cutoff) – λ_c = 0.8 mm,
- The measuring range – 360 µm,
- Velocity of the needle travel – V_t = 0.50 mm/s

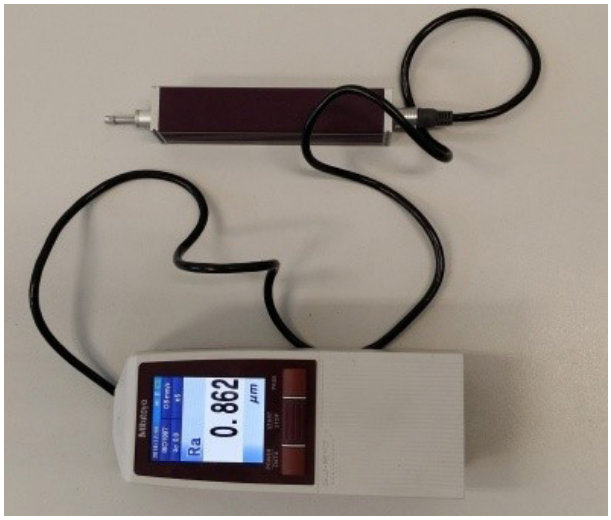

Fig. 1. A view of Mitutoyo SJ 210 profilometer

To determine the necessary number of the measurements n, the preliminary studies were carried out. There were adopted: significance level α = 0.05 and the number of preliminary measurements n_0 = 10; the level of estimate error was assumed as d = 0.1. For the adopted values, the coefficient t_α = 2.262 [12] was read out. Then, the arithmetical mean $\bar{y}$ of *Ra* and *Rz*, standard deviation *S* were calculated and the number of measurements n from the following relationship was estimated [8, 12]:

$$n = \frac{t_\alpha^2 \times s^2}{d^2} \leq n_0$$

where:
n_0 = size of the preliminary test,
t_α = value of T-Student variable,
s^2 = variance from the preliminary test,
d – maximum estimate error, equal to the measurement error

Tab. 2. The results of the measurements of the preliminary tests

n_0	Steel S355	
	Ra [mm]	*Rz* [mm]
1.	1,521	8,545
2.	1,741	8,378
3.	1,813	8,265
4.	1,673	8,234
5.	1,579	7,965
6.	1,685	8,251
7.	1,668	8,344
8.	1,643	8,434
9.	1,454	8,314
10.	1,585	8,515
$\bar{y}$	**1,636**	**8,325**
S	**0,15090**	**0,165538**
S^2	**0,011043956**	**0,027402944**
n	**5,65**	**14,021**

Tab. 2 shows the results of the preliminary measurements of roughness of steel S355 subjected to the machining by head, equipped in standard cutting inserts with the following parameters: cutting speed V_c = 160 m/min., feed per tooth f_z = 0.05 mm/tooth.

On the grounds of the conducted statistical analysis, based upon the results of the preliminary measurements for parameter *Rz*, the number of the measurements was adopted with a certain reserve n = 16.

The results of the tests

Fig. 2 ─ 9 show the change in parameters 2 D of the surface roughness *Ra* and *Rz* as a function of changes in feed F_z and cutting speed V_c for standard cutting inserts and Wiper inserts. Standard deviation was given as dispersion.

The results of the surface roughness measurements for steel S355JR as illustrated in Fig. 2-5 indicate the improvement of the quality of the surface after cutting with the Wiper insert.

During the milling with the feed f_z = 0.5 mm/tooth, the difference in the surface roughness, resulting from the application of Wiper insert is practically invisible. We should however remember that the mentioned value of feed f_z is not recommended by the producer of the inserts. The highest differences in the surface roughness were obtained during the treatment with the feed f_z = 0.1 mm/tooth. It may be observed that the surface roughness as obtained after the treatment with the use of Wiper insert demonstrates a slightly declining trend together with the increase of the value of feed f_z.

The increase of the cutting velocity V_c causes a reduction in the surface roughness of steel S355JP; it is especially visible after the machining with the standard inserts and at higher cutting speed V_c >140 m/min – Fig. 4÷5.

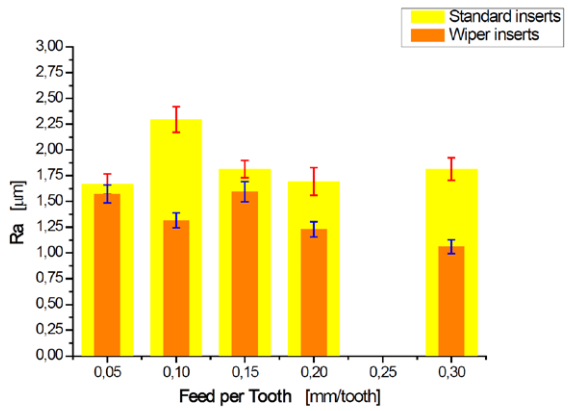

Fig. 2. The changes in the roughness parameter *Ra* for steel S355 in function of feed f_z after milling with standard inserts and Wiper inserts

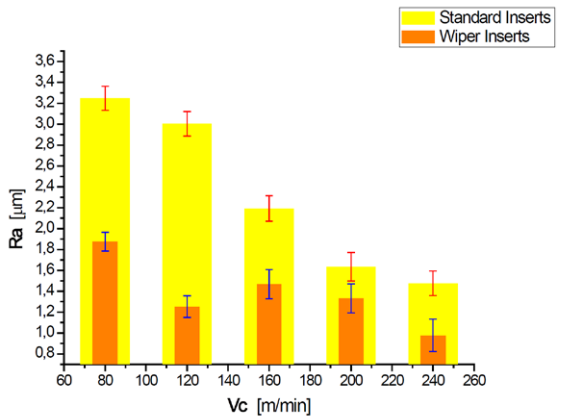

Fig. 4. The changes in the roughness parameter *Ra* for steel S355 in function of cutting speed V_c after milling with standard inserts and Wiper inserts

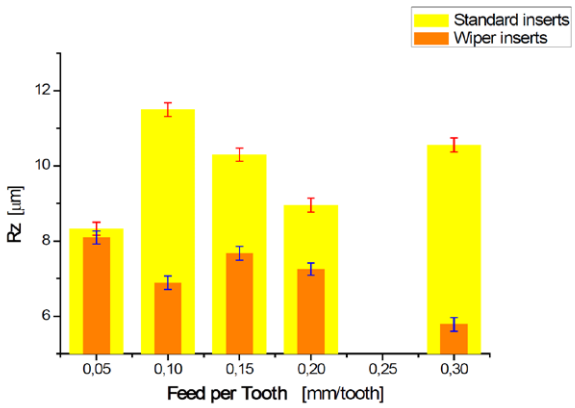

Fig. 3. The changes in the roughness parameter *Rz* for steel S355 in function of feed f_z after milling with standard inserts and Wiper inserts

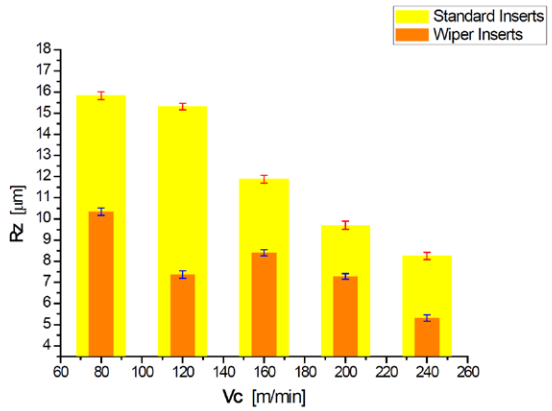

Fig. 5. The changes in the roughness parameter *Rz* for steel S355 in function of cutting speed V_c after milling with standard inserts and Wiper inserts

In the case of the machining of steel X40CrMoV511, the advantages resulting from the application of Wiper inserts are most visible – Fig. 6-8. The increase of the feed f_z in the case of the standard inserts use leads to a distinct increase of the parameters *Ra* and *Rz* – Fig. 6-7. The situation is different in the case of treatment with Wiper insert. Together with the increase of feed fz, the increase of the roughness parameters is practically not recorded. The most significant differences between the obtained parameters were found for feed f_z = 0.2 mm/tooth. After cutting with the Wiper insert, there was obtained five times lower parameter *Ra* as compared to the surface, treated by the standard inserts.

The effect of cutting speed of steel X40CrMoV511 on the surface roughness after the machining is visible in Fig. 8÷9. Together with the increase of cutting speed V_c, a small declining tendency of parameters *Ra* and *Rz* is observed.

The situation visible in Fig. 2-3 requires a separate explanation as well as in Fig. 6-7 where the increase of feed fz caused a decline in the roughness. It results probably from the fact that at lower feed velocities, the roughness becomes independent on the feed velocity and is only a function of the radius of the insert rounding and the type of the treated material [3]. It causes a higher micro-roughness, i.e. the overlapping uneven roughness on the produced grooves when removing the chips. In the area of edge, relatively more plastic flowing of the machining material is generated. Similarly when the feed is high and the corner of the insert has a small radius, the roughness of the surface is mainly dependent on the feed. The mentioned plastic flowing of the material is directed opposite to the direction of the feed and leads to formation of higher unevenness [1]. A similar phenomenon was presented in the paper [2] where a lower surface roughness occurred at higher feed due to “a clear cut” of the material and a relative lack of plastic deformations in the area of the blade work. The discussed theory may be supported by the fact that in the case of Wiper inserts, having a completely different cutting edge and the corner, the mentioned above phenomenon is practically not observed – Fig. 6-7.

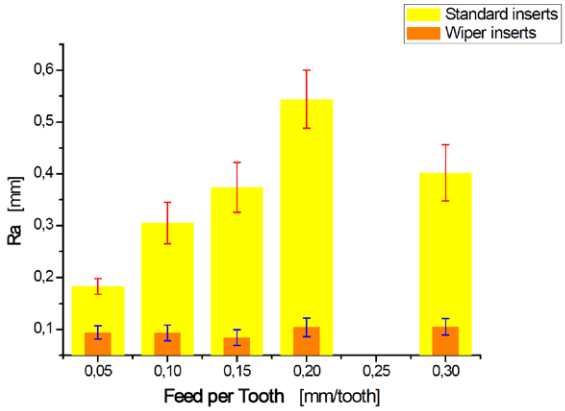

Fig. 6. The changes in the roughness parameter *Ra* for steel X40CrMoV511 in function of feed f_z after machining with standard inserts and Wiper inserts

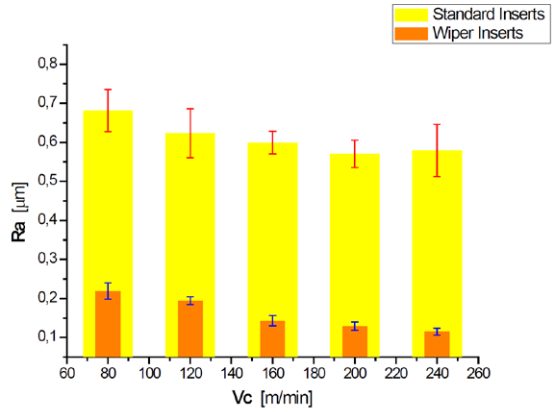

Fig. 8. The changes in the roughness parameter *Ra* for steel X40CrMoV511 in function of cutting velocity V_c after machining with standard inserts and Wiper inserts

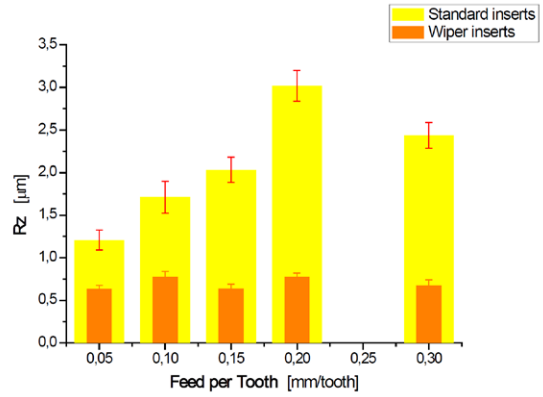

Fig. 7. The changes in the roughness parameter *Rz* for steel X40CrMoV511 in function of feed f_z after machining with standard inserts and Wiper inserts

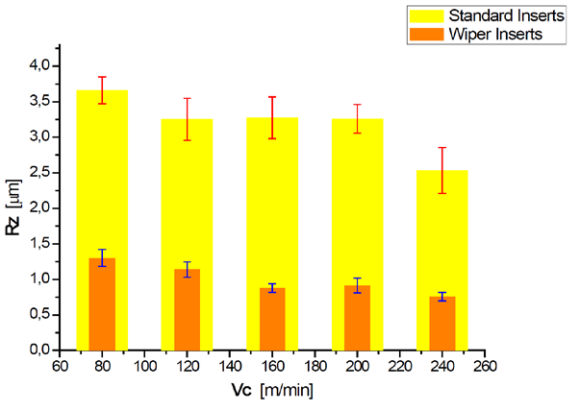

Fig. 9. The changes in the roughness parameter Rz for steel X40CrMoV511 in function of cutting speed V_c after machining with standard inserts and Wiper inserts

It should be remembered that vibrations, generated during the treatment are the reason for the changes in the surface roughness. They may cause "flattening" of the traces after the machining due to the relative vibrations of the tool's work [14].

Summary and concluisions

The conducted tests allowed carrying out the general verification of advantages coming form the application of smoothing inserts during the process of face milling as affected by the variable technological parameters V_c and f_z. On the grounds of the above, it is possible to formulate the following conclusions:

1. The application of cutting Wiper inserts in the process of face milling allows obtaining the lower surface roughness as compared to the machining with the standard inserts.
2. The decline in the surface roughness after the machining with the application of a single Wiper insert is dependent on the type of the steel. A considerable improvement of the surface quality is observed after the machining of the alloy steel.
3. In the case of using Wipert inserts, the increase in the feed value allows maintaining a low value of roughness what may be manifested in the increase of productivity, especially in the conditions of series and mass manufacture of the products.
4. The increase of the feed value in certain circumstances of the blade work may also lead to the lowering of the roughness of the surface after machining.

References

[1] Abouelatta O. B., Madi J. 2001. „Surface roughness prediction based on cutting parameters and tool vibration in turning operations". Journal of Materials Processing Technology 118: 269-277.

[2] Astakhov V. P., Shvets S. 2004. „The Assessment of plastic deformation in metal cutting". Journal of Materials Processing Technology 146(02): 193-202.

[3] Childs T. H. C., Sekiya K., Tezuka R., Yamane Y., Dornfeld D., Lee D. E., Min S. and Wright P. K. 2008. „Surface finishes from turning and facing with round nosed tools". Annals of CIRP 57(1): 89-92.

[4] Fedai Y. et. al. 2018. „Optimization of machining parameters in face milling using multi-objective Taguchi technique". Technical Journal 12: 104-18.

[5] Greń J. 1987. „Statystyka matematyczna podręcznik programowany". Warszawa: PWN.

[6] Jarosz K., Löschner P. 2018. „The effect of changes in depth of cut on surface roughness in machining of AISI 316 stainless steel". Journal of Machine Engineering 18(1): 72-79.

[7] Kadirgama K. et al. 2008. „Optimization of Surface Roughness in End Milling on Mould Aluminium Alloys (AA6061-T6) Using Response Surface Method and Radian Basis Function Network". JJMIE 2(4): 209-124.

[8] Kłonica M. 2017. „Wykorzystanie elementów statystyki w procesie badawczym na przykładzie pomiarów wybranych parametrów chropowatości powierzchni". W Innowacje w zarządzaniu inżynierii produkcji, 772-782, tom I. Opole: Oficyna Wydawnicza Polskiego Towarzystwa Zarządzania Produkcją.

[9] Mayur N. et. al. 2017. „Optimization of CNC Face Milling Process Parameters for Inconel 718 by Using Taguchi Method – A Review". IRJET 04: 806-810.

[10] Mitsubishi, face mills. Available from: http://www.mhuk-carbide.co.uk/technical_information/tec_rotating_tools/face_mills/tec_milling_guide/tec_milling_precautions/tec_milling_precautions_asx445 [Accessed: 02/12/2019].

[11] Mitsubishi, face mills. Available from: http://www.mitsubishicarbide.net/mhg/pl/face_mills/20000020/20066004 [Accessed: 02/12/2019].

[12] Mitsubishi, face mills. Available from: http://www.mitsubishicarbide.com/application/files/9014/4643/8968/b034g-f.pdf [Accessed: 02/12/2019].

[13] Mourão A. et. al. 2010. „The effect of wiper edge inserts on the specific cutting energy in face milling of aluminium alloys". International Journal of Modern Manufacturing Technologies II(2): 71-75.

[14] Reddy M. R., Kumar P. R., Mohana Rao G. K. 2011. „Effect of feed rate on the generation of surface roughness in turning", International Journal of Engineering Science and Technology 3(11): 8099-8105.

[15] Toledo J. V. R. et. al. 2018. „Performance of wiper geometry carbide tools in face milling of AISI 1045 steel". Journal of the Brazilian Society of Mechanical Sciences and Engineering 40: 478.

[16] Zalewski K., Matuszak J. 2017. „Badania porównawcze wpływu parametrów technologicznych frezowania wybranych stopów tytanu na moment skrawania i chropowatość obrobionej powierzchni". RUTMech XXXIV(89) (4/17): 563-572.

Dr inż. Adam Frączyk
Department of Materials and Machine Technology
University of Warmia and Mazury in Olsztyn, Poland
e-mail: adam.fraczyk@uwm.edu.pl

TiAM kwartalnik naukowo-techniczny
TECHNOLOGIA I AUTOMATYZACJA MONTAŻU
ZESPOŁÓW • MASZYN • URZĄDZEŃ

Zapraszamy Autorów do współpracy!
www.tiam.pl
tiam@sigma-not.pl

ASSEMBLY AUTOMATION

Emerald Publishing Limited
Howard House
Wagon Lane
Bingley BD16 1WA
United Kingdom
e-mail: emerald@emeraldinsight.com

Volume 39, Issue 4

ABSTRACTS:

1. Design and analysis of output feedback constraint control for antilock braking system based on Burckhardt's model

Authors: Youguo He, Chuandao Lu, Jie Shen, Chaochun Yuan

The purpose of this study is to improve vehicles' brake stability, the problem of constraint control for an antilock braking system (ABS) with asymmetric slip ratio constraints is concerned. A nonlinear control method based on barrier Lyapunov function (BLF) is proposed not only to track the optimal slip ratio but also to guarantee no violation on slip ratio constraints.

A quarter vehicle braking model and Burckhardt's tire model are considered. The asymmetric BLF is introduced into the controller for solving asymmetric slip ratio constraint problems.

The proposed controller can implement ABS zero steady-state error tracking of the optimal wheel slip ratio and make slip ratio constraints flexible for various runway surfaces and runway transitions. Simulation and experimental results show that the control scheme can guarantee no violation on slip ratio constraints and avoid self-locking.

The slip rate equation with uncertainties is established, and BLF is introduced into the design process of the constrained controller to realize the slip rate constrained control.

2. Combination modeling of auto body assembly dimension propagation considering multi-source information for variation reduction

Authors: Yinhua Liu, Shiming Zhang, Guoping Chu

This paper aims to present a combination modeling method using multi-source information in the process to improve the accuracy of the dimension propagation relationship for assembly variation reduction.

Based on a variable weight combination prediction method, the combination model that takes the mechanism model and data-driven model based on inspection data into consideration is established. Furthermore, the combination model is applied to qualification rate prediction for process alarming based on the Monte Carlo simulation and also used in engineering tolerance confirmation in mass production stage.

The combination model of variable weights considers both the static theoretical mechanic variation propagation model and the dynamic variation relationships from the regression model based on data collections, and provides more accurate assembly deviation predictions for process alarming.

A combination modeling method could be used to provide more accurate variation predictions and new engineering tolerance design procedures for the assembly process.

3. Numerical and experimental investigation of bulk stress distribution in edge under different clamping sequence

Authors: Hua Wang, Hailong Wang

The edge is a typical aero-structural compliant part, whose length-width ratio is about 60:1 and height-thickness ratio is about 30:1. Distortion of the edge is mainly caused by the bulk stresses which come from the manufacturing process of the plates. This paper aims to investigate the effect of clamping sequence on the bulk stress distribution in the edge.

The paper conducts the numerical and experimental investigations to predict the bulk stress distribution in the edge under different clamping sequences. A finite element model of the plate with residual stress after quenching and stretching is constructed. The edge is milled from the plate numerically and is ready for clamping. The contact model between the clamper and the edge is constructed

to simulate the clamping process. Then the edge is virtually clamped in different clamping sequences, and different deformations and bulk stresses are obtained. An experimental edge milled from the plate and a designed clamping platform are used to precisely control clamping force to verify the effect of clamping sequence on the bulk stress distribution in the edge. The experimental edge's distortions, relative displacements between the edge and the clamper and clamping forces validate the proposed numerical model.

4. A flexible resource investment problem based on project splitting for aircraft moving assembly line

Authors: Yifei Ren, Zhiqiang Lu

This paper represents a new extension of the resource investment problem based on aircraft moving assembly line. An effective integrated nested optimization algorithm is proposed to specify station splitting scheme, job scheduling scheme and resources allocation in the assembly lines, which is significant for practical engineering applications.

In response to the station design and flexible resources allocation of the aircraft moving assembly line, a new problem named flexible resource investment problem based on project splitting (FRIP_PS), which minimizes total cost of resources with a given deadline are proposed in this paper.

First, a corresponding mathematical model considering project splitting is constructed, which needs to be simultaneously determined together with job scheduling to acquire the optimized project scheduling scheme and resource configurations. Then, an integrated nested optimization algorithm including project splitting policy and job scheduling policy is designed in this paper. In the first stage of the algorithm, a heuristic algorithm designed to get the project splitting scheme and then in the second stage a genetic algorithm with local prospective scheduling strategy is adopted to solve the flexible resource investment problem.

5. The coupling mechanism of reassembly quality with uncertainty of remanufactured parts

Authors: Cuixia Zhang, Conghu Liu, Jianqing Chen, Qiang Li, Kang He, Mengdi Gao, Wei Cai

This study provides practical implications by developing a multivariate nonlinear mapping model for reassembly quality based on entropy to determine the uncertainty factors that affect the reassembly quality significantly and then correct the reassembly operation to better optimize the allocation of remanufacturing production resources. The study also theoretically contributes to reveal the coupling mechanism of reassembly quality with the uncertainty of remanufactured parts.

The uncertainty of remanufacturing parts is a key factor affecting the quality of remanufactured products. Therefore, the purpose of this paper is to measure the uncertainty of remanufactured parts and study the coupling mechanism of reassembly quality.

First, uncertainty of remanufactured parts is analyzed, and the uncertainty measure model for remanufacturing parts based on entropy is constructed. Second, the nonlinear mapping model between the uncertainty and reassembly quality were studied using Gauss-Newton iterative method to reveal the coupling mechanism between uncertainty of remanufacturing parts and reassembly quality. Finally, the model is verified in the reassembly process of remanufacturing cylinder head.

The method can guide reassembly operations to improve the reassembly quality with uncertainty of remanufactured parts.

6. A 3D assembly model retrieval method based on assembly information

Authors: Hu Qiao, Qingyun Wu, Songlin Yu, Jiang Du, Ying Xiang

The purpose of this paper is to propose a three-dimensional (3D) assembly model retrieval method based on assembling semantic information to address semantic mismatches, poor accuracy and low efficiency in existing 3D assembly model retrieval methods.

The paper proposes an assembly model retrieval method. First, assembly information retrieval is performed, and 3D models that conform to the design intention of the assembly are found by retrieving the code. On this basis, because there are conjugate subgraphs between attributed adjacency graphs (AAG) that have an assembly relationship, the assembly model geometric retrieval is translated into a problem of finding AAGs with a conjugate subgraph. Finally, the frequent subgraph mining method is used to retrieve AAGs with conjugate subgraphs.

The method improved the efficiency and accuracy of assembly model retrieval.

The examples illustrate the specific retrieval process and verify the feasibility and reasonability of the assembly model retrieval method in practical applications.

The assembly model retrieval method in the paper is an original method. Compared with other methods, good results were obtained.

7. A study on product assembly and disassembly time prediction methodology based on virtual maintenance

Authors: Kaijun Cai, Weiming Zhang, Wenzhuo Chen, Hongfei Zhao

Based on virtual maintenance, this paper aims to propose a time prediction method of assembly and disassembly (A&D) actions of product maintenance process to enhance existing methods' prediction accuracy, applicability and efficiency.

First, a framework of A&D time prediction model is constructed, which describes the time prediction process in detail. Then, basic maintenance motions which can comprise a whole A&D process are classified into five categories: body movement, working posture change, upper limb movement, operation and grasp/placement. A standard posture library is developed based on the classification. Next, according to motion characteristics, different time prediction methods for each motion category are proposed based on virtual maintenance simulation, modular arrangement of predetermined time standard theory and the statistics acquired from motion experiment. Finally, time correction based on the quantitative evaluation method of motion time influence factors is studied so that A&D time could be predicted with more accuracy.

This paper proposes a more accurate, efficient and applicable product A&D time prediction method. It can help designers predict A&D time of a product maintenance accurately in early design phases without a physical prototype. It can also provide basis for the verification of maintainability, the balance of the design of product structure and system layout.

8. An efficient algorithm for U-type assembly line re-balancing problem with stochastic task times

Authors: Faruk Serin, Süleyman Mete, Erkan Çelik

In this paper, a genetic algorithm is proposed to solve approach for U-type assembly line re-balancing problem using stochastic task times.

Changing the product characteristics and demand quantity resulting from the variability of the modern market leads to re-assigned tasks and changing the cycle time on the production line. Therefore, companies need re-balancing of their assembly line instead of balancing. The purpose of this paper is to propose an efficient algorithm approach for U-type assembly line re-balancing problem using stochastic task times.

The performance of the genetic algorithm is tested on a wide variety of data sets from literature. The task times are assumed normal distribution. The objective is to minimize total re-balancing cost, which consists of workstation cost, operating cost and task transposition cost. The test results show that proposed genetic algorithm approach for U-type assembly line re-balancing problem performs well in terms of minimizing total re-balancing cost.

Demand variation is considered for stochastic U-type re balancing problem. Demand change also affects cycle time of the line. Hence, the stochastic U-type re-balancing problem under four different cycle times are analyzed to present practical case.

9. Precise on-line non-target pose measurement for cylindrical components based on laser scanning

Authors: Jieyu Zhang, Yuanying Qiu, Xuechao Duan, Changqi Yang

Thus, this paper aims to provide a precise on-line non-target scanning method based on 3D vision.

Cylindrical components are common in industry assembly areas. It is necessary to obtain their precise positions and orientations for their assemblies. But some measurement approaches relying on measuring targets are not allowed, as they may not meet the efficiency requirement of on-line measurement or may cause surface damages to the components.

First, a laser profile sensor is used to acquire point cloud of the side surface of the measured cylindrical component. Then a composite process is conducted to estimate the pose and position of the axis. Aiming at this purpose, two fitting approaches, i.e., axis fitting and generatrix fitting, are tried respectively to estimate the pose parameters from the point cloud.

The results of Monte Carlo simulations demonstrate that neither the axis fitting nor the generatrix fitting could solely obtain the needed accuracy and precisions roundly. Thus, a new synthesis method is presented. And the results of prototype experiments validate the excellent accuracy and precision of the synthesis method.

This proposed new synthesis method combines the advantages of both the above fitting methods and can be easily integrated into the assembly line to guide the automation assembly process of the cylindrical components precisely.

10. Classification, representation and automatic extraction of adhesively bonded assembly features

Authors: Shantanu Kumar Das, Abinash Kumar Swain

This paper aims to present the classification, representation and extraction of adhesively bonded assembly features (ABAFs) from the computer-aided design (CAD) model.

The ABAFs are represented as a set of faces with a characteristic arrangement among the faces among parts in proximity suitable for adhesive bonding. The characteristics combination of the faying surfaces and their topological relationships help in classification of ABAFs. The ABAFs are classified into elementary and compound types based on the number of assembly features exist at the joint location.

A set of algorithms is developed to extract and identify the ABAFs from CAD model. Typical automotive and aerospace CAD assembly models have been used to illustrate and validate the proposed approach.

New classification and extraction methods for ABAFs are proposed, which are useful for variant design.

11. Precise on-line non-target pose measurement for cylindrical components based on laser scanning

Authors: Hui Wang, Jingsong Peng, Bing Zhao, Xin-Dong Zhang, Jie Yu, Yuan Li, Mao-Min Wang

This paper aims to present a fundamental approach on modeling and performance analysis of the blade–fixture system.

Near-net-shaped processes of jet engine blade have better performance in both reducing the material waste during production and improving work reliability in service, while the geometric features of blade, both sculptured surface and thin-walled shape, make the precise machining of blade challenging and difficult owing to its dynamics behaviors under complex clamping and machining loads.

A computerized framework on the complex blade–fixture dynamic behavior has been developed. Theoretical mechanic analysis on blade fixturing and machining is proposed with an especial emphasis on the boundary conditions of the blade–fixture system. Then the finite element analysis (FEA) method is used to simulate the variation trend of preloads, stiffness and blade distortion. The strong influence of parameters of workpiece–fixture configuration on blade distortion and machining error is investigated.

The adaptive machining of near-net-shaped jet engine blade is a new high-performance manufacturing technology in aerospace production. This study provides a fundamental methodology for the performance analysis of blade-fixture system, to clear the variation law of blade distortion during preloading and machining, which will contribute to minimize the machining error and improve productivity.

12. Structure-function correlations analysis and functional semantic annotation of mechanical CAD assembly model

Authors: Zhoupeng Han, Rong Mo, Haicheng Yang, Li Hao

This paper aims to find an approach for structure-function correlations analysis and functional semantic annotation of mechanical CAD assembly model before functional semantic-based assembly retrieval.

Three-dimensional computer-aided design (CAD) assembly model has become important resource for design reuse in enterprises, which implicates plenty of design intent, assembly intent, design experience knowledge and functional structures. To acquire quickly CAD assembly models associated with specific functions by using product function requirement information in the product conceptual design phase for model reuse.

An approach for structure-function correlations analysis and functional semantic annotation of CAD assembly model is proposed.

The correlation between structure and function is analyzed effectively, and functional semantics corresponding to structures in CAD assembly model are labeled. Additionally, the relationships between functional structures, assembled parts and functional semantics can be described explicitly and formally.

The paper proposes a novel approach for structure-function correlations analysis and functional semantic annotation of mechanical CAD assembly model. Functional structures in assembly model are extracted and analyzed from the point of view of assembly structure and function part structure. Furthermore, the correlation relation between structures, assembled parts and functional semantics is expressed explicitly and formally based on polychromatic sets.

13. RFID-based tracking and monitoring approach of real-time data in production workshop

Authors: Xixing Li, Baigang Du, Yibing Li, Kejia Zhuang

This paper aims to develop a novel RFID-based tracking and monitoring approach of real-time data in production workshop (TMrfid) to solve them.

In practical workshop production process, there are many production emergencies, e.g. new manufacturing tasks, facilities failure and tasks change. On one hand,

it results in poor timeliness and reliability of real-time production data collection, acquisition and transmission; on the other hand, it increases the difficulty of real-time data tracking and monitoring. At first, a three-layer model of real-time data based on RFID has been constructed, which contains RFID-based integrated acquisition center; “RFID & Cloud-service-rules”-based calculation and analysis center; and “RFID & Ontology-knowledge-base”-based monitoring and scheduling center. Then, a targeted analysis and evaluation method of TMrfid with feasibility, quality and performance has been proposed. Finally, a prototype platform of a textile machinery manufacturing enterprise has been built to verify the effective of TMrfid.

The effectiveness of TMrfid is verified by applying two groups of actual experimental data from the case enterprise, the results show that TMrfid can promote the efficiency, reliability and feasibility of tacking and monitoring of real-time data in production workshop.

RFID-based tracking and monitoring approach of real-time data in production workshop has been developed to solve the data information transmission and sharing problem. Three analysis and evaluation approaches have been introduced to solve the un-standardized evaluation problem of RFID application. A prototype platform of a textile machinery manufacturing enterprise has been constructed.

14. Integrated design environment for reusable modular assembly systems

Authors: Pedro Ferreira, Paul Danny Anandan, Ivo Pereira, Vikrant Hiwarkar, Mohmed Sayed, Niels Lohse, Susana Aguiar, Gil Gonçalves, Joana Gonçalves, Fabian Bottinger

This paper aims to provide a service-based integrated prototype framework for the design of reusable modular assembly systems (RMAS) incorporating reusability of equipment into the process. It extends AutomationML (AML) developments for an engineering data exchange to integrate and standardize the data formats that support the design of RMAS.

The approach provides a set of systematic procedures and support tools for the design of RMAS. This includes enhanced domain knowledge models that facilitate the interpretation and integration of information across the design phases.

The inclusion of reusability aspects in the design phase improves the sustainability of future assembly systems, by ensuring equipment use until its end-of-life. Moreover, the integrated support tools reduce the design time, while improving the quality/performance of the system design solution, as it enables the exploration of a larger solution space. This will result in a better response to dynamic and rapidly changing system requirements.

This work provides a sustainable approach for the design of modular assembly systems (MAS), which will ensure better resource utilization. Additionally, the standardization of the data and the support of low cost tools is expected to benefit industrial companies, particularly the small- and medium-sized enterprises.

15. A multimedia case-based reasoning framework for assembly sequence planning

Authors: Junhao Chen, Xiaoliang Jia

Assembly sequence planning (ASP) is a crucial job during assembly process design. However, it is still difficult to reuse the existing solution to solve a new ASP problem. In particular, with the rapid development of digital technologies, the reusable assembly information of an existing solution is not concentrated in one multimedia but dispersed in multiple heterogeneous multimedia, e.g. text, three-dimensional graphics, even images and videos. This paper aims to propose a multimedia case (MC)-based reasoning framework to solve ASP by reusing the existing solution whose assembly information is dispersed in multimedia.

The proposed framework is designed with the introduction of the MC. An MC seamlessly integrates the dispersed assembly information of an existing solution. Under the proposed concept and architecture, the assembly information of an existing solution is extracted to build assembly descriptors of multimedia. Therefore, the MC is captured by organizing the assembly descriptors of corresponding multimedia.

By means of the framework proposed, it is possible to reuse the existing solution whose assembly information is dispersed in multimedia to solve ASP. Moreover, the extraction method of assembly information can flexibly parse most of the multimedia. Finally, the MC has the capability to represent the existing solution by collecting dispersed assembly information.

The proposed framework can discover the similar existing solution and avoid the potential failures confronted in the past so that the feasibility of ASP result can be improved as much as possible.

16. An MBD based framework for relative position accuracy measurement in digital assembly of large-scale component

Authors: Guijiang Duan, Zhibang Shen, Rui Liu

This paper aims to promote the integration of the relative position accuracy (RPA) measurement and

evaluation in digital assembly process by adopting the model-based method. An integrated framework for RPA measurement is proposed based on a model-based definition (MBD) data set. The study also aims to promote the efficiency of inspection planning of RPA measurement by improving the reusability and configurability of the inspection planning.

The works have been carried out on three layers. In the data layer, an extended MBD data set is constructed to describe the objects and data for defining RPA measurement items; In definition layer, a model based and hierarchical structure for RPA item definition is constructed to support quick definition for RPA measurement items. In function layer, a toolset consisting three modules is constructed in a sequence from measurement planning to RPA value solving to visualized displaying again. Based on this framework, a prototype system is developed.

The paper provides an identified practice of model-based inspection. It suggests that MBD is valuable in promoting both the integration and efficiency of digital inspection.

The templates and constructed geometry objects given in this paper are still limited in a scenario of aircraft assembly. The integrity and universality of them still need follow-up works.

The paper includes implications for the model based digital inspection, the digital assembly and the extended application of MBD.

17. Complementary projector for null-space stiffness control of redundant assembly robot arm

Authors: Nikola Lukic, Petar B. Petrovic

Stiffness control of redundant robot arm, aimed at using extra degrees of freedom (DoF) to shape the robot tool center point (TCP) elastomechanical behavior to be consistent with the essential requirements needed for a successful part mating process, i.e., to mimic part supporting mechanism with selective quasi-isotropic compliance (Remote Center of Compliance – RCC), with additional properties of inherent flexibility.

Theoretical analysis and synthesis of the complementary projector for null-space stiffness control of kinematically redundant robot arm. Practical feasibility of the proposed approach was proven by extensive computer simulations and physical experiments, based on commercially available 7 DoF SIA 10 F Yaskawa articulated robot arm, equipped with the open-architecture control system, system for generating excitation force, dedicated sensory system for displacement measurement and a system for real-time acquisition of sensory data.

A novel complementary projector was synthesized based on the adopted objective function. Practical verification was conducted using computer simulations and physical experiments. For the needs of physical experiments, an adequate open-architecture control system was developed and upgraded through the implementation of the proposed complementary projector and an adequate system for generating excitation and measuring displacement of the robot TCP. Experiments demonstrated that the proposed complementary projector for null-space stiffness control is capable of producing the task-space TCP stiffness, which can satisfy the essential requirements needed for a successful part-mating process, thus allowing the redundant robot arm to mimic the RCC supporting mechanism behavior in a programmable manner.

18. Design and human–machine compatibility analysis of Co-Exos II for upper-limb rehabilitation

Authors: Leiyu Zhang, Jianfeng Li, Shuting Ji, Peng Su, Chunjing Tao, Run Ji

Upper-limb joint kinematics are highly complex and the kinematics of rehabilitation exoskeletons fail to reproduce them, resulting in hyperstaticity and human–machine incompatibility. The purpose of this paper is to design and develop a compatible exoskeleton robot (Co-Exos II) to address these problems.

The configuration synthesis of Co-Exos II is completed using advanced mechanism theory. A compatible configuration is selected and four passive joints are introduced into the connecting interfaces based on optimal configuration principles. A Co-Exos II prototype with nine degrees of freedom (DOFs) is developed and still owns a compact structure and volume. A new approach is presented to compensate the vertical glenohumeral (GH) movements. Co-Exos II and the upper arm are simplified as a guide-bar mechanism at the elevating plane. The theoretical displacements of passive joints are calculated by the kinematic model of the shoulder loop. The compatible experiments are completed to measure the kinematics of passive joints.

The compatible configuration of the passive joints can effectively reduce the gravity influences of the exoskeleton device and the upper extremities. The passive joints exhibit excellent compensation effect for the GH joint movements by comparing the theoretical and measured results. Passive joints can compensate for most GH movements, especially vertical movements.

Co-Exos II possesses good human–machine compatibility and wearable comfort for the affected upper limbs. The proposed compensation method is convenient to therapists and stroke patients during the rehabilitation trainings.

19. A survey on data-driven process monitoring and diagnostic methods for variation reduction in multi-station assembly systems
Authors: Yinhua Liu, Rui Sun, Sun Jin

Driven by the development in sensing techniques and information and communications technology, and their applications in the manufacturing system, data-driven quality control methods play an essential role in the quality improvement of assembly products. This paper aims to review the development of data-driven modeling methods for process monitoring and fault diagnosis in multi-station assembly systems. Furthermore, the authors discuss the applications of the methods proposed and present suggestions for future studies in data mining for quality control in product assembly.

This paper provides an outline of data-driven process monitoring and fault diagnosis methods for reduction in variation. The development of statistical process monitoring techniques and diagnosis methods, such as pattern matching, estimation-based analysis and artificial intelligence-based diagnostics, is introduced.

A classification structure for data-driven process control techniques and the limitations of their applications in multi-station assembly processes are discussed. From the perspective of the engineering requirements of real, dynamic, nonlinear and uncertain assembly systems, future trends in sensing system location, data mining and data fusion techniques for variation reduction are suggested.

This paper reveals the development of process monitoring and fault diagnosis techniques, and their applications in variation reduction in multi-station assembly.

20. Assembly variation analysis of compliant mechanisms by combining direct linearization method and Lagrange's equations
Authors: Zhihua Niu, Zhimin Li, Sun Jin, Tao Liu

This paper aims to carry out assembly variation analysis for mechanisms with compliant joints by considering deformations induced by manufactured deviations. Such an analysis procedure extends the application area of direct linearization method (DLM) to compliant mechanisms and also illustrates the dimensional interaction within multi-loop compliant structures.

By applying DLM to both geometrical equations and Lagrange's equations of the second kind, an analytical deviation modeling method for mechanisms with compliant joints are proposed and further used for statistical assembly variation analysis. The precision of this method is verified by comparing it with finite element simulation and traditional DLM.

A new modeling method is proposed to represent kinematic relationships between joint deformations and parts/components deviations. Based on a case evaluation, the computational efficiency is improved greatly while the modeling accuracy is maintained at more than 94% rate comparing with the benchmark finite element simulation.

The Equilibrium Equations of Incremental Forces derived from Lagrange's equations are proposed to quantitatively represent the relationships between manufactured deviations and assembly deformations. The present method extends the application area of DLM to compliant structures, such as automobile suspension systems and some Micro-Electro-Mechanical-Systems.

korozja kosztuje! *

***) straty korozyjne szacuje się na 3-6% PKB**

Forum wymiany wiedzy i doświadczeń na temat ochrony materiałów przed skutkami korozji

na życzenie wysyłamy bezpłatny egzemplarz okazowy:
redakcja@ochronaprzedkorozja.pl

www.ochronaprzedkorozja.pl
www.sigma-not.pl

TiAM kwartalnik naukowo-techniczny
TECHNOLOGIA I AUTOMATYZACJA MONTAŻU
ZESPOŁÓW • MASZYN • URZĄDZEŃ

ASSEMBLY TECHNIQUES AND TECHNOLOGIES

INFORMATION FOR AUTHORS

Please submit to the editorial office author's application form with contact details, a title of the proposed article, number of pages, illustrations and tables and a brief abstract. After receiving information about the acceptance of the proposed paper submit the entire text prepared according to the editorial instructions as well as a complete declaration form.
Submitted articles are subjected to editorial assessment and receive a formal editorial identification number used in further stages of the editorial process. Every submitted article is reviewed. Publication is possible after receiving positive reviews (see review procedure).
The editorial office does not pay royalties.

GUIDELINES FOR PREPARING PAPERS

- Articles for publication in POLISH TECHNICAL REVIEW should have scientific and research character and deal with current issues of the industry.
- Articles must be original, not previously published (if the article is a part of another work i.e. PhD thesis, Habilitation etc. the information about that should be placed in the reference section) .
- The article should involve a narrow topic but treated thoroughly without repeating general knowledge information included in the widely known literature.
- If the problem is extensive break it into articles for separate publications.
- Articles should be of a clear and logical structure: the material should be divided into parts with titles reflecting its content. The conclusions should be clearly stated at the end of the paper.
- The article should be adequately supplemented with illustrations, photographs, tables etc. however, their number should be limited to absolute necessity.
- The title of the article should be given in Polish and English as well as the abstract and key words.
- The article should not exceed 8 pages (1 page – 1 800 characters).
- The article should include mailing and e-mail addresses of the author(s).
- The article should be electronically submitted in * doc or * docx format. Equations should be written in the editors, with a clear distinction between 0 and O. If the equations exceed the width of column (8 cm) they must be moved, otherwise use double width column (16 cm).
- The editorial staff does not rewrite the texts or prepare illustrations. Apart from doc, * docx formats it is recommended to submit the source files of illustrations (in *.eps, *jpg or * tif format).
- Drawings and graphs must be clear, taking into account the fact that the width of the columns in the magazine is 8 cm, width of the single column - 17 cm, height of the column - 24.5 cm.
- The text on the drawings cut to the size must be legible and not less than 2 mm.
- The authors are required to give at the end of the article a full list of sources used for the paper. The text must include citation references to the position of cited work in the bibliography. The bibliography prepared according to the references in the text must include: books – surname and first letter of the author's name, title, publisher, year and a place of publication (optionally page numbers), magazines – author's name and surname, title of the article, title of the magazine, number, year and optionally page numbers. The bibliography should present the current state of knowledge and take into account publications of world literature.
- The authors guarantee that the contents of the paper and the drawings are originally their property (if not, the source should be indicated). The authors who submit the paper, will receive the following documents from the Publisher SIGMA-NOT to be signed by them:
  - The declaration on granting a licence
  - The licence agreement
  - The Authors' agreement

  on the right of the Publisher to:
  a) Preservation and reproduction of the article, via production of its copies by paper and electronic way,
  b) Turnover of the copies on which the article has been preserved – by introduction to market, lending or lease of the copies,
  c) Making available to the public, including the Internet pages,
  d) Dissemination as a whole or of its parts for advertisement and/or promotional purposes.
- The editorial staff will document all forms of scientific misconduct, especially violations of the rules of ethics applicable in science.

Zapraszamy Autorów do współpracy!

www.tiam.pl

tiam@sigma-not.pl

tel. 22 853 81 13

TiAM kwartalnik naukowo-techniczny
TECHNOLOGIA I AUTOMATYZACJA MONTAŻU
ZESPOŁÓW • MASZYN • URZĄDZEŃ


WYDAWNICTWO SIGMA-NOT
34 TYTUŁY
123 000 PUBLIKACJI
on-line
WYGODNY DOSTĘP
DO ARTYKUŁÓW FACHOWYCH
on-line
WIRTUALNA CZYTELNIA
NA PORTALU INFORMACJI TECHNICZNEJ
www.sigma-not.pl

WIEDZA TWOJĄ PRZEWAGĄ

WIRTUALNA CZYTELNIA

NA PORTALU INFORMACJI TECHNICZNEJ

www.sigma-not.pl

również na urządzenia mobilne

WYGODNY DOSTĘP
DO **POLSKIEJ** PRASY FACHOWEJ
W KAŻDEJ CHWILI

więcej informacji:
22 840 30 86, prenumerata@sigma-not.pl
22 827 43 65, reklama@sigma-not.pl

70 lat
WYDAWNICTWO *SIGMA-NOT*

/sigmanot